論文 / 著書情報
Article / Book Information

題目(和文)	
Title(English)	Electrom-transfer reactions of 2,2'-bipyridine complexes of transition metals
著者(和文)	佐治 哲夫
Author(English)	T.Saji
出典(和文)	学位:博士(工学), 学位授与機関:東京工業大学, 報告番号:甲第741号, 授与年月日:1975年3月26日, 学位の種別:課程博士, 審査員:青柳茂
Citation(English)	Degree:Doctor (Engineering), Conferring organization: Tokyo Institute of Technology, Report number:甲第741号, Conferred date:1975/3/26, Degree Type:Course doctor, Examiner:
学位種別(和文)	博士論文
Type(English)	Doctoral Thesis

ELECTRON TRANSFER REACTIONS OF 2,2'-BIPYRIDINE COMPLEXES OF TRANSITION METALS

ELECTRON TRANSFER REACTIONS OF 2,2'-BIPYRIDINE COMPLEXES OF TRANSITION METALS

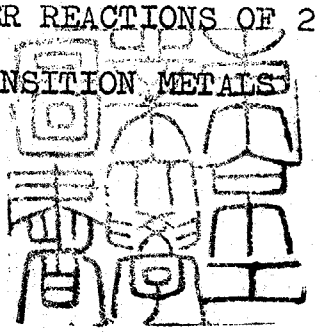

A

DISSERTATION

Presented to the Faculty of the Graduated School of

Tokyo Institute of Technology

in Partial Fulfillment of the Requirements

for the Degree of

DOCTOR OF ENGINEERING

by

Tetsuo Saji, B. S., M. S.

March, 1975

ACKNOWLEDGEMENTS

Sincere and grateful appreciation is expressed to Dr. Shigeru Aoyagui for his patience and generous guidance given to me during the preparation of this dissertation. My grateful acknowledgement is also given to my colleagues for their kind help.

Tetsuo Saji

Tokyo Institute of Technology
Ohokayama, Meguro-ku
Tokyo

March, 1975

TABLE OF CONTENTS

CHAPTER I

INTRODUCTION

Pure electron-transfer reactions occurring in solution and at electrodes are the simplest of all the elementary processes of chemical reactions, because they are unaccompanied by bond-formation or bond-rupture. Both types of electron-transfer reactions have many features in common. A particularly simple reaction of the former type is the transfer of one electron from a reduced species to an oxidized one with no change in concentration of either species. It can be classified into so-called homonuclear electron-exchange reactions where the standard free energy change is zero. It is termed a homogeneous electron-exchange reaction or more briefly a homogeneous reaction in this article. The electrochemical redox reactions of substances soluble in solution are quite similar schematically to the homogeneous electron-exchange reaction in solution. They are termed electrochemical electron-transfer reactions or electrochemical reactions. The two reaction types are represented by the following equations:

$$A^z + A^{z-1} \rightleftharpoons A^{z-1} + A^z \quad \text{(homogeneous reactn.)} \quad (1)$$

$$A^z + e^- \rightleftharpoons A^{z-1} \quad \text{(electrochemical reactn.)} \quad (2)$$

where z is the number of the ionic charge of the oxidized

species and e^- an electron in the electrode. We may expect more success in calculations of absolute reaction rate constants for such reactions than is generally obtained for other types of chemical reaction. In fact most of the major theoretical treatments of electron-transfer reactions can be applied straightforwards only to these simple reactions[1].

The electrochemical electron-transfer reactions, however, cannot be so simple as the homogeneous reactions, because they are heterogeneous in nature. It is quite probable that the reaction kinetics are much affected by the electrical double-layer at the metal-solution interface, the conditions of matal surface and some other unknown factors. The non-empirical calculation of the electrochemical rate constant can only be made by neglecting the heterogeneity and introducing some inhomogeneity in potential at the location where the electron-transfer occurs. It is also true that there exists a far smaller body of experimental results suitable for testing theoretically calculated rate constants of electrochemical reactions than homogeneous ones[2]. Much more systematic studies on electrochemical electron-transfer reactions are required. If we are successful in finding some correlation between electrochemical rate constants and homogeneous

ones, we may have a sound reason for the credibility of the discussions on electrochemical rates based on the analogy to those on homogeneous ones.

The mechanism of homogeneous electron-transfer reactions, especially of transition metal complexes, has been widely studied experimentally and theoretically[1,3]. They are divided into two groups: one is the group of reactions proceeding via an outer-sphere activated complex, and the other, an inner-sphere activated complex. In the reactions of the former group, the inner coordination shells of the reactant complex ions are left intact in the transition state; in the latter, two reactants share the ligands of their first coordination spheres in the transition state. When an electron-transfer rate theory is tested by comparing the rate constant calculated theoretically with the observed one, experiments should be made on reactions with an outer-sphere mechanism, becasue the representative theories are based on the assumption of this mechanism. Unfortunately, it is often difficult to know which mechanism is realized in a homogeneous electron-exchange reaction and there are not many reactions that have been confirmed to proceed via an outer-sphere activated complex. Even the concept of outer- and inner-sphere mechanisms have never been established in electrochemical electron-

transfer reactions. In this regard the following proposals are made for selecting a reaction suitable for testing the theory of the electrochemical electron-transfer reactions. First, an electrode reaction is favourable when the corresponding homogeneous electron-exchange reaction is known to be definitely of outer-sphere type. Secondly, reversible electrode reactions are more favourable than irreversible ones, because it can be reasonably considered that there are chances of finding an outer-sphere electrochemical reaction among reactions with large standard rate constants than among those with small standard rate constants. The latter reactions may be associated with bond-breaking or bond-making reactions.

In connection with the first criterion, now it is necessary to choose outer-sphere reactions for the theoretical prediction to be compared with the experimental results. There is some reason to believe that very fast exchange reactions are of outer-sphere type[3]. The systems $Fe(CN)_6^{3-}/Fe(CN)_6^{4-}$ (9×10^4)[4], $Fe(phen)_3^{3+}/Fe(phen)_3^{2+}$ (3×10^8)[5], $Fe(C_5H_5)_2^{+}/Fe(C_5H_5)_2$ (3×10^8)[6], are examples; they are classified into outer-sphere reactions on the basis of certain experimental evidence. Here phen is 1,10-phenanthroline and C_5H_5 cyclopentadienyl. The numbers in parentheses are the second order rate constants in $M^{-1}\ s^{-1}$. The term "system" is defined in this article

to be a couple of complexes which undergo either a homogeneous electron-exchange reaction of eqn. (1) or an electrochemical electron-transfer reaction of eqn. (2) and is designated by a symbol A^z/A^{z-1}.

Generally an electron-exchange reaction is very fast, if it satisfies the following conditions[3]: (1) the reactants have "conducting" unsaturated ligands, such as cyanide, phenanthroline, bipyridine and cyclopentadienyl, that is, the reactants are characterized by a highly delocalized π-electron distribution, and (2) the reactants are a pair of complexes differing by one in the number of electrons in the low-lying orbitals not used in ligand bondings. The electron-exchange reactions such as $Fe(phen)_3^{3+}/Fe(phen)_3^{2+}$ [5], $Fe(C_5H_5)_2^{+}/Fe(C_5H_5)_2$ [6], $Fe(bipy)_3^{3+}/Fe(bipy)_3^{2+}$ [7] (bipy = 2,2'-bipyridine) and $Os(bipy)_3^{3+}/Os(bipy)_3^{2+}$ [8] satisfy these conditions; their second order rate constants are larger than 10^7 M^{-1} s^{-1}.

In this thesis attempts are made to obtain some basic data suitable for testing the non-empirical elucidation of electrode kineics. Experiments are carried out on the complexes of a variety of transition metals with 2,2'-bipyridine as ligands. They are well suited for the present purpose because of the following reasons.

(1) Most of them are inert with respect to ligand substitution.

(2) All redox systems satisfy the first condition described above. When they are in certain oxidation states, they satisfy the second condition, too.

(3) A wide variety of oxidation states and electronic configurations can be obtained[9].

The homogeneous electron-exchange reactions of the systems composed of an aromatic hydrocarbon and its anion radical are known to be very fast or possibly the fastest, when anion radicals are not in strong ion-pairing with counter cations[10]. Under such circumstances there is no reason for classifying these systems into reactions with an inner-sphere mechanism. Their second order rate constants are of the order 10^9 M^{-1} s^{-1}. It is true that there have been systematic studies on their homogeneous and electrochemical reactions and attempts have been made to test the theories with these systems[11]. The oxidation states of hydrocarbons, however, can only be varied within a very limited range. A series of redox systems perylene$^+$/perylene, perylene/perylene$^-$ and perylene$^-$/perylene^{2-} is the most extensive one ever reported[12,13].

In Chapter II, the electronic configurations of bipyridine complexes of transition metals are determined by a new electrochemical method. In Chapter III, the electrochemical electron-transfer rates of these

complexes are measured by the galvanostatic double-pulse method. The correlation between the rate constants and the electronic configurations determined in Chapter II is discussed. In Chapter IV, the correlation between the rate constants for the homogeneous electron-exchange reactions and those for the electrochemical electron-transfer reactions is discussed on the basis of the theoretical equation of Marcus.

REFERENCES

1 W. L. Reynolds and R. W. Lamry, Mechanisms of Electron Transfer, The Ronald Press Co., New York, N. Y. (1966).

2 R. A. Marcus, J. Phys. Chem., 67, 853 (1963).

3 F. Basolo and R. G. Pearson, Mechanisms of Inorganic Reactions, 2nd ed., John Wiley & Sons Inc., New York, N. Y. (1967), Chap. 6.

4 M. Shporer, G. R. A. Loemenstein and G. Novan, Inorg. Chem., 4, 361 (1965).

5 I. Ruff and M. Zimonyi, Electrochimica Acta, 18, 515 (1973).

6 J. R. Pladziewicz and J. H. Espensen, J. Am..Chem. Soc., 95, 56(1973).

7 R. Stasiw and R. G. Wilkins, Inorg. Chem., 8, 156 (1969).

8 R. Campin, N. Purdie and N. Sutin, J. Am. Chem. Soc., 85, 3528 (1963).

9 W. R. McWhinnie and J. D. Mitter in H. J. Emeleus and A. G. Sharpe (Eds.), Advances in Inorganic Chemistry and Radiochemistry, Vol. XII, Academic Press, New York, 1969, p. 134.

10 K. Suga, S. Ishikawa and S. Aoyagui, Bull. Chem. Soc. Japan, 46, 808 (1973).

11 M. E. Peover in N. S. Hush (Eds.) Reactions of Molecules at Electrode, Wiley-Interscience, London, 1971, p. 259.

12 H. Mizota, K. Suga, Y. Kanzaki and S. Aoyagui, J. Electroanal. Chem., 44, 471 (1973).

13 N. Koizumi and S. Aoyagui, Electroanal. Chem., 55, 452 (1974).

CHAPTER II

POLAROGRAPHIC STUDIES ON TRIS(2,2'-BIPYRIDINE) COMPLEXES

A. Correlation between Reduction Potentials of Iron(II), Ruthenium(II), Osmium(II) Complexes and Those of Free Ligands

a. INTRODUCTION

It is known that the ligand 2,2'-bipyridine (bipy) stabilizes low oxidation states for a wide variety of both transition and nontransition metals[1]. Most of these complexes in low oxidation states have been prepared by Herzog and coworkers[2]. Their physical properties have been investigated experimentally and theoretically[1]. The electronic configuration of a complex in a low oxidation state can be determined by electronic absorption spectroscopy and electron spin resonance (e.s.r) spectroscopy. When available, e.s.r spectra with hyperfine splittings may offer the most straightforward method for this purpose. The unpaired electrons in a nontransition metal complex, e.g. Li(bipy) and $Be(bipy)_2$, have been concluded to occupy molecular orbitals composed mainly of ligand π^*-orbitals, on the basis of their e.s.r spectra exhibiting hyperfine splittings due to nitrogen nuclei and protons with or without an admixture of metal hyperfine lines[3-7]. Transition metal complexes, on the other hand,

can be divided into two groups according to their electronic configurations in low oxidation states. In some complexes, e.g. $Cr(bipy)_3^+$ and $V(bipy)_3$, the highest occupied orbital is a delocalized molecular orbital composed mainly of a metal t_{2g}-orbital. This is supported by their e.s.r spectra exhibiting hyperfine splittings due to central metal nuclei with some admixture of splittings due to bipyridine nitrogen nuclei but no admixture of proton lines[3-8]. Complexes belonging to the other group, e.g. $Fe(bipy)_3$ and $Fe(bipy)_3^-$, have an electronic configuration similar to that of the nontransition metal complexes[9-11].

In this section we present a new method to determine which molecular orbital an electron in a low oxidation state complex occupies, a molecular orbital mainly of metal orbital character or a molecular orbital mainly of ligand orbital character. It is based on an empirical rule concerning the correlation between the polarographic half-wave potentials of complexes and their electronic configurations. Polarography has been extensively used to investigate bipyridine complexes. Especially when aprotic solvents such as acetonitrile or N,N-dimethylformamide (DMF) are used, it provides valuable informations about the low oxidation states of many complexes[12-19]. A series

of low oxidation states is revealed by the polarographic reduction of a complex in a high oxidation state. Such a complex is stable under usual conditions. Thus the in situ investigation of a less stable complex in a low oxidation state can be easily performed. In the assignement of elecronic states based on the e.s.r method, on the other hand, it is necessary to prepare and handle complexes in a low oxidation state. This is a drawback in the e.s.r method because most of complexes in low oxidation states are unstable when allowed to atand in contact with the atmosphere. Besides, not every complex in a low oxidation atate provides an e.s.r spectrum exhibiting hyperfine splittings. Attempts have been made to assign an unpaired electron to either a metal orbital or a ligand orbital with the aid of g-value analysis of an unresolved e.s.r spectrum[9,13]. However, this method is less reliable.

b. EXPERIMENTAL

Reagents

4,4'-dimethyl-2,2'-bipyridine (4-dmbipy) and 5,5'-dimethyl-2,2'-bipyridine (5-dmbipy) were prepared according to the method of Sasse and Whittle[19]. Bipy and 2,2',2''-terpyridine (terpy) were supplied by the Wako Pure Chemical Industries and the Tokyo Chemical

Industries, respectively. DMF was dried over potassium carbonate, distilled in vacuo and stored under a nitrogen atmosphere. Tetra-n-butylammonium perchlorate (TBAP) was prepared from tri-n-butylamine and n-butyl iodide.

Complexes

Tris(2,2'-bipyridine)iron(II) perchlorate[20], bis(2,2',2"-terpyridine)iron(II) perchlorate[15], tris (4,4'-dimethyl-2,2'-bipyridine)iron(II) perchlorate[21], tris(5,5'-dimethyl-2,2'-bipyridine)iron(II) perchlorate[22], tris(2,2'-bipyridine)ruthenium(II) perchlorate[23] and tris(2,2'-bipyridine)osmium(II) perchlorate[24] were prepared according to the procedures described in the literature cited. 4,4'- and 5,5'-dimethyl derivatives of tris(2,2'-bipyridine)ruthenium(II) perchlorate and tris(2,2'-bipyridine)osmium(II) perchlorate were prepared according to procedures similar to those for the unsubstituted complexes.

Solutions

The electrolytic solutions contained 0.1 M TBAP and 1 mM electroactive substances, i.e. complexes or ligands, in DMF. They were handled under an atmosphere of nitrogen.

Voltammetric measurements

Dc polarograms and cyclic voltammograms were obtained with a conventional potentiostat assembled from solid-state operational amplifiers and recorded on a Riken Denshi F-3D X-Y plotter. An H-type cell with a glass frit was used. A dropping mercury electrode served as a working electrode in measurements of polarograms and a platinum spherical electrode in measurements of cyclic voltammograms. The scan rate in the latter measurements was 0.1 V s^{-1}. The counter electrode was a mercury pool placed in the compartment of working electrode. The other compartment was connected with a saturated calomel electrode (SCE) via an aqueous agar bridge. All data on electrode potentials are referred to the SCE. Measurements were carried out at 20 ± 2 °C.

c. RESULTS

Polarography of bipy, 4-dmbipy, 5-dmbipy and terpy

Table 1 shows the reduction half-wave potentials of the ligands used in this experiment. The second wave of 5-dmbipy is possibly masked by the ultimate current rise. Reversibility of each wave was examined on the basis of log-plot analysis of the polarogram together with peak-potential separation and peak-current ratio of the cyclic voltammogram. The first waves were found to be reversible

one-electron waves, whereas the second waves were irreversible. Half-wave potentials for bipy in DMF have been reported by DuBois et al.[26] to be -2.11 and -2.5 V vs. SCE. Their second wave was less negative than ours. It is very likely that the half-wave potential of the second wave is a function of impurities in the sample solution.

The half-wave potentials of the first waves of the free ligands become more negative in the order terpy < bipy<4-dmbipy < 5-dmbipy. When the contribution from the solvation energy to the reduction potential of a ligand is constant in the four ligands, the π^*-levels in the free ligands increase in the order terpy<bipy<4-dmbipy< 5-dmbipy.

Polarography of $Fe(bipy)_3(ClO_4)_2$

Figure 1 shows a cathodic polarogram for $Fe(bipy)_3(ClO_4)_2$. It exhibits four reduction waves with half-wave potentials of -1.26, -1.44, -1.70 and -2.43 V. Each plot of $\log[i/(i_1-i)]$ vs. E for these waves gave a straight line with a slope shown in Table 2. Here i is the polarographic current at a potential E and i_1 the limiting current. The wave heights of the first three waves were identical. By the addition of a small amount of water into the solution, these wave heights were

scarcely affected, while the height of the fourth wave increased and its half-wave potential was shifted to a less negative potential.

Figure 2 shows a cyclic voltammogram for $Fe(bipy)_3(ClO_4)_2$ obtained with the platinum working electrode. The conventional reversibility criteria of peak-potential separation and peak-current ratio show that the three waves in the figure are reversible one-electron waves. The three waves in Fig. 3 with the half-wave potentials of -1.26, -1.44 and -1.70 V can thus be assigned to the $Fe(bipy)_3^{2+}/Fe(bipy)_3^{+}$, $Fe(bipy)_3^{+}/Fe(bipy)_3$ and $Fe(bipy)_3/Fe(bipy)_3^{-}$ redox systems respectively. The assignment was supported by the following fact. After the $Fe(bipy)_3^{2+}$ had been partially reduced to $Fe(bipy)_3^{+}$ by a controlled-potential electrolysis at -1.4 V, the polarogram of the resultant solution showed a wave passing through the line of zero current and having a half-wave potential of -1.25 V, although the half-wave potential is rather obscured by a maximum current in the anodic wave falling abruptly at -0.44 V into a diffusion plateau at more positive potentials. The three waves assigned above were in qualitative agreement with the waves observed in acetonitrile by Tanaka and Sato[12,13].

Polarography of $Fe(terpy)_2(ClO_4)_2$

The cathodic polarogram of $Fe(terpy)_2(ClO_4)_2$ exhibited five waves. The two waves at -1.99 and -2.35 V were much lower in height compared with other waves. They may be attributed to reduction of free terpy, because a polarogram of the latter substance showed two reduction waves at -2.00 and -2.4 V. The first three waves with half-wave potentials of -1.17, -1.34 and -1.99 V were reversible one-electron waves. The first two waves are shown in Fig. 3 in comparison with the first three waves for $Fe(bipy)_3^{2+}$. The waves at -1.17 and -1.34 V may be assigned to the redox systems $Fe(terpy)_2^{2+}/Fe(terpy)_2^{+}$ and $Fe(terpy)_2^{+}/Fe(terpy)_2$ respectively. This is consistent with the conclusion of Musumeci et al.[15] who made a detailed examination of polarograms for $Fe(terpy)_2(ClO_4)_2$ in acetonitrile.

Polarography of $Fe(4\text{-dmbipy})_3(ClO_4)_2$ and $Fe(5\text{-dmbipy})_3(ClO_4)_2$

The polarograms and cyclic voltammograms for $Fe(4\text{-dmbipy})_3(ClO_4)_2$ and $Fe(5\text{-dmbipy})_3(ClO_4)_2$ were quite similar to those of the unsubstituted bipyridine complexes. Figure 4 shows the first three reduction waves for these complexes together with the first three waves for $Fe(bipy)_3^{2+}$. They were reversible one-electron waves. Table 2 shows that the half-wave potentials of the first reduction waves for the iron complexes become more

negative in the following order of ligands, terpy < bipy < 4-dmbipy < 5-dmbipy. The same relation holds for the second waves and the third ones, with terpy excluded from the relation for the third waves.

Polarography of $Ru(bipy)_3(ClO_4)_2$, $Ru(4\text{-}dmbipy)_3(ClO_4)_2$ and $Ru(5\text{-}dmbipy)_3(ClO_4)_2$

The cathodic polarogram of $Ru(bipy)_3(ClO_4)_2$ was almost identical with that of the iron complex except for the fourth wave. The half-wave potential of the fourth wave, -2.3 V, was less negative than that of $Fe(bipy)_3^{2+}$, -2.43 V. In so far as the first three reduction waves were concerned, the polarogram and the cyclic voltammogram of $Ru(bipy)_3^{2+}$ were quite similar to those obtained previously in acetonitrile[17,26]. The polarograms in Fig. 5 show the first three reduction waves for $Ru(bipy)_3^{2+}$ and its methyl derivatives. They were all reversible one-electron waves. Their half-wave potentials listed in Table 2 show that the same substitution effect on the half-wave potential that was found in the iron complexes holds in the case of ruthenium complexes, too.

Polarography of $Os(bipy)_3(ClO_4)_2$, $Os(4\text{-}dmbipy)_3(ClO_4)_2$ and $Os(5\text{-}dmbipy)_3(ClO_4)_2$

The first three waves in the cathodic polarograms

for $Os(bipy)_3(ClO_4)_2$, $Os(4\text{-}dmbipy)_3(ClO_4)_2$ and $Os(5\text{-}dmbipy)_3(ClO_4)_2$ are shown in Fig. 6. They behaved in almost the same way as the corresponding waves in polarograms for the iron and ruthenium complexes, although the osmium waves appeared at slightly less negative potentials than the iron and ruthenium waves. The nine waves in Fig. 6 were all reversible one-electron waves. Table 2 shows that their half-wave potentials follow the same sequence as in the iron and ruthenium complexes.

d. DISCUSSION

The reduction half-wave potential of free ligand molecules, $E^{red}_{1/2,L}$, and that of complex molecules, $E^{red}_{1/2,C}$, can be written as follows:

$$E^{red}_{1/2,L} = A_L - \Delta E_{s,L} + T\Delta S^{o}_{L}/nF - (RT/nF)\ln(f_r D_o^{1/2}/f_o D_r^{1/2})_L + \beta \quad (3)$$

$$E^{red}_{1/2,C} = A_C - \Delta E_{s,C} + T\Delta S^{o}_{C}/nF - (RT/nF)\ln(f_r D_o^{1/2}/f_o D_r^{1/2})_C + \beta \quad (4)$$

where A's are electron affinities of oxidants, ΔE_s's differences in solvation energy for couples of reductant and oxidant species, D's diffusion coefficients, f's activity coefficinets and ΔS^o's standard entropies of reaction; the subscripts C and L designate a metal

and a free ligand respectively, and o and r the oxidant and the reductant species, respectively; β is a constant appropriate to the reference electrode employed, n is the number of electrons transferred and F, R and T have usual significance.

If the reduction of a complex is the reduction of its coordinated ligand, a linear relationship may exist between the electron affinity of the complex, A_C, and that of the free ligand, A_L, for a series of complexes of the same metal ion. Furthermore, if it is assumed that every term in eqns. (3) and (4) except electron affinity terms is identical for a series of complexes of a metal ion with different ligand species, the following relation can be written:

$$E^{red}_{1/2,C} = E^{red}_{1/2,L} + c \qquad (5)$$

where c is a constant.

Figure 7 shows a plot of half-wave potentials of the first waves of iron complexes vs. those of free ligands and the same kinds of plots corresponding to the second waves and the third ones. Plots for ruthenium and osmium complexes are shown in Figs. 8 and 9 respectively. Straight lines were drawn so as to have a slope predicted by the theoretical equation (5). The nine plots show that the linear relationship between the half-wave potentials of a complex and its ligand as predicted by eqn. (5) holds

approximately. The same relationship, though less quantitative, can be drawn on the basis of the polarographic data in acetonitrile reported by Musumeci et.al.: the order of half-wave potentials for complexes of iron(II) perchlorate with 1,10-phenanthroline, 4,7-dimethyl-1,10-phenanthroline and 4,7-diphenyl-1,10-phenanthroline is in accordance with the order of half-wave potentials for the free ligands[14]. These facts may be evidence for the validity of the assumptions made in derivation of eqn. (5). Especially they may support the premise that in the one-electron reduction of complexes ML_3^{2+}, ML_3^{+} and ML_3 (M = Fe, Ru, Os; L = bipy, 4-dmbipy, 5-dmbipy) the added electron occupies a molecular orbital contributed mainly by a ligand π^*-orbital. Further support to the premise may be provided by the fact that the half-wave potentials for complexes with the same oxidation state and the same ligands vary no more than 80 mV regardless of kind of metal. The oxidation half-wave potential of $Ru(bipy)_3^{2+}$ was more positive by 0.42 V than that of $Os(bipy)_3^{2+}$. In these cases it is believed that an electron in a t_{2g}-orbital is removed[27]; thus the difference in half-wave potential may be caused by a difference in ionization potential of the central metal.

It may be reasonable to consider that the solvation energy of a terpyridine complex does not differ much

from that of a corresponding bipyridine complex, because the number of pyridine rings is equal in these complexes and their molecular dimentions are similar. It is evident that the same reasoning cannot be applied to solvation energies of free bipyridines and terpyridines. However, the assumption of equal solvation energy for the free ligands may be supported by the experimental fact that the half-wave potential difference between the first wave for free bipyridines and that for free terpyridines was almost identical with the difference between the first wave for $Fe(bipy)_3^{2+}$ and that for $Fe(terpy)_2^{2+}$ as well as difference between their second waves.

Table 2 shows that the half-wave potential difference between a couple of successive waves for every complex studied, including $Fe(terpy)_2^{2+}$, is rather small compared with the difference between two waves in which metal d-electrons are transferred[18,25]. This is quite reasonable if one imagines that the electron transferred in the former case occupies a ligand orbital. To a first approximation, the lowest π^*-orbital in the bipyridine complexes and the terpyridine complexe is triply or doubly degenerate and localized in a bipyridine or a terpyridine molecule respectively. In the first three reduction waves for bipyridine complexes and the first two waves for the terpyridine complex, each added electron may occupy one of the vacant localized π^*-orbitals. Electronic repulsion

between the added electron and others can thus be much smaller than that between electrons in partially filled t_{2g}-orbitals. A support to this reasoning is the experimental fact that the third wave nearly neighbouring to the second wave was not found in a polarogram for terpyridine complex in contrast with the bipyridine complexes. We do not agree with Musumeci et al.[15,16] who gave the following interpretation to the same experimental finding: the lowering in symmetry from O_h causes the splitting of the twofold degenerate e_g-orbitals in terpyridine complexes of iron into two nondegenerate orbitals and the high-lying e_g-orbital can account for non-existence of $Fe(terpy)_2^-$.

Thus it is concluded that in the first three reduction steps for the bipyridine complexes of Iron(II), ruthenium(II) and osmium(II) as well as the first two reduction steps for the terpyridine complex of iron(II), each added electron occupies a ligand π^*-orbital. A part of this conclution is supported by spectroscopic investigations[9,10] on the complexes $Fe(bipy)_3$ and $Fe(bipy)_3^-$.

e. REFERENCES

1 W. R. McWhinnie and J. D. Miller in H. J. Emeleus and A. G. Sharpe (Eds.), Advances in Inorganic Chemistry and Radiochemistry, Vol. XII, Academic Press, New York, 1969, p.134.

2 S. Herzog and R. Taube, Z. Chem., 2, 208 (1962)

3 B. Elschner and S. Herzog, Arch. Sci. Geneva, 11, 160 (1958).

4 E. König and H. Fischer, Z. Naturforsch., 17a, 1063 (1962).

5 J. Dos Santos Veiga, W. L. Reynolds and J. R. Bolton, J. Chem. Phys., 44, 2214 (1966).

6 I. M. Brown and S. I. Weissman, J. Amer. Chem. Soc., 85, 2528 (1963).

7 I. M. Brown, S. I. Weissman and L. C. Snyder, J. Chem. Phys., 42, 1105 (1965).

8 E. König, Z. Naturforsch., 19a, 1139 (1964).

9 F. S. Hall and W. L. Reynolds, Inorg. Chem., 5, 931 (1966).

10 C. Mahon and W. L. Reynolds, ibid, 6,1927 (1967).

11 Y. Kaizu, T. Yazaki, Y. Torii and H. Kobayashi, Bull. Chem. Soc. Japan, 43, 2068 (1970).

12 N. Tanaka and Y. Sato, Electrochim. Acta, 13,335 (1968).

13 N. Tanaka, Y. Ogata and S. Niizuma, Bull. Chem. Soc. Japan, 46, 3299 (1973).

14 S. Musumeci, E. Rizzarelli, I. Fragala, S. Sammartano and R. P. Bonomo, Inorg. Chim. Acta, 7, 660 (1973).

15 S. Musumeci, E. Rizzarelli, S. Sammartano and R. P. Bonomo, J. Inorg. Nucl. Chem., 36, 853 (1974).

16 S. Musumeci, E. Rizzarelli, S. Sammartano and R. P. Bonomo, J. Electroanal. Chem., 46, 109 (1973).

17 N. E. Tokel and A. J. Bard, J. Amer. Chem. Soc., 94, 2862 (1972).

18 Y. Sato and N. Tanaka, Bull. Chem. Soc. Japan, 42, 1021 (1969).

19 W. H. F. Sasse and C. P. Whittle, J. Chem. Soc., (1961) 1347.

20 F. H. Burstall and R. S. Nyholm, ibid, (1952) 3570.

21 H. Irring, ibid, (1959) 2977.

22 F. W. Cagle and C. F. Smith, J. Amer. Chem. Soc., 69, 1860 (1947).

23 F. H. Burstall, J. Chem. Soc., (1936) 173.

24 F. H. Burstall, F. P. Dwyer and E. C. Gyarfas, ibid, (1950) 953.

25 D. W. DuBois, R. T. Iwamoto and J. Kleinberg, Inorg. Nucl. Chem. Lett., 6, 53 (1970).

26 I. Shimizu, K. Sato, J. Oura and G. P. Sato, The 18th Symposium on Polarography and Electroanalytical

Chemistry, Tokyo, Oct.,1972, The Polarographic Society of Japan, Kyoto, 1972, p. 51.

27 Table 6 in Ref. 1.

Table 1. Polarographic data for reduction of free ligands in DMF solutions containing 0.1 M TBAP

Compound	1st wave			2nd wave
	a	b	c	a
bipy	-2.10	60	65	-2.66
4-dmbipy	-2.15	58	65	-2.63
5-dmbipy	-2.23	60	70	—
terpy	-2.00	58	70	-2.4

a: Half-wave potential in V. vs. SCE.

b: Slope of log-plot of polarogram in mV.

c: Peak separation of cyclic voltammogram in mV.

Table 2. Polarographic data for reduction of iron(II), ruthenium(II) and osmium(II) complexes in DMF solutions containing 0.1 M TBAP

Complex	1st wave			2nd wave			3rd wave			4th wave
	a	b	c	a	b	c	a	b	c	a
$Fe(bipy)_3^{2+}$	-1.26	66	60	-1.44	58	60	-1.70	64	65	-2.43
$Fe(4\text{-dmbipy})_3^{2+}$	-1.34	62	70	-1.53	59	65	-1.81	61	70	-2.53
$Fe(5\text{-dmbipy})_3^{2+}$	-1.39	60	75	-1.58	58	65	-1.85	62	70	-2.5
$Ru(bipy)_3^{2+}$	-1.25	64	65	-1.43	60	70	-1.68	62	65	-2.30
$Ru(4\text{-dmbipy})_3^{2+}$	-1.34	64	60	-1.53	63	60	-1.78	63	65	-2.37
$Ru(5\text{-dmbipy})_3^{2+}$	-1.39	63	60	-1.57	60	60	-1.85	58	65	-2.51
$Os(bipy)_3^{2+}$	-1.19	64	60	-1.37	61	60	-1.69	59	65	-2.37
$Os(4\text{-dmbipy})_3^{2+}$	-1.28	66	60	-1.47	64	60	-1.79	66	70	-2.40
$Os(5\text{-dmbipy})_3^{2+}$	-1.32	61	70	-1.50	60	65	-1.86	60	70	-2.55
$Fe(terpy)_2^{2+}$	-1.17	61	60	-1.34	58	65	—	—	—	—

a: Half-wave potential in V vs. SCE

b: Slope of log-plot of polarogram in mV

c: Peak separation of cyclic voltammogram in mV

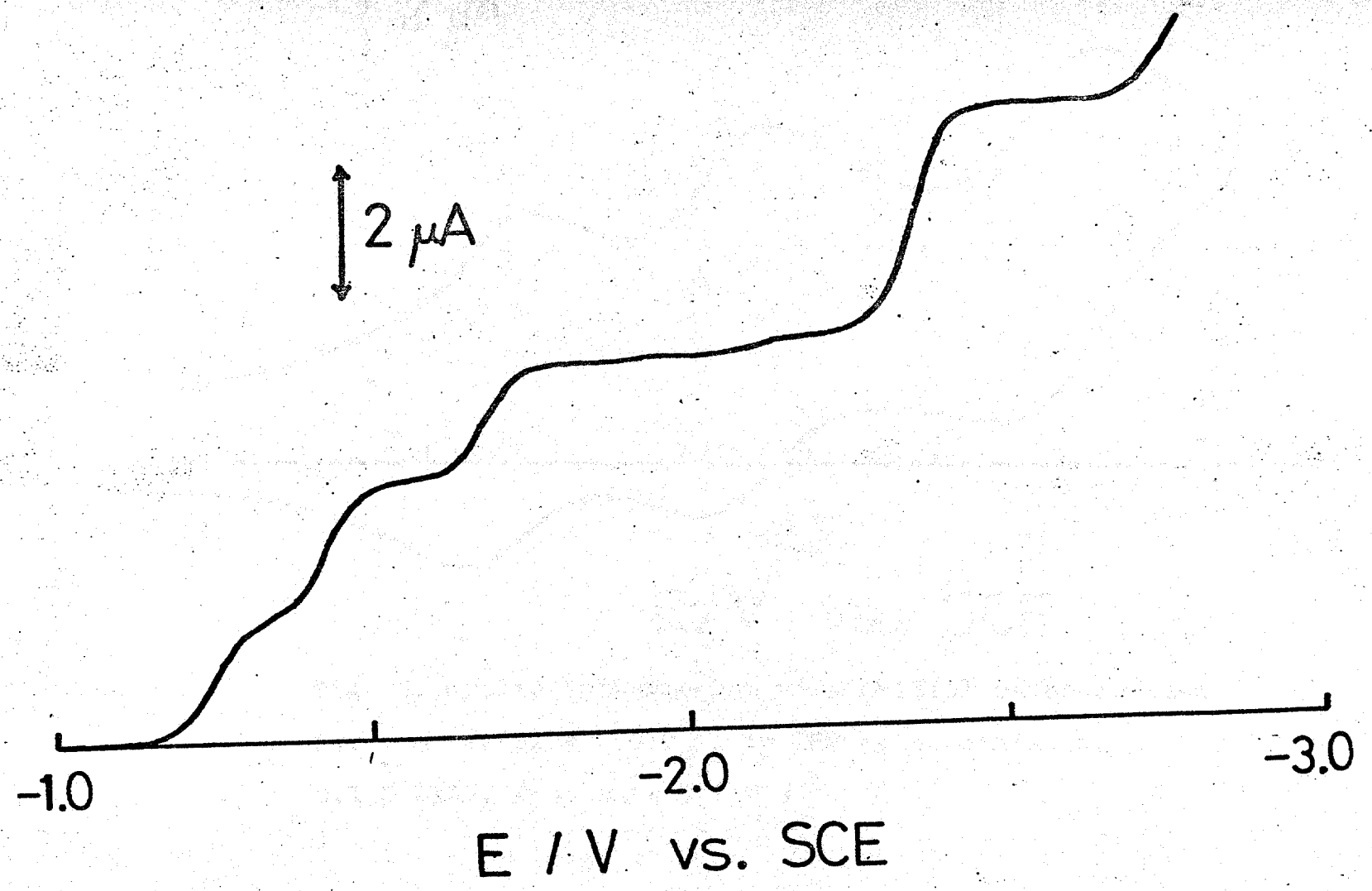

Fig. 1. Cathodic polarogram for 1 mM $Fe(bipy)_3(ClO_4)_2$ in DMF soln. containing 0.1 M TBAP.

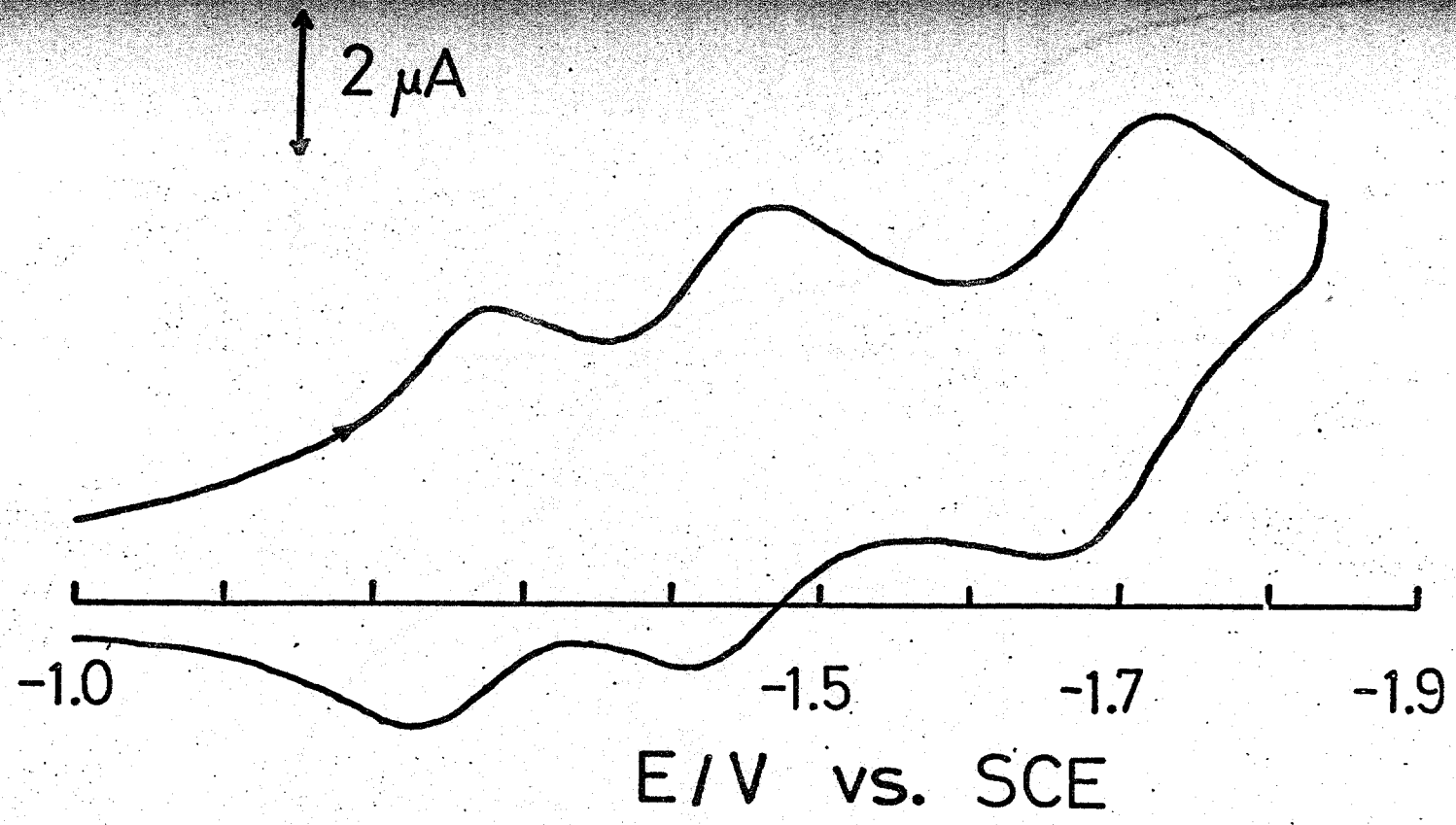

Fig. 2. Cyclic voltammogram with initial cathodic scan for 1 mM $Fe(bipy)_3(ClO_4)_2$ in DMF soln. containing 0.1 M TBAP. Scan rate 0.1 V s^{-1}.

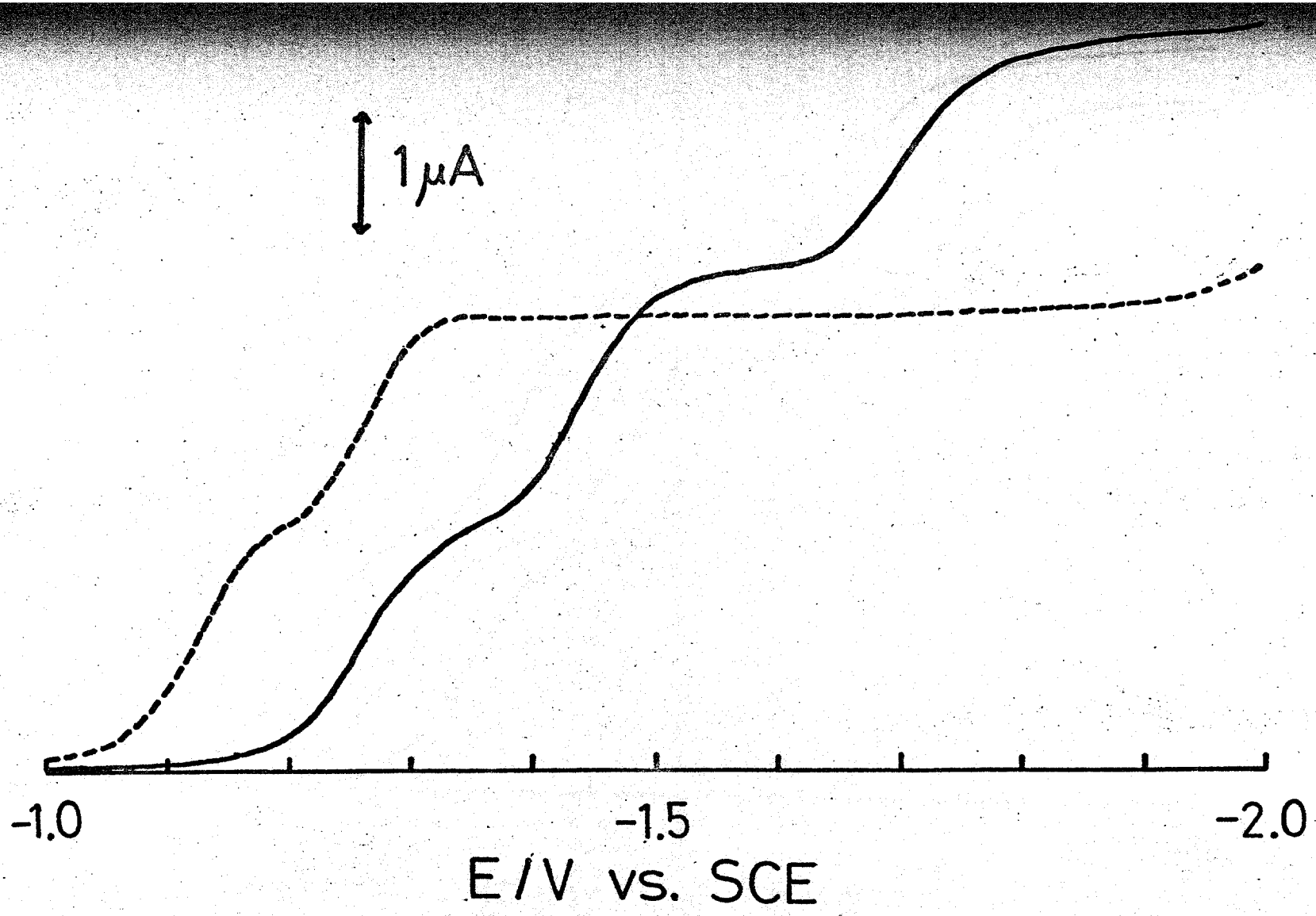

Fig. 3. Cathodic polarograms for 1 mM iron(II) complexes in DMF soln. containing 0.1 M TBAP. (——) $Fe(bipy)_3(ClO_4)_2$; (----) $Fe(terpy)_2(ClO_4)_2$.

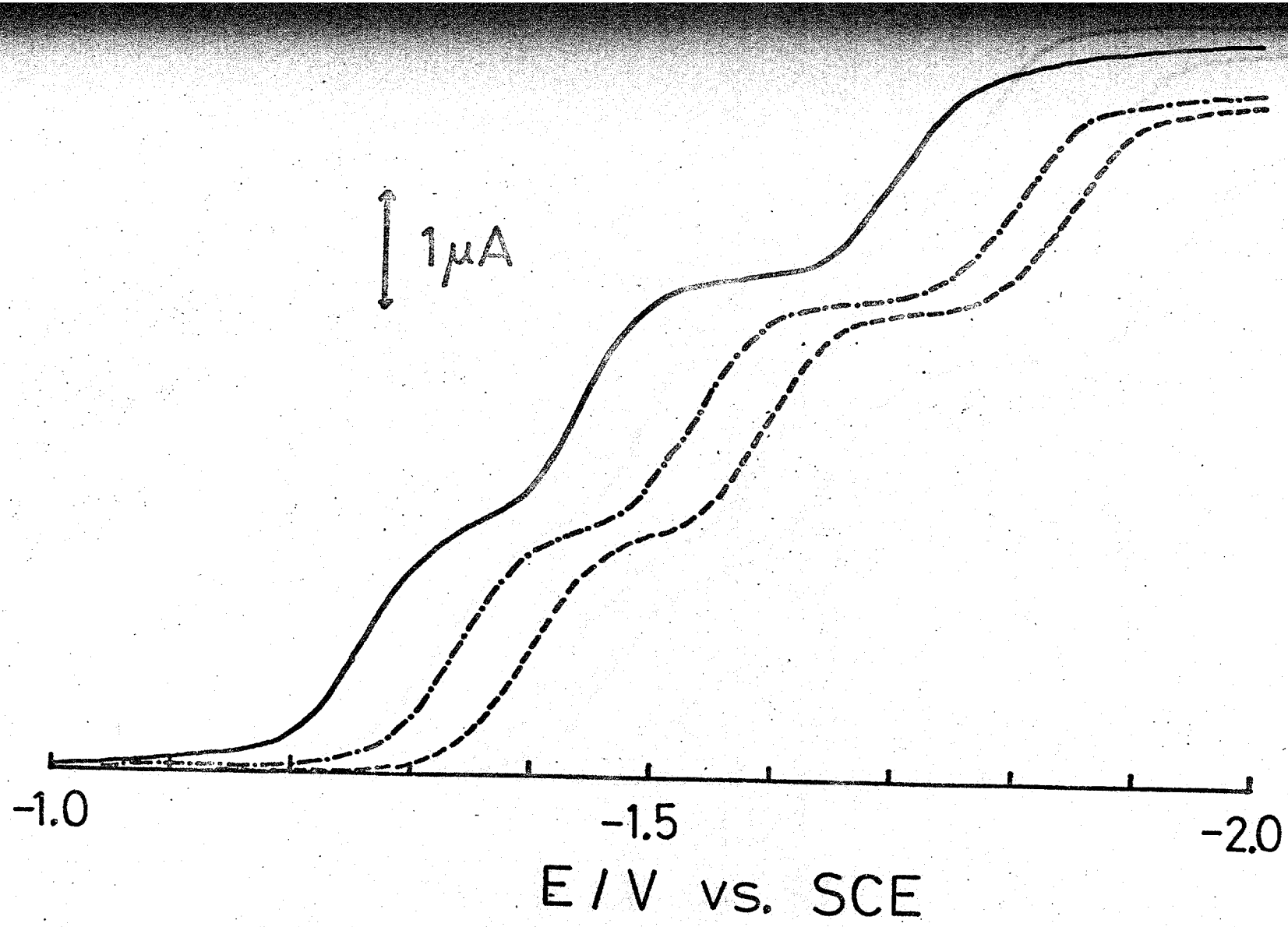

Fig. 4. Cathodic polarograms for 1 mM $FeL_3(ClO_4)_2$ in DMF soln. containing 0.1 M TBAP. L = (——) bipy, (-·-·-) 4-dmbipy, (----) 5-dmbipy.

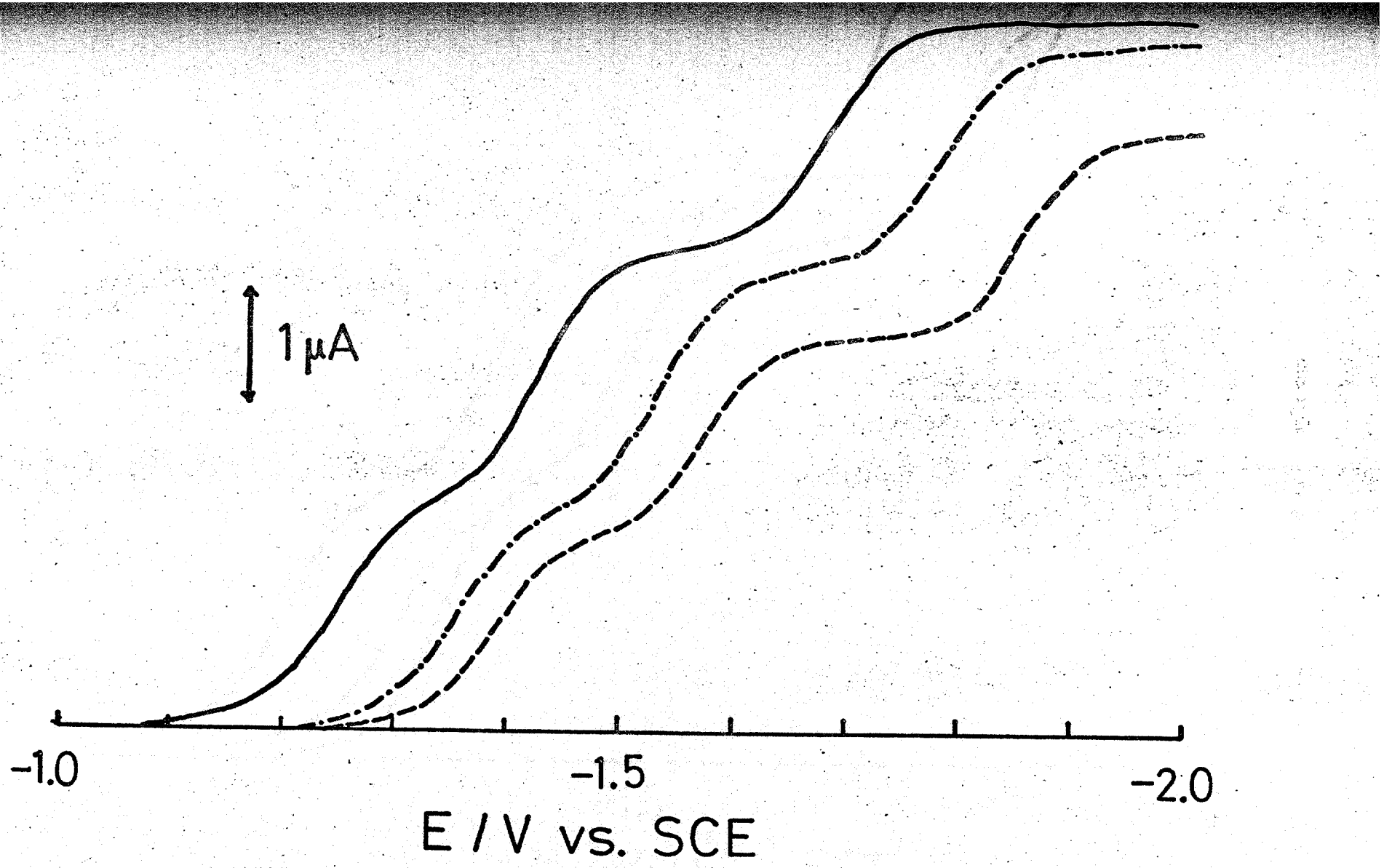

Fig. 5. Cathodic polarograms for 1 mM $RuL_3(ClO_4)_2$ in DMF soln. containing 0.1 M TBAP. L = (——)bipy, (-·-·-) 4-dmbipy, (----) 5-dmbipy

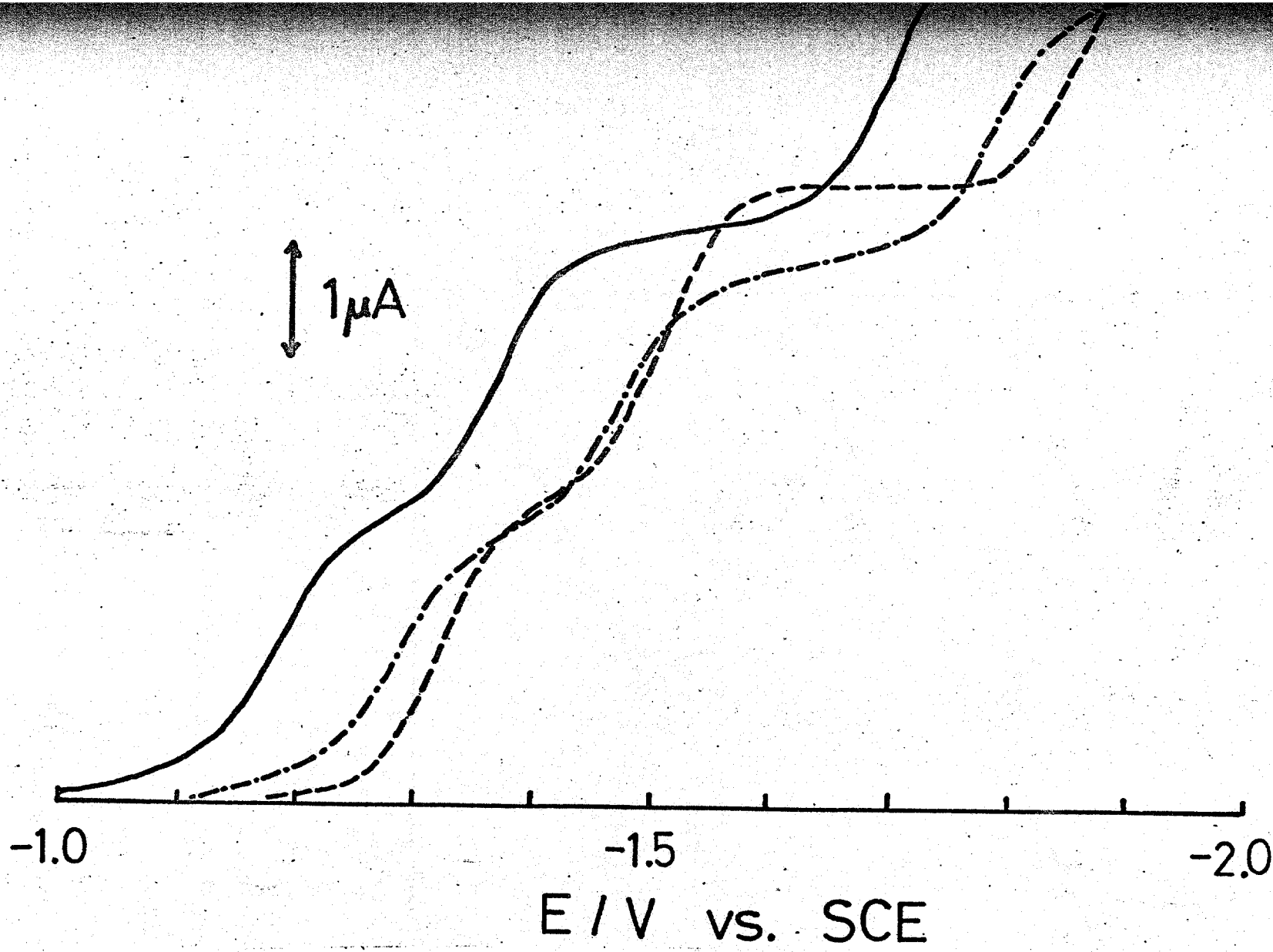

Fig. 6. Cathodic polarograms for 1 mM $OsL_3(ClO_4)_2$ in DMF soln. containing 0.1 M TBAP. L = (——) bipy,

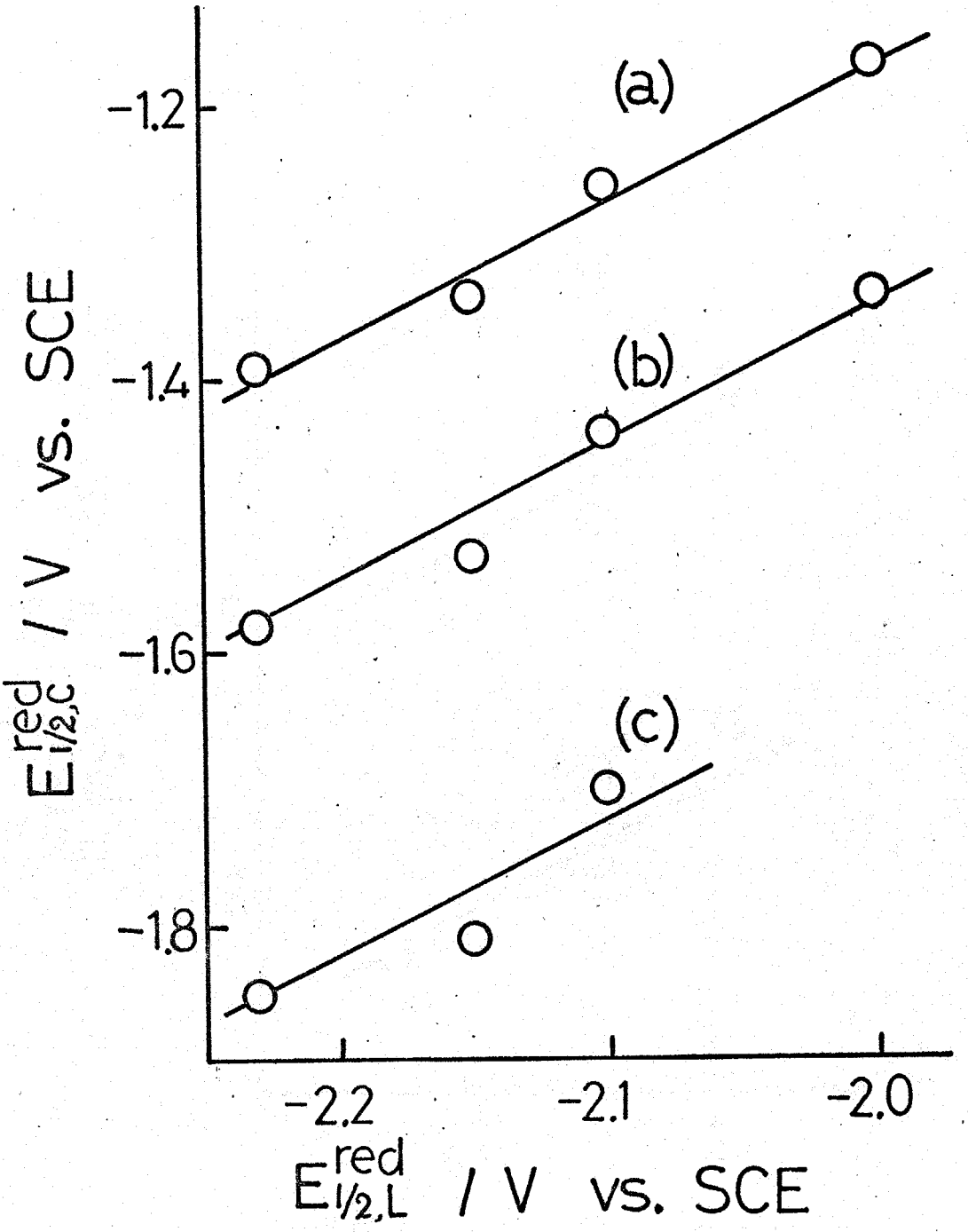

Fig. 7. Plot of half-wave potentials for (a) FeL_3^{2+}/FeL_3^{+}, (b) FeL_3^{+}/FeL_3 and (c) FeL_3/FeL_3^{-} systems, $E^{red}_{1/2,C}$, vs. those f L/L^{-} systems, E^{red}_{L}. L = bipy, 4-dmbipy, 5-dmbipy. Experimental points for $Fe(terpy)_2^{2+}/Fe(terpy)_2^{+}$ and $Fe(terpy)_2^{+}/Fe(terpy)_2$ systems are also included.

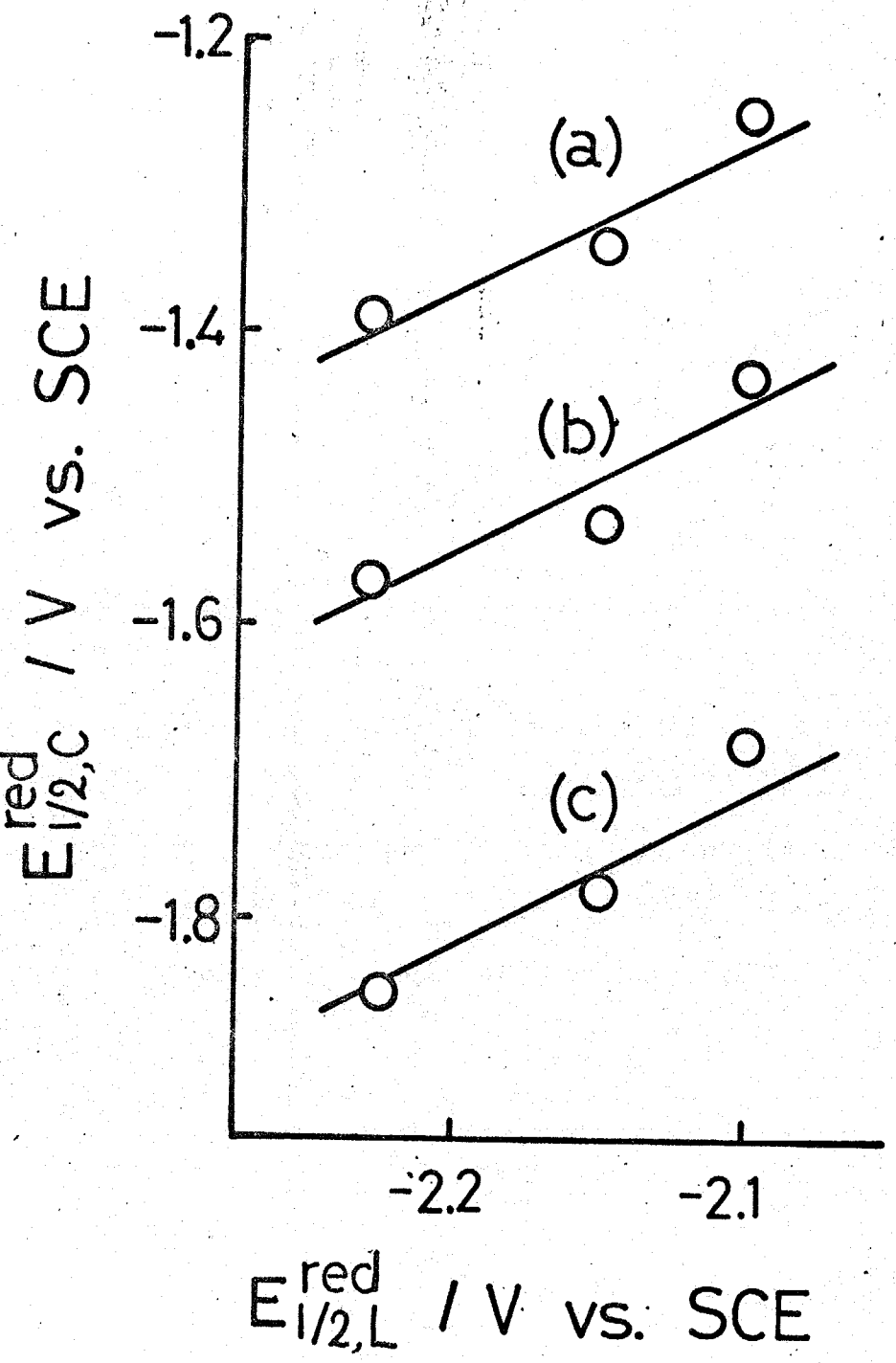

Fig. 8. Plot of half-wave potentials for (a) RuL_3^{2+}/RuL_3^{+}, (b) RuL_3^{+}/RuL_3 and (c) RuL_3/RuL_3^{-} systems, $E^{red}_{1/2,C}$, vs. those for L/L^{-} systems, E^{red}_{L}. L = bipy, 4-dmbipy, 5-dmbipy.

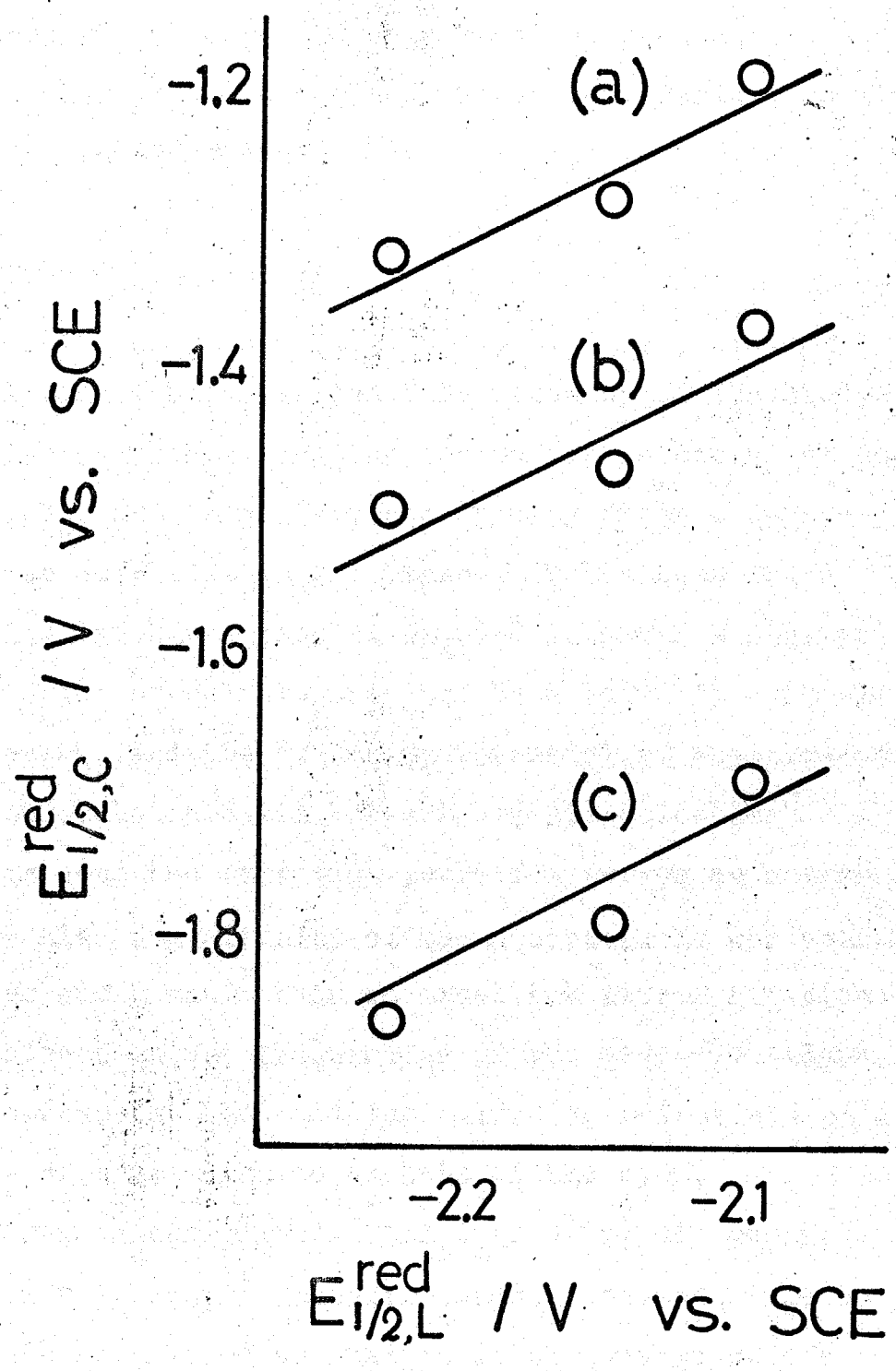

Fig. 9. Plot of half-wave potentials for (a) OsL_3^{2+}/OsL_3^{+}, (b) OsL_3^{+}/OsL_3 and (c) OsL_3/OsL_3^{-} systems, E^{red}_{C}, vs. those for L/L^{-} systems, $E^{red}_{1/2,L}$. L = bipy, 4-dmbipy, 5-dmbipy.

B. Correlation between Charge-transfer Frequencies and Oxidation Potentials of Iron, Ruthenium, Osmium, Cobalt and Chromium Complexes

a. INTRODUCTION

A correlation between the frequency of the charge-transfer band, ν_{CT}, and the ionization potential of the donor, I_D, has been discussed on many organic donor-acceptor complexes in gas phase[1]. It has been found empirically that a plot of ν_{CT} vs. I_D gives a straight line. A linear relationship has been found to hold also between ν_{CT} and the reduction potential of the acceptor of a molecular complex between organic molecules[2]. In this case the reduction potential serves as a measure of the electron affinity of the acceptor. It has been found by Shriver and Posnor[3] that an excellent linear relationship exists between the frequencies of the metal-to-ligand charge-transfer band and the oxidation potentials of a series of metal-cyanide adducts of the type, $Fe(1,10\text{-phenanthroline})_2(CNBX_3)_2$(X = Br, Cl, methyl). The shift in charge-transfer bands of these complexes has been attributed to changes in the energy of the highest occupied metal orbitals in the ground state of the complex, on addition of a Lewis acid.

The intense red-coloured diamagnetic complexes of tris(2,2'-bipyridine)iron(II) and tris(1,10-phenanthroline)iron(II) have been widely studied spectroscopically as well as electrochemically[4]. The adsorption bands near 20,000 cm^{-1} have been assigned to metal-to-ligand charge-transfer transitions on the basis of the substituent effect[5,6]. The visible and near-infrared absorption bands of tris(2,2'-bipyridine) complexes of vanadium(II), chromium(II) and cobalt(I) have on the same basis been assigned to this kind of transition[7,8]. However, no simple correlation between their electrochemical energies and spectroscopic ones have been observed. In Section A of this chapter[9], we predicted a linear relationship between the reduction half-wave potential of a transition metal complex and that of its free ligand, assuming that the electron added to the complex in the course of electrochemical reduction occupies a molecular orbital mainly composed of a ligand π^*-orbital. The following complexes were found to obey the predicted relation: ML_3^{2+}, ML_3^{+} and ML_3. Here M is iron, ruthenium or osmium and L is bipy, 4-dmbipy or 5-dmbipy. Present investigation deals with the correlation between the oxidation potentials and the charge-transfer frequencies of tris(2,2'-bipyridine) complexes of iron, ruthenium, osmium, cobalt and chromium,

in which the change in the electron affinity of ligand molecules on coordination is taken into consideration.

b. EXPERIMENTAL

Acetonitrile (AN) was dried over calcium hydride, distilled and then stored under a nitrogen atmosphere. Tris(2,2'-bipyridine)cobalt(II) perchlorate and tris-(2,2'-bipyridine)chromium(III) perchlorate were prepared by the methods of Burstall and Nyholm[10]. 4,4'- and 5,5'-dimethyl derivatives of these complexes were prepared respectively according to the procedures similar to those for the unsubstituted complexes. Other chemicals, including complexes, solvent and supporting electrolyte, were described in the section A of this chapter[9], as well as all operations in preparing solutions and measuring polarograms and cyclic voltammograms. A supporting electrolyte was 0.1 M TBAP for DMF and AN solutions and 0.1 M potasium chloride for aqueous solutions. Electronic absorption spectra were recorded on a Shimazu UV-200 spectrophotometer.

c. RESULTS

Polarography of 2,2'-bipyridine and 4,4'- and 5,5'-dimethyl derivatives

The reduction half-wave potentials for bipy, 4-dmbipy and 5-dmbipy obtained in AN solutions are listed in Table 3 together with the previous data obtained in DMF. The half-wave potentials in each solvent become more negative in the order bipy < 4-dmbipy < 5-dmbipy.

Cyclic voltammetry of iron complexes

Figure 10 shows cyclic voltammograms for $Fe(bipy)_3(ClO_4)_2$ and its methyl derivatives obtained in AN with initial anodic scan. Cyclic voltammograms in DMF and aqueous solutions were also obtained. They were similar to those in Fig. 10. The conventional reversibility criteria of peak-current ratio and peak separation show that these waves are all reversible one-electron waves. Their polarographic half-wave potentials obtained from peak potentials of cyclic voltammograms are listed in Table 4. It is seen that the oxidation half-wave potentials of bivalent iron complexes become more negative in the order of ligand, bipy < 5-dmbipy < 4-dmbipy, in all solvents studied. The same relation can be found between the previous data on the half-wave potentials of the redox systems $Fe(bipy)_3^{3+}/Fe(bipy)_3^{2+}$ and $Fe(4\text{-}dmbipy)_3^{3+}/Fe(4\text{-}dmbipy)_3^{2+}$ obtained in aqueous solutions[11,12].

Cyclic voltammetry of ruthenium complexes and osmium complexes

Table 4 involves the anodic half-wave potentials for $RuL_3(ClO_4)_2$ obtained in AN and those for $OsL_3(ClO_4)_2$ in DMF and AN. Throughout this section L designates any one of the following ligands: bipy, 4-dmbipy and 5-dmbipy. The half-wave potentials were evaluated from cyclic voltammograms with initial anodic scan. The anodic waves for $RuL_3(ClO_4)_2$ in DMF and aqueous solutions could not be observed. They might be masked by the ultimate current rise, because the half-wave potentials for ruthenium complexes in these solvents were possibly more positive by about 0.2 V than those for the corresponding iron complexes as seen in the data obtained in AN. The half-wave potentials for osmium complexes, on the other hand, were more negative by about 0.2 V than those for iron complexes. Such a difference in half-wave potential among complexes with the same kind of ligand molecules and the different kind of central metals has been reported previously on the unsubstituted trisbipyridine complexes of iron, ruthenium and osmium[13]. Table 4 shows that the same substitution effect on the half-wave potential that was found in the iron complexes holds for the redox systems of RuL_3^{3+}/RuL_3^{2+} and OsL_3^{3+}/OsL_3^{2+}.

Polarography and cyclic voltammetry of cobalt complexes

A cathodic polarogram for $Co(bipy)_3(ClO_4)_2$ in DMF exhibited two reduction waves with half-wave potentials of -0.88 and -1.46 V. The limiting current of the wave at -1.46 V was nearly twice as high as that of the other wave. Figure 11 shows two cyclic voltammograms for this complex in DMF; one with initial cathodic scan and the other with anodic scan. Similar polarograms and cyclic voltammograms were also observed for the substituted complexes in DMF as well as the substituted and unsubstituted complexes in AN. The polarogram for the unsubstituted complex in AN was in quantitative agreement with the one obtained by Tanaka and Sato[14]. On the basis of the criteria described above the first reduction step and the first oxidation step for every cobalt(II) complex studied were reversible one-electron steps in DMF and AN. Table 3 shows that the half-wave potentials for the redox systems CoL_3^{3+}/CoL_3^{2+} and CoL_3^{2+}/CoL^{+} in both solvents follow the same sequence as in the iron, ruthenium and osmium complexes.

Polarography and cyclic voltammetry of chromium complexes

The cathodic polarogram for $Cr(bipy)_3(ClO_4)_2$ in AN exhibited six waves; the fifth and the sixth waves were not well-defined. Figure 12 shows the first four waves

for this complex and its methyl derivatives. The corresponding cyclic voltammograms were also obtained. They were quite similar. On the basis of the reversibility criteria the four steps were concluded to be reversible one-electron steps. They may be assigned[15] to the redox systems CrL_3^{3+}/CrL_3^{2+}, CrL_3^{2+}/CrL_3^{+}, CrL_3^{+}/CrL_3 and CrL_3/CrL_3^{-}. The waves corresponding to the first four waves in AN were also found in a polarogram taken in DMF, although they were accompanied by several small waves which were not found in polarograms obtained in AN. Poor stability of bivalent chromium complexes in DMF may account for the additional waves. Each polarogram for $CrL_3(ClO_4)_2$ taken in an aqueous solution exhibited only one reversible wave followed by several irreversible waves possibly complicated by chemical reactions[16]. The former was attributed to a redox system of the type CrL_3^{3+}/CrL_3^{2+}. The reversible half-wave potentials obtained are listed in Table 4. The same correlation between half-wave potentials and kind of ligand that was found for the redox systems, FeL_3^{3+}/FeL_3^{2+}, RuL_3^{3+}/RuL_3^{2+}, OsL_3^{3+}/OsL_3^{2+}, CoL_3^{3+}/CoL_3^{2+} and CoL_3^{2+}/CoL_3^{+}, holds for the systems CrL_3^{3+}/CrL_3^{2+} and CrL_3^{2+}/CrL_3^{+} but does not for CrL_3^{+}/CrL_3 or CrL_3/CrL_3^{-}. In the latter two systems the half-wave potential become more negative in the following sequence of ligands: bipy < 4-dmbipy < 5-dmbipy.

Electronic absorption spectra of $RuL_3(ClO_4)_2$ and $OsL_3(ClO_4)_2$

The methyl substitution effect on the charge-transfer bands of FeL_3^{2+}, CoL_3^{+} and CrL_3^{2+} has been reported[5,7,8]. The absorption wave numbers for a series of complexes with the same central metal have been found to be shifted to some larger values in the following order of ligands: 4-dmbipy < bipy < 5-dmbipy. The absorption bands for the $Ru(bipy)_3^{2+}$ and $Os(bipy)_3^{2+}$ complexes in the vicinity of 19,000 cm^{-1} have been assigned to charge-transfer transitions[17,18]. The absorption spectra of RuL_3^{2+} and OsL_3^{2+}, including $Ru(bipy)_3^{2+}$ and $Os(bipy)_3^{2+}$, were measured in aqueous solutions. The charge-transfer frequencies for dimethyl derivatives were determined in analogy with the unsubstituted complexes. Data obtained in this experiment are listed in Table 4 together with the literature values for FeL_3^{2+}, CoL_3^{+} and CrL_3^{2+}. They are blue-shifted according to the order of ligand as 4-dmbipy <bipy < 5-dmbipy; the sequence was the same as in the FeL_3^{2+}, CoL_3^{+} and CrL_3^{2+} complexes. The charge-transfer bands for CoL_3^{2+}, CrL_3^{+}, CrL and CrL_3^{-} except $Cr(bipy)_3^{+}$ and $Cr(bipy)_3$ have never been reported[19,20]. They are not discussed in this thesis .

d. DISCUSSION

A plot of the reduction half-wave potentials for FeL_3^{3+} vs those for free ligands did not yield a straight line. According to our previous findings such a plot should be a straight line, if an electron added to the oxidant species occupies a molecular orbital of the reductant species mainly of ligand π^*-orbital character[9]. The trend of the plot for any of the redox systems, RuL_3^{3+}/RuL_3^{2+}, OsL_3^{3+}/OsL_3^{2+}, CoL_3^{3+}/CoL_3^{2+}, CoL_3^{2+}/CoL_3^{+}, CrL_3^{3+}/CrL_3^{2+} and CrL_3^{2+}/CrL_3^{+}, were similar to that for the FeL_3^{3+}/FeL_3^{2+} system. The plots for the CrL_3^{+}/CrL_3 and CrL_3/CrL_3^{-} systems, on the other hand, satisfied the linear relationship as shown in Fig. 13. Straight lines were drawn so as to have a slope predicted by the theoretical equation (5) in section A of this chapter.

The lowest charge-transfer transition energy, ν_{CT}, is given by

$$h\nu_{CT} = I_C - A_L^C \qquad (6)$$

where I_C is the vertical ionization potential of a t_{2g}-orbital in metal complexes and A_L^C the vertical electron affinity of the lowest antibonding π^*-orbital in coordinated ligands. When it is assumed that a t_{2g}-electron is removed in electrochemical oxidation of a metal complex, the oxidation half-wave potential, $E_{1/2,C}^{ox}$,

can be expressed as follows:

$$E^{ox}_{1/2,C} = I_C - \Delta E_{s,C} + T\Delta S^{o}_{C}/nF - (RT/nF)\ln(f_r D_o^{1/2}/f_o D_r^{1/2})_C + \beta \qquad (7)$$

and the reduction half-wave potential of free ligands, $E^{red}_{1/2,L}$:

$$E^{red}_{1/2,L} = A_L - \Delta E_{s,L} + T\Delta S^{o}_{L}/nF - (RT/nF)\ln(f_r D_o^{1/2}/f_o D_r^{1/2})_L + \beta \qquad (8)$$

The explanations of notations are given in Section A of this chapter. If it is assumed that a linear relationship exists between the electron affinities of the coordinated ligand and the free ligand for a series of complexes of the same metal ion with different ligand species and, moreover, if it is assumed that other terms in eqns. (7) and (8) are practically invariant, the following relation can be obtained:

$$E^{ox}_{1/2,C} - E^{red}_{1/2,L} = h\nu_{CT} + c \qquad (9)$$

where c is a constant.

Table 3 shows that no simple correlation exists between $E^{ox}_{1/2,C}$ and $h\nu_{CT}$ of the following complexes: FeL_3^{2+}, RuL_3^{2+}, OsL_3^{2+}, CrL_3^{2+} and CoL_3^{+}. This is also true for tris(1,10-phenanthroline)iron(II) and its methyl derivatives, as is evident from the inspection of the potentiometric and spectroscopic data reported by Brandt and Smith[21]. However, when the half-wave potential difference $E^{ox}_{1/2,C} - E^{red}_{1/2,L}$, in the place of $E^{ox}_{1/2,C}$, is plotted against $h\nu_{CT}$, a nearly linear relation was

revealed for each of these complexes. Some typical plots are shown in Figs. 14 and 15. Each straight line was drawn in accordance with eqn. (9) with an arbitrary choice of the c value. This finding suggests that the simple energetics leading to eqn. (9) was successful. The agreement between theory and experiment on nine plots for five families of complexes is encouraging, although each plot consists of only three experimental points. The following discussion is based on the premise that the coincidence is not fortuitous.

Because of the lack of data on $h\nu_{CT}$ for the CoL_3^{2+}, CrL_3^{+}, CrL_3 and CrL_3^{-} complexes, the correlation between $E^{ox}_{1/2,C} - E^{red}_{1/2,L}$ and $h\nu_{CT}$ for these complexes could not be discussed. However, the former two fall into the same class as the above five complexes with respect to the dependence of the half-wave potential difference on the kind of ligand: the $E^{ox}_{1/2,C} - E^{red}_{1/2,L}$ values become more positive in the following order of ligand, 4-dmbipy < bipy < 5-dmbipy. On the other hand, the latter two complexes have another dependence, 4-dmbipy < 5-dmbipy < bipy.

In conclution, the methyl substitution effect on the half-wave potential discussed in this section and the previous section provides a new criterion applicable to assignment of the molecular orbital occupied by the electron added to the oxidant species in the course of reduction. Fortunately, the magnetic moments of most

unsubstituted bipyridine complexes discussed in this section are known[10,22,23]. The electronic configurations of these complexes can thus be presumed. In the following presentation the electronic configurations and spin numbers of all complexes with methyl-substituted bipyridines as well as those of ruthenium and osmium complexes are written by analogy: $FeL_3^{3+}(t_{2g}^5, s = 1/2)$, $FeL_3^{2+}(t_{2g}^6, s = 0)$, $RuL_3^{3+}(t_{2g}^5, s = 1/2)$, $RuL_3^{2+}(t_{2g}^6, s = 0)$, $OsL_3^{3+}(t_{2g}^5, s = 1/2)$, $OsL_3^{2+}(t_{2g}^6, s = 0)$, $CoL_3^{3+}(t_{2g}^6, s = 0)$, $CoL_3^{2+}(t_{2g}^5 e_g^2, s = 3/2)$, $CoL_3^{+}(t_{2g}^6 e_g^2, s = 1)$, $CrL_3^{3+}(t_{2g}^3, s = 3/2)$, $CrL_3^{2+}(t_{2g}^4, s = 1)$, $CrL_3^{+}(t_{2g}^5, s = 1/2)$, $CrL_3(t_{2g}^6, s = 0)$ and $CrL_3^{-}(t_{2g}^6 e_g$ or $t_{2g}^6 \pi^*, s = 1/2)$. The redox systems composed of a pair of these complexes differing by one in the number of electrons can be divided into three groups according to their electronic configurations. The excess electron in the reductant species of a redox system of Group 1 occupies a t_{2g}-orbital and that of a system belonging to Group 2 a metal e_g- or a ligand π^*-orbital. In a redox system of Group 3, one of the redox species is in a high spin state and the other in a low spin state. The redox systems belonging to Group 1 are as follows: FeL_3^{3+}/FeL_3^{2+}, RuL_3^{3+}/RuL_3^{2+}, OsL_3^{3+}/OsL_3^{2+},

CoL_3^{2+}/CoL_3^{+}, CrL_3^{3+}/CrL_3^{2+}, CrL_3^{2+}/CrL_3^{+} and CrL_3^{+}/CrL_3. It is seen that the half-wave potentials for all but one of these complexes obey eqn. (9) or at least depend on the kind of ligand in such a way as they become more negative in the order bipy < 5-dmbipy < 4-dmbipy. The only exception is CrL_3^{+}/CrL_3. The complexes of this type belong to Group 2 from the viewpoint of substitution effect. Considering that they are in low oxidation states, this contradiction may be due to the strong π-bondings between t_{2g}-orbitals of a central metal atom and ligand π^*-orbitals caused by the decrease in the charge of the central metal atom[20,24]. Among the redox systems discussed in this section only the CrL_3/CrL_3^{-} system belongs to Group 2. On the basis of the methyl substitution effect shown in Fig. 13(b), it falls into the same category with the following redox systems whose reductant species has been concluded in the previous section to have an excess electron in its π^*-orbital: FeL_3^{2+}/FeL_3^{+}, FeL_3^{+}/FeL_3, FeL_3/FeL_3^{-}, RuL_3^{2+}/RuL_3^{+}, RuL_3^{+}/RuL_3, RuL_3/RuL_3^{-}, OsL_3^{2+}/OsL_3^{+}, OsL_3^{+}/OsL_3 and OsL_3/OsL_3^{-}. The CoL_3^{3+}/CoL_3^{2+} system belongs to Group 3. It is not certain whether there can be any meaning in the fact that this redox system is classified into Group 1 on the basis of the methyl substitution effect.

e. REFERENCES

1 R. S. Mulliken and W. B. Person, Ann. Rev. Phys. Chem., 13, 107 (1962). W. B. Person, J. Chem. Phys., 38, 109 (1963).

2 M. E. Peover, Electrochim. Acta, 13, 1083 (1968).

3 D. F. Shriver and J. Posner, J. Amer. Chem. Soc., 88, 1672 (1966).

4 W. R. McWhinnie and J. D. Miller in H. J. Emeleus and A. G. Sharpe (Eds.), Advances in Inorganic Chemistry and Radiochemistry, Vol. 12, Academic Press, New York, 1969, p. 134.

5 F. W. Cagle and G. F. Smith, J. Amer. Chem. Soc.,69, 1860 (1947).

6 R. J. P. Williams, J. Chem. Soc., 1955, 137.

7 I. Fujita, T. Yazaki, Y. Torii and H. Kobayashi, Bull. Chem. Soc. Japan, 45, 2156 (1972).

8 Y. Kaizu, Y. Torii and H. Kobayashi, ibid, 43, 3296 (1970).

9 T. Saji and S. Aoyagui, J. Electroanal. Chem., in press. JEC 3407.

10 F. H. Burstall and R. S. Nyholm, J. Chem. Soc., 1952, 3570.

11 P. Geoge, G. I. H. Hanania and D. H. Irvine, ibid, 1959, 2548.

12 D. H. Irvine, J. Chem. Soc., 1959, 2977.

13 Table VI in Ref. 4.

14 N. Tanaka and Y. Sato, Bull. Chem. Soc. Japan, 41, 2059 (1968).

15 Y. Sato and N. Tanaka, ibid, 42, 1021 (1969).

16 B. R. Baker and B. Dev Mehta, Inorg. Chem., 4, 848 (1965).

17 J. E. Fergusson and G. M. Harris, J. Chem. Soc., 1966, 1293.

18 R. A. Palmer and T. S. Piper, Inorg. Chem., 5, 864 (1966).

19 E. König and S. Herzog, J. Inorg. Nucl. Chem., 32, 585 (1970).

20 Y. Kaizu, T. Yazaki, Y. Torii and H. Kobayashi, Bull. Chem. Soc. Japan, 43, 2068 (1970).

21 W. W. Brandt and G. F. Smith, Anal. Chem., 21, 1313 (1949).

22 R. Perthel, Z. Phys. Chem., 211, 74 (1959).

23 S. Herzog, U. Grimm and W. Waicenbauer, Z. Chem., 7, 355 (1967).

24 Y. Kaizu and H. Kobayashi, Bull. Chem. Soc. Japan, 45, 470 (1972).

TABLE 3

REDUCTION HALF-WAVE POTENTIALS $E^{red}_{\frac{1}{2},L}$ FOR TRIS-2,2'-BIPYRIDINE AND ITS DIMETHYL DERIVATIVES

LIGAND	$E^{red}_{\frac{1}{2},L}$/V	
	DMF	AN
bipy	-2.10[a]	-2.12
4-dmbipy	-2.15[a]	-2.17
5-dmbipy	-2.23[a]	-2.25

a: Ref. 9

TABLE 4

OXIDATION HALF-WAVE POTENTIALS $E^{ox}_{\frac{1}{2},C}$ AND CHARGE-TRANSFER TRANSITION ENERGIES $h\nu_{CT}$ FOR TRIS-2,2'-BIPYRIDINE COMPLEXES OF IRON, RUTHENIUM, OSMIUM, COBALT AND CHROMIUM AND HALF-WAVE POTENTIALS CORRECTED FOR REDUCTION HALF-WAVE POTENTIALS $E^{red}_{\frac{1}{2},L}$ OF FREE LIGAND MOLECULES

COMPLEX	DMF		AN		aq		$h\nu_{CT}$/eV
	a/V	b/V	a/V	b/V	a/V	b/V	
$Fe(bipy)_3^{2+}$	+1.06	3.16	+1.03	3.15	+0.81	2.91	2.38[c]
$Fe(4\text{-dmbipy})_3^{2+}$	+0.92	3.07	+0.87	3.04	+0.65	2.80	2.35[c]
$Fe(5\text{-dmbipy})_3^{2+}$	+0.96	3.19	+0.92	3.17	+0.73	2.96	2.43[c]
$Ru(bipy)_3^{2+}$	----	----	+1.20	3.32	----	----	2.74
$Ru(4\text{-dmbipy})_3^{2+}$	----	----	+1.09	3.26	----	----	2.72
$Ru(5\text{-dmbipy})_3^{2+}$	----	----	+1.13	3.38	----	----	2.80
$Os(bipy)_3^{2+}$	+0.83	2.93	+0.81	2.93			2.59
$Os(4\text{-dmbipy})_3^{2+}$	+0.71	2.86	+0.65	2.82			2.53
$Os(5\text{-dmbipy})_3^{2+}$	+0.76	2.99	+0.70	2.95			2.66

TABLE 4 (continued)

$Co(bipy)_3^{2+}$	+0.31	2.41	+0.28	2.40			
$Co(4\text{-}dmbipy)_3^{2+}$	+0.21	2.36	+0.15	2.32			
$Co(5\text{-}dmbipy)_3^{2+}$	+0.26	2.49	+0.19	2.44			
$Co(bipy)_3^{+}$	-0.88	1.22	-0.97	1.15			0.89[d]
$Co(4\text{-}dmbipy)_3^{+}$	-1.02	1.13	-1.12	1.05			0.83[d]
$Co(5\text{-}dmbipy)_3^{+}$	-0.97	1.26	-1.07	1.18			0.93[d]
$Cr(bipy)_3^{2+}$	-0.23	1.87	-0.26	1.86	-0.47	1.63	1.05[e]
$Cr(4\text{-}dmbipy)_3^{2+}$	-0.37	1.78	-0.42	1.75	-0.66	1.49	1.02[e]
$Cr(5\text{-}dmbipy)_3^{2+}$	-0.32	1.91	-0.36	1.89	-0.54	1.69	1.11[e]
$Cr(bipy)_3^{+}$	-0.69	1.41	-0.76	1.36	-----	----	
$Cr(4\text{-}dmbipy)_3^{+}$	-0.82	1.33	-0.91	1.26	-----	----	
$Cr(5\text{-}dmbipy)_3^{+}$	-0.79	1.44	-0.87	1.38	-----	----	
$Cr(bipy)_3$	-1.21	0.89	-1.32	0.80	-----	----	
$Cr(4\text{-}dmbipy)_3$	-1.34	0.81	-1 42	0.75	-----	----	
$Cr(5\text{-}dmbipy)_3$	-1.37	0.86	-1.48	0.77	-----	----	
$Cr(bipy)_3^{-}$	-1.87	0.23	-1.94	0.18	-----	----	
$Cr(4\text{-}dmbipy)_3^{-}$	-1.94	0.21	-2.00	0.17	-----	----	
$Cr(5\text{-}dmbipy)_3^{-}$	-2.01	0.22	-2.08	0.17	-----	----	

a: $E^{ox}_{\frac{1}{2},C}$ b: $E^{ox}_{\frac{1}{2},C} - E^{red}_{\frac{1}{2},L}$ c: Ref. 5 d: Ref. 8 e: Ref. 7

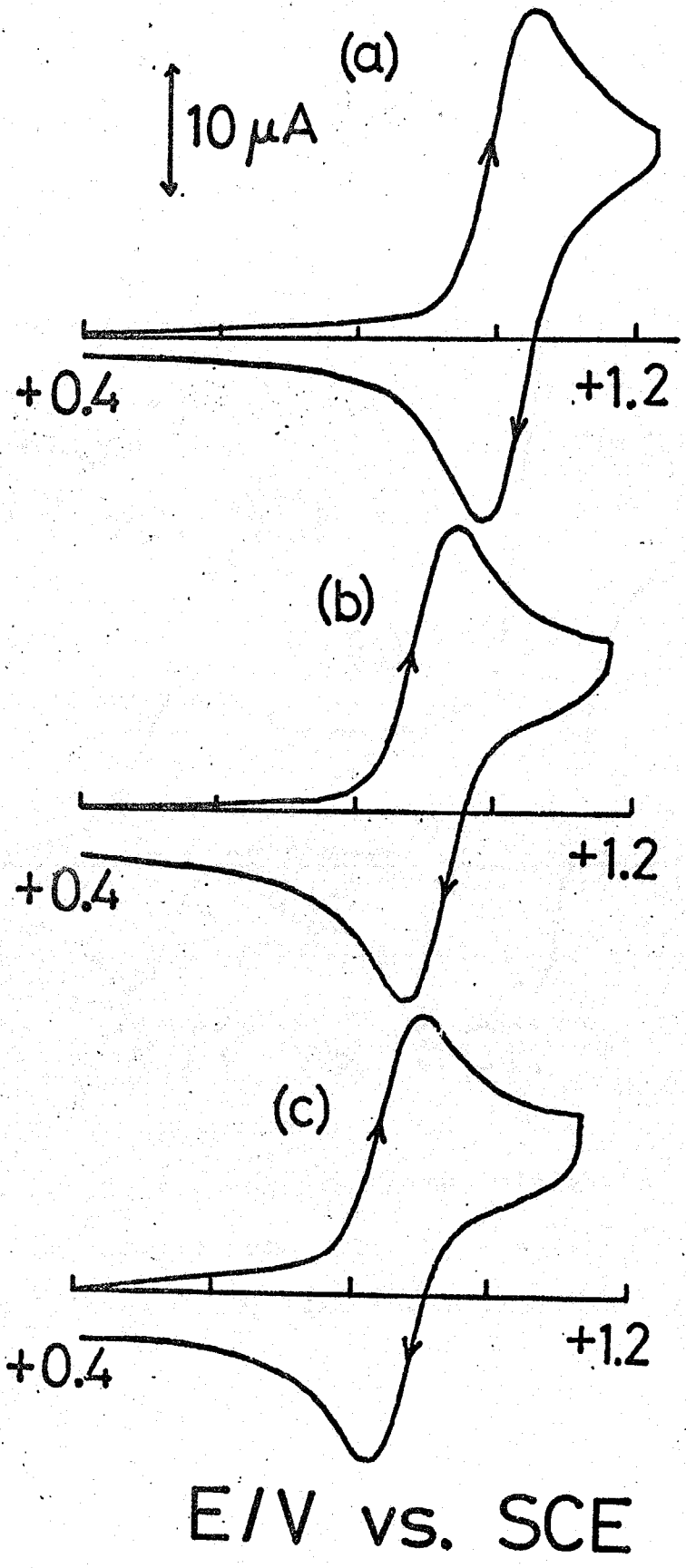

Fig. 10. Cyclic voltammogram with initial anodic scan for (a) $Fe(bipy)_3(ClO_4)_2$, (b) $Fe(5\text{-}dmbipy)_3(ClO_4)_2$ and (c) $Fe(4\text{-}dmbipy)_3(ClO_4)_2$ in AN soln. containing 1 mM complex and 0.1 M TBAP. Scan rate 0.1 V s^{-1}.

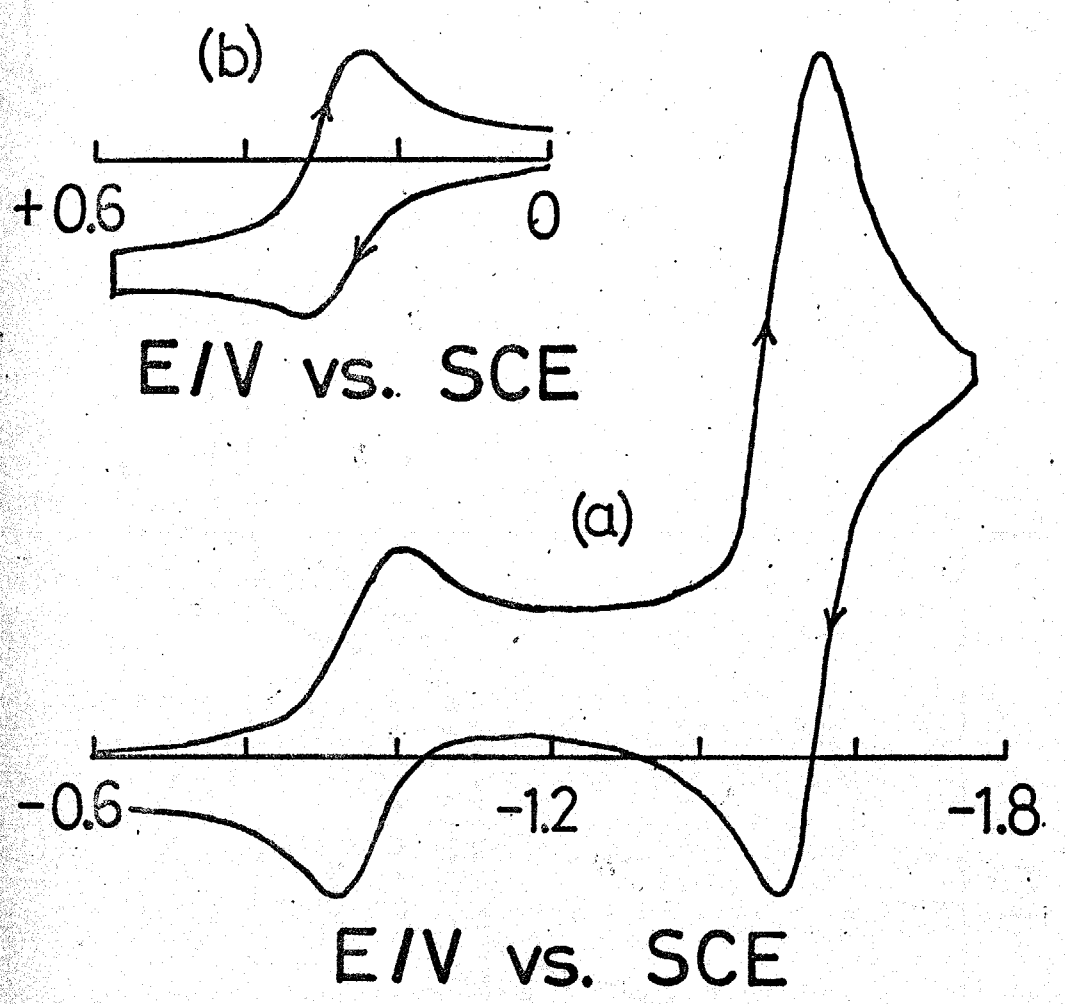

Fig. 11. Cyclic voltammogram with initial (a) cathodic scan and (b) anodic scan for 1 mM $Co(bipy)_3(ClO_4)_2$ in DMF soln. containing 0.1 M TBAP. Scan rate 0.1 V s^{-1}.

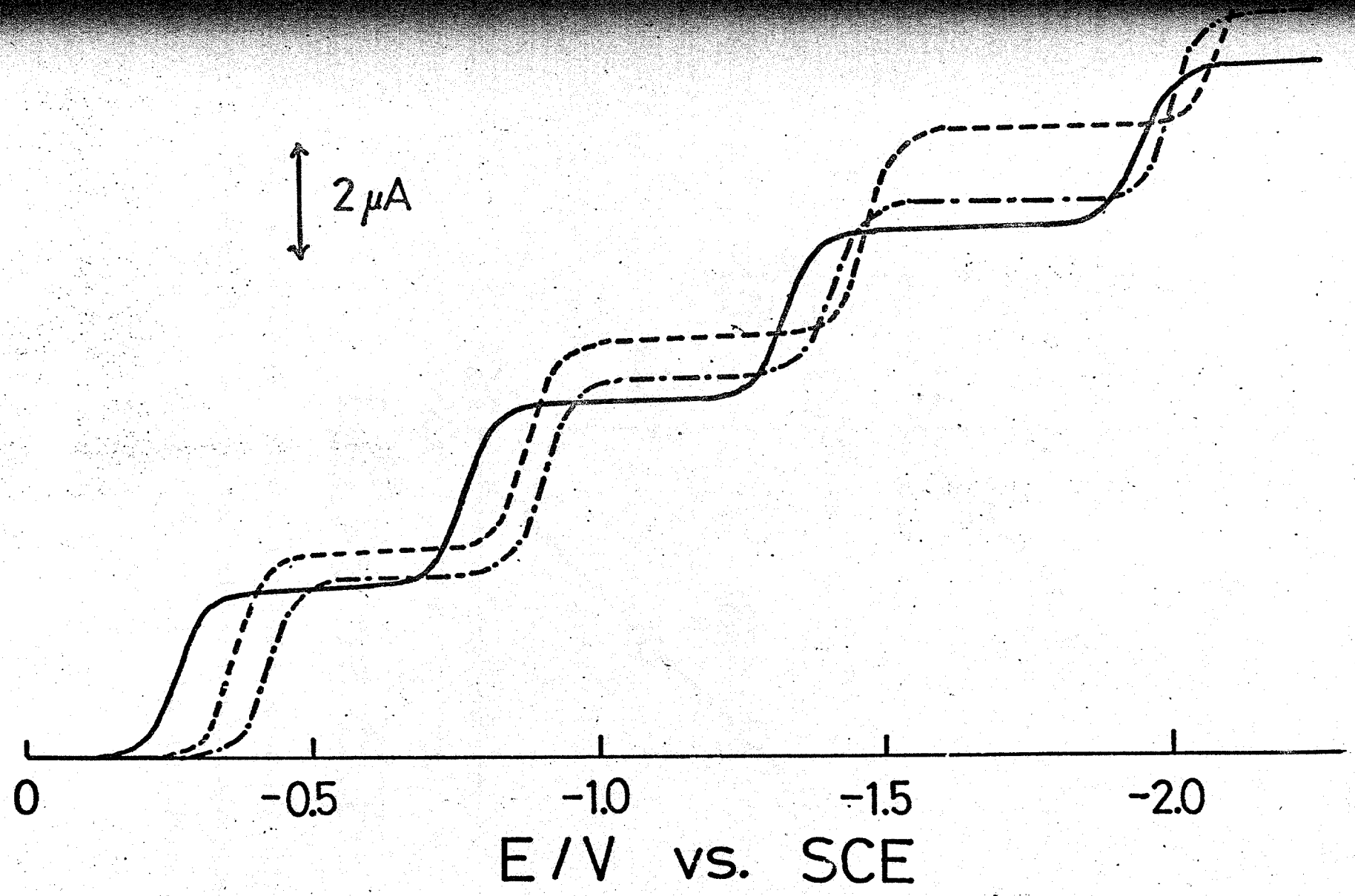

Fig. 12. Cathodic polarogram for 1 mM chromium(III) complex in AN soln. containing 0.1 M TBAP. (——) $Cr(bipy)_3(ClO_4)_3$; (----) $Cr(5\text{-}dmbipy)_3(ClO_4)_3$; (—·—·) $Cr(4\text{-}dmbipy)_3(ClO_4)_3$.

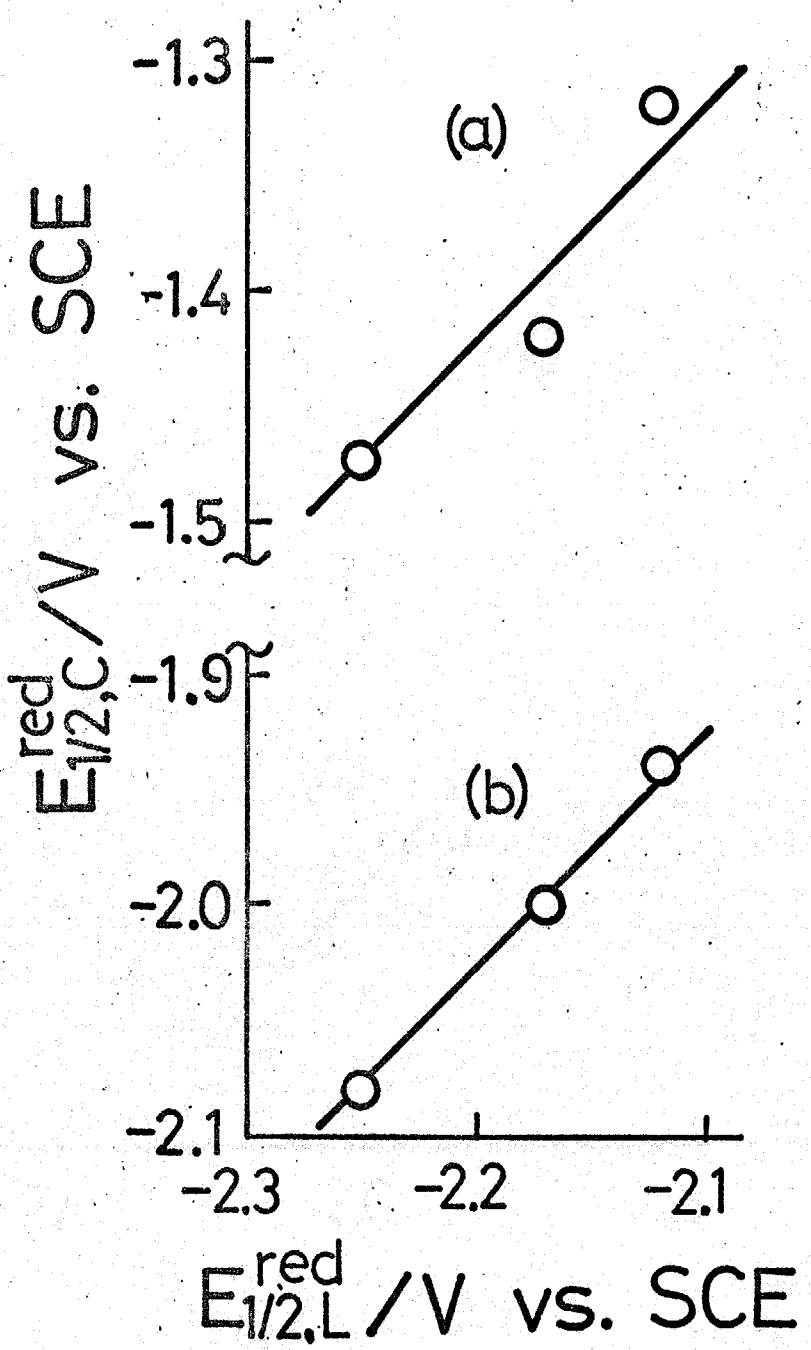

Fig. 13. Plot of reduction half-wave potential $E^{red}_{½,C}$ of (a) CrL_3^+ and (b) CrL_3 vs. reduction half-wave potential of free ligand molecule, $E^{red}_{½,L}$, in AN soln. containing 0.1 M TBAP. L = bipy, 4-dmbipy, 5-dmbipy.

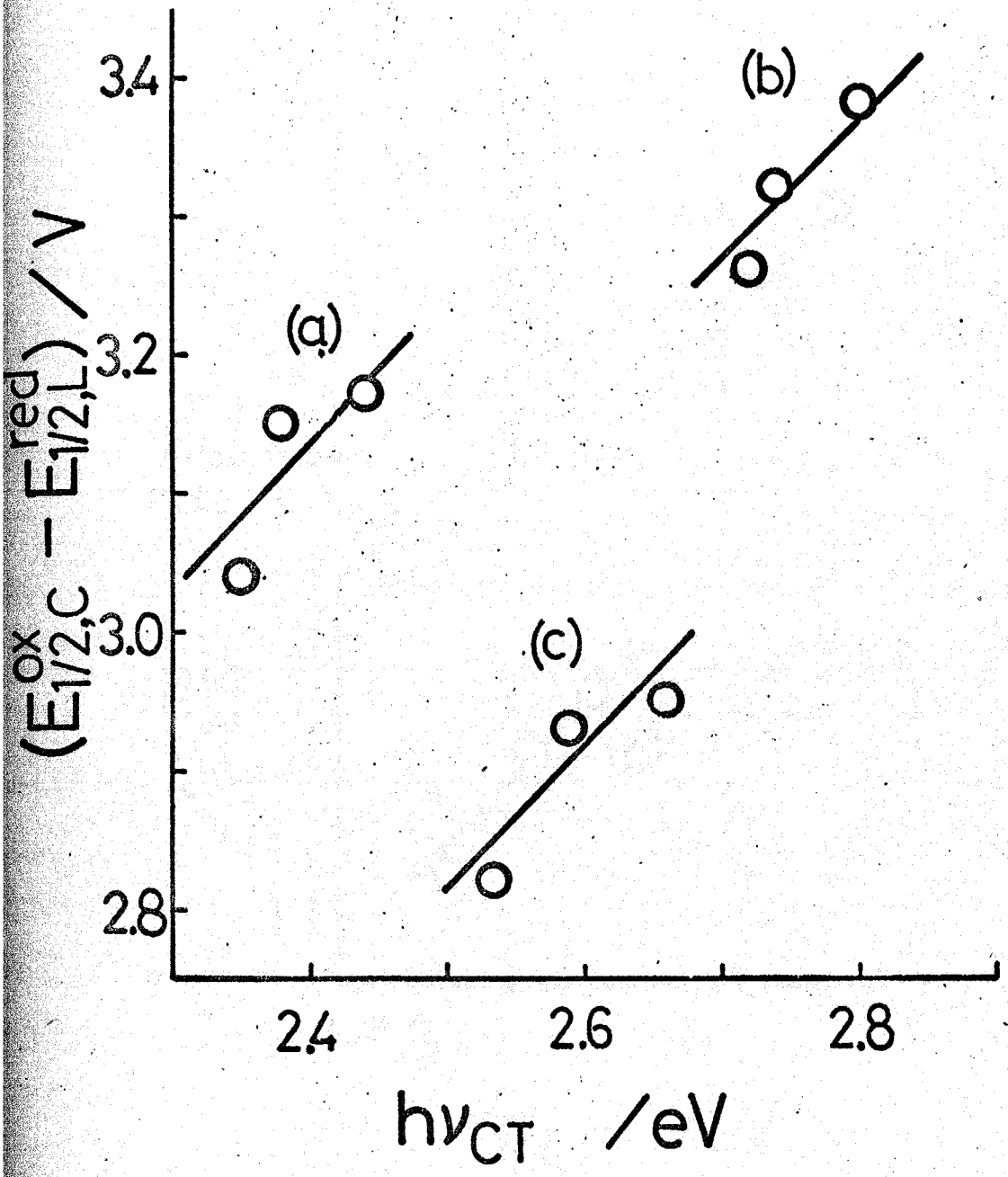

Fig. 14. Plot of half-wave potential difference $E^{ox}_{½,C} - E^{red}_{½,L}$ vs. charge-transfer energy $h\nu_{CT}$ for (a) FeL_3^{2+}, (b) RuL_3^{2+} and (c) OsL_3^{2+} in AN soln. containing 0.1 M TBAP. L = bipy, 4-dmbipy, 5-dmbipy.

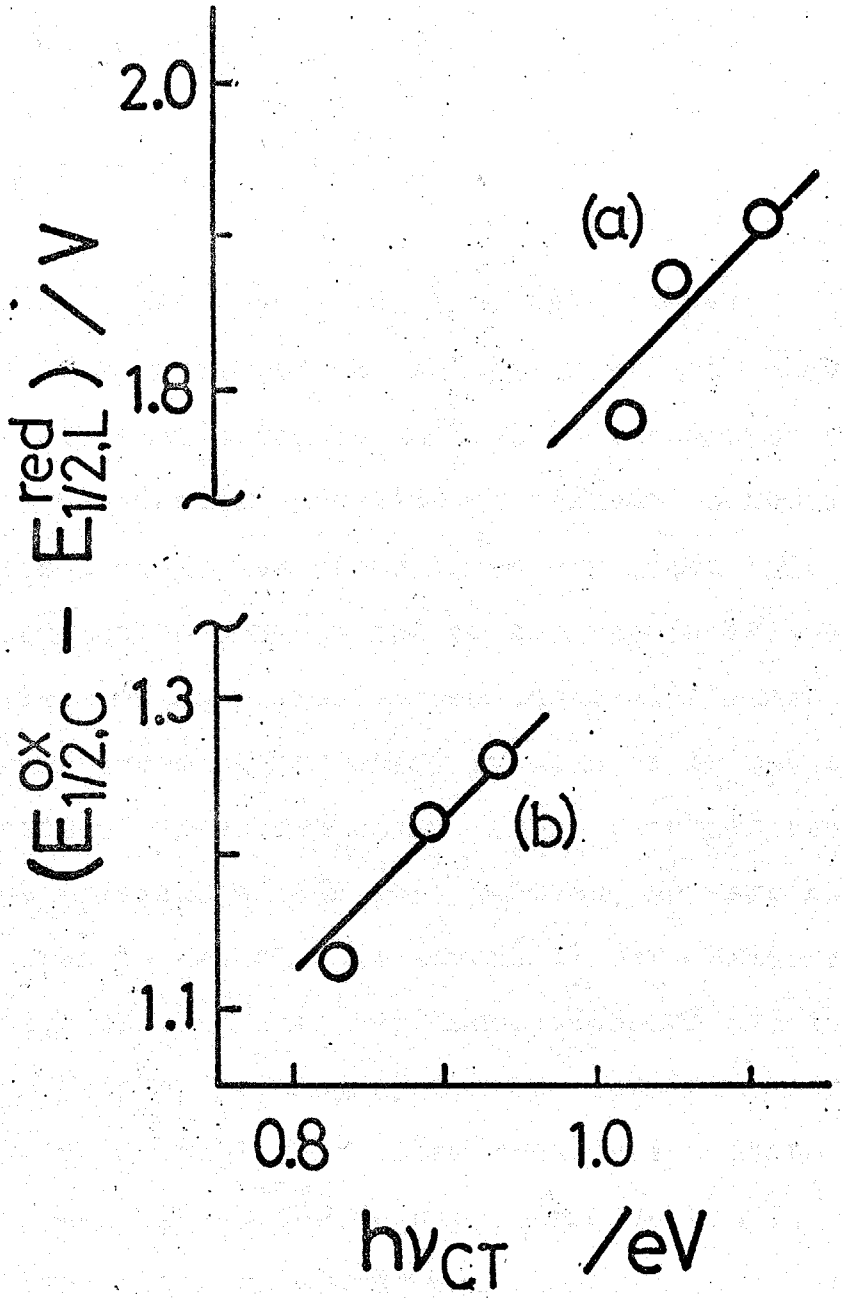

Fig. 15. Plot of half-wave potential difference $E^{ox}_{½,C} - E^{red}_{½,L}$ vs. charge-transfer energy $h\nu_{CT}$ for (a) CrL_3^{2+} and CoL_3^{+} in DMF soln. containing 0.1 M TBAP. L = bipy, 4-dmbipy, 5-dmbipy.

C. Polarography of Chromium(I,0), vanadium(0), Titanium(0) and Molybdenum(0) Complexes

a. INTRODUCTION

In Sections A and B of this chapter, a new method of determining the molecular orbital occupied by the electron added or removed in the course of an oxidation-reduction reaction of transition metal complexes was proposed. It was based on an empirical rule concernig the correlation between the polarographic half-wave potentials of complexes and their electronic configurations. Twenty redox systems of tris-bipyridine complexes of iron, ruthenium, osmium, cobalt and chromium have been discussed. In this section the same kind of discussion is extended to several lower-oxidation state complexes of vanadium, chromium, titanium and molybdenum on the basis of polarographic data obtained with solutions containing a complex in a lower oxidation state. Such polarograms except those for $Mo(bipy)_3^1$ and $Fe(bipy)_3^2$ have never been reported elsewhere.

b. EXPERIMENTAL

Reagents

All the reagents and solvents were commercially obtained. TBAP was recrystalized from an oxygen-free ethyl acetate solution under a nitrogen atmosphere and then dried in vacuo.

Solvent

DMF was purified in a way described in Section A of this chapter. Residual water and oxygen were removed by sodium anthracenide according to the conventional procedure, and then distilled and stored in an evacuated glass ampoule. All operations in purifying the solvent were performed under a nitrogen atmosphere or in vacuo.

Complexes

All complexes discussed in this section were very sensitive to air. The preparations and handling of the complexes were performed under a nitrogen atmosphere or in vacuo.

Tris(2,2'-bipyridine)chromium(I)[3] perchlorate and tris(2,2'-bipyridine)chromium(0)[4] were prepared according to the procedures in the literature cited. 4,4'- and 5, 5'-dimethyl derivatives of tris(2,2'-bipyridine)-chromium(I) perchlorate were prepared by the

disproportionation of the corresponding divalent complexes in dilute NaOH solutions.

Calcd. for $Cr(bipy)_3(ClO_4)$: C, 58.1; H, 3.90; N, 13.6.
Found: C, 57.8; H, 3.79; N, 13.9.

Calcd. for $Cr(bipy)_3$: C, 69.2; H, 4.65; N, 16.2.
Found: C, 67.0; H, 4.60; N, 16.0.

Calcd. for $Cr(4,4'\text{-dmbipy})_3(ClO_4)$: C, 61.3; H, 5.15; N, 11.9.
Found: C, 59.8; H, 5.01; N, 11.0.

Calcd. for $Cr(5,5'\text{-dmbipy})_3(ClO_4)$: C, 61.3; H, 5.15; N, 11.9.
Found: C, 59.4; H, 5.02; N, 10.9.

Tris(2,2'-bipyridine)vanadium(0) and its 4,4'- and 5,5'-dimethyl derivatives were prepared from vanadium trichloride and bipyridine dinegative ion (lithium salt) in tetrahydrofran.

Calcd. for $V(bipy)_3$: C, 69.3; H, 4.66; N, 16.2.
Found: C, 68.3; H, 4.40; N, 15.9.

Calcd. for $V(4,4'\text{-dmbipy})_3$: C, 69.4; H, 4.66; N, 16.2.
Found: C, 65.3; H, 4.63; N, 15.6.

Calcd. for $V(5,5'\text{-dmbipy})_3$: C, 69.4; H, 4.66; N, 16.2.
Found: C, 67.4; H, 4.57; N, 15.3.

Tris(2,2'-bipyridine)titanium(0)[5] was prepared

according to the procedure in the literature cited.

Calcd. for $Ti(bipy)_3$: C, 69.8; H, 4.68; N, 16.3. Found: C, 68.9; H, 4.51; N, 16.1.

Tris(2,2'-bipyridine)molybdenum(0) was prepared from molybdenum pentachloride and bipyridine dinegative ions in tetrahydrofran.

Calcd. for $Mo(bipy)_3$: C, 63.8; H, 4.29; N, 14.9. Found: C, 60.0; H, 4.10; N, 13.4.

Solutions

Required amounts of a complex and TBAP were sealed in an evacuated glass ampoule equipped breakable seals. A DMF solution was prepared by transferring the purified solvent into this ampoule by ampoule-to-ampoule distillation on a vacuum line. Each solution ampoule was connected with the cell via a tapered joint and a breakable seal.

Cell

The Pyrex-glass electrolysis cell shown in Fig. 16 was used. After the cell had been evacuated, nitrogen gas was introduced into it until an atmospheric pressure was reached. An aqueous agar-bridge, was then connected with the cell via a tapered joint under a nitrogen counter flow. The electrolytic solution was transferred

into the cell through the breakable-seal by the appropriate rotation of the ampoule around the tapered joint. A SCE was connected with the subsidiary compartment via the agar-bridge. The DME, the SCE and a mercury pool electrode were used in the polarographic measurements. The platinum spherical electrode A, the SCE, and the mercury pool electrode were used in the cyclic voltammetric measurements. The mercury pool electrode and the platinum plate electrode B served as the working and the counter electrode in controlled potential electrolyses respectively. The compartment of the latter electrode was separated by a fritted glass from that of the former electrode. The progress of the controlled potential electrolysis was followed polarographically. Measurements were made at room temperature maintained at 25 °C.

c. RESULTS

Polarography and cyclic voltammetry of vanadium(0) complexes

Figure 17 shows a cathodic polarogram for $V(bipy)_3$. It exhibits five reduction waves with half-wave potentials -1.55, -2.10, -2.23, -2.6 and -2.73 V. The heights of the waves at -1.55 and -2.23 V are identical. The wave at

-2.73 V is almost the same in height with these waves when corrected for the ultimate current rise. The waves at -2.10 and -2.6 V are much lower than others. They are attributable to reduction of free 2.2'-bipyridnine molecules.

Figure 18 shows a polarogram in the cathodic-anodic polarozation. The anodic wave has a maximum falling abruptly at -0.44 V and a diffusion plateau at more positive potentials. The plateau height is twice the height of the reduction wave at -1.55 V. The potential at which the maximum current ends is approximately the point of zero-charge in this solution. The anodic maximum of this kind has rarely been reported for metal complexes though it has been observed in the anodic polarization of several hydrocarbon anion radicals. The same maximum was found in the polarograms for the complexes of titanium, chromium and molybdenum. Both maxima in hydrocarbons and metal complexes may be considered to have a common origin.

Figure 19 shows two cyclic voltammograms for $V(bipy)_3$: (a) one with an initial cathodic scan and (b) the other anodic scan. The latter exhibits two peaks partly overlapped with each other. The polarographic half-wave potentials corresponding to these peak potentials are -1.01 and -1.11 V. The four oxidation-

reduction steps at -1.01, -1.11, -1.55 and -2.23 V were concluded to be reversible one-electron steps on the basis of the conventional reversibility criterion of the peak-potential separation and the peak-current ratio. Polarograms corresponding to $V(bipy)_3^+$ and $V(bipy)_3^{2+}$ were obtained successively in the course of a controlled-potential electrolysis of $V(bipy)_3$ at -0.8 V. This is the evidence for the electrochemical generation and the stability of these complexes. The half-wave potentials -1.01, -1.11, -1.55, -2.23 and -2.73 V may be assigned to the redox systems $V(bipy)_3^{2+}/V(bipy)_3^+$, $V(bipy)_3^+/V(bipy)_3$, $V(bipy)_3/V(bipy)_3^-$, $V(bipy)_3^-/V(bipy)_3^{2-}$ and $V(bipy)_3^{2-}/V(bipy)_3^{3-}$ respectively. The polarograms and cyclic voltammograms for $V(4\text{-dmbipy})_3$ and $V(5\text{-dmbipy})_3$ were also obtained. They were quite similar to those for $V(bipy)_3$.

The half-wave potentials obtained are listed in Table 5. It can be seen that the half-wave potentials of VL_3^{2+}/VL_3^+ and VL_3^+/VL_3 become more negative in the order of ligand, bipy < 5-dmbipy < 4-dmbipy, and those of VL_3/VL_3^- and VL_3^-/VL_3^{2-} in the order bipy < 4-dmbipy < 5-dmbipy. L degignates bipy, 4-dmbipy and 5-dmbipy throughout this section. Figure 20 shows the relation between the reduction half-wave potentials of the complexes and those of the free ligands. The latter data

are available in Section A of this chapter. Each straight line was drawn in accordance with the following equation with an arbitrary choice of the c^{red} value:

$$E^{red}_{1/2,C} = E^{red}_{1/2,L} + c^{red} \qquad (10)$$

Equation (10) was derived by assuming that the reduction of a complex is the reduction of its coordinated ligand, in other words an excess electron in a reductant species occupies a π^*-orbital* of the coordinated ligand and not a metal d-orbital. It is seen that the redox systems VL_3/VL_3^- and VL_3^-/VL_3^{2-} obey eqn. (10) but VL_3^{2+}/VL_3^+ and VL_3^+/VL_3 do not. As shown in Fig. 21, the VL_3^+/VL_3 system obey the order the other equation derived in Section B of this chapter:

$$E^{ox}_{1/2,C} - E^{red}_{1/2,L} = h\nu_{CT} + c^{ox} \qquad (11)$$

Equation (12) is based on the assumption that the oxidation of a complex is a removal of an electron from a metal t_{2g}-orbital. Applicability of eqn. (12) to the VL_3^{2+}/VL_3^+ system could not be examined because of the lacking of data on $h\nu_{CT}$.

---

* The term "π^*-orbital" does not necessarily mean a pure π^*-orbital in this chapter. A molecular orbital contributed mainly from ligand π^*-orbitals is called a π^*-orbital and that from metal t_{2g}-orbitals a t_{2g}-orbital.

Polarography and cyclic voltammetry of chromium(I) and chromium(0) complexes

Figure 22 shows a cathodic-anodic polarogram for $Cr(bipy)_3(ClO_4)$ in DMF. It exhibits six reduction waves with half-wave potentials -1.22, -1.85, -2.10, -2.20, -2.45 and -2.6 V and two oxidation waves at -0.72 and -0.23 V. The heights of the waves at -1.22, -1.85, -2.20 and -2.45 V were almost identical when corrected for mercury drop area. The waves at -2.10 and -2.6 V were lower than these. They are attributable to reduction of free 2,2'-bipyridine molecules. The wave at -0.72 V was slightly higher than the wave at -1.22 V, while the wave at -0.23 V was slightly lower. The sum of the height of the waves at -0.23 and -0.72 V was twice the height of the wave at -1.22 V.

A polarogram for $Cr(bipy)_3$ exhibited five reduction waves and three oxidation waves. It was consistent with the the one for $Cr(bipy)_3(ClO_4)$.

Figure 23 shows cyclic voltammograms for $Cr(bipy)_3(ClO_4)$ in DMF; one with initial cathodic scan and others with anodic scan. On the basis of the reversibility creteria, the five waves at -1.22, -1.85, -2.10, -2.20 and -2.45 V were concluded to be reversible one-electron waves. The waves at -1.22, -1.85, -2.20 and -2.45 V can be assigned to the redox systems $Cr(bipy)_3^+/Cr(bipy)_3$,

$Cr(bipy)_3/Cr(bipy)_3^-$, $Cr(bipy)_3^-/Cr(bipy)_3^{2-}$ and $Cr(bipy)_3^{2-}/Cr(bipy)_3^{3-}$, respectively. The cyclic voltammograms with initial anodic scan showed a new peak at about -0.8 V (Fig. 23-b). The same peak appeared also in the voltammogram with the scan direction reversed at -0.4 V (Fig. 23-c). Its peak-height became smaller relatively to others as the scan rate became higher. These facts means that the reduction of $Cr(bipy)_3^+$ is coupled by chemical reactions. The cyclic voltammogram for $Cr(bipy)_3$ was in consistence with the one for $Cr(bipy)_3(ClO_4)$.

Polarograms and cyclic voltammograms were also obtained for $Cr(4\text{-dmbipy})_3(ClO_4)$ and $Cr(5\text{-dmbipy})_3(ClO_4)$ in DMF. They were quite similar to those for $Cr(bipy)_3(ClO_4)$. The observed reversible half-wave potentials are listed in Table 5. It is seen that the half-wave potentials of CrL_3^+/CrL_3 become more negative in the order bipy < 4-dmbipy < 5-dmbipy. The same half-wave potential order holds for CrL_3/CrL_3^-, CrL_3^-/CrL_3^{2-} and CrL_3^{2-}/CrL_3^{3-}. Figure 24 shows the $E^{red}_{1/2,C}$ vs. $E^{red}_{1/2,L}$ plots for the latter redox systems. They obey eqn. (10).

Polarography and cyclic voltammetry of titanium(0) complexes

Figure 25 shows a cathodic polarogram for $Ti(bipy)_3$. It exhibits four reduction waves of which half-wave potentials are -1.51, -1.97, -2.1 and -2.6 V. The heights

of the waves at -1.51 and -1.97 V are almost identical. The waves at -2.1 and -2.6 V are higher than these. They may be attributed to reduction of free bipyridine molecules. An anodic polarogram exhibited a wave at -1.0 V. It was twice as high as the reduction wave at -1.51. The cyclic voltammogram in Fig. 26 shows that the waves at -1.51, -1.97 and -2.1 V are reversible one-electron waves and those at -1.0 and -2.6 V irreversible. The waves at -1.51 and -1.97 V became lower and those at -2.1 and -2.6 V higher during several hours later than the preparation of the sample solutions. This may be due to the liberation of bipyridine from the complex $Ti(bipy)_3$ caused by its gradual decomposition. After a controlled-potential electrolysis of $Ti(bipy)_3$ at -2.0 V, a polarogram corresponding to $Ti(bipy)_3^-$ was obtained. The waves at -1.51 and -1.97 V were assigned to the redox systems $Ti(bipy)_3/Ti(bipy)_3^-$ and $Ti(bipy)_3^-/Ti(bipy)_3^{2-}$ respectively.

Polarography and cyclic voltammetry of molybdenum(0) complexes

As shown in Fig. 27 a polarogram for $Mo(bipy)_3$ exhibited three reduction waves with half-wave potentials -1.72, -2.14 and -2.65 V and two oxidation waves, -1.13

and -0.47 V. The waves at -1.13 and -1.72 V were almost identical in height. The wave at -2.14 V was slightly higher than these. This may be due to its overlapping with the reduction wave for free bipyridine. The small wave at -2.65 V may be the second reduction wave for the free bipyridine. According to DuBois et al.[1] the waves at -2.14 and -2.65 V were four and two times as high as the wave at -1.72 V respectively. This might be due to the contamination of their sample solutions by bipyridine to a larger extent than ours.

On the basis of the cyclic voltammogram for this complex, the waves at -1.13, -1.72 and -2.14 V were concluded to be reversible one-electron waves, and the waves at -0.47 V irreversible. The reversible waves may be assigned to the redox systems $Mo(bipy)_3^+/Mo(bipy)_3$, $Mo(bipy)_3/Mo(bipy)_3^-$ and $Mo(bipy)_3^-/Mo(bipy)_3^{2-}$ respectively.

A polarogram for $Mo(bipy)_3$ in THF exhibited three reduction waves at -1.80, -2.15 and -2.9 V as well as an oxidation wave at -1.11 V. The wave at -2.9 V was partly overlapped by the ultimate current rise. Bipyridine waves were not observed. The half-wave potentials obtained in both solvents are listed in Table 6.

d. DISCUSSION

The electronic configurations of tris-bipyridine complexes including those treated in Sections A and B of this chapter are now discussed on the basis of the following points of view:

(1) An empirical rule concerning the shift in half-wave potential caused by methyl-substitution of ligand. If the reduction half-wave potentials of complexes of a transition metal with bipy, 4-dmbipy and 5-dmbipy as ligands become more negative in the order of ligand, bipy < 5-dmbipy < 4-dmbipy, the excess electron in the reductant species occupies a metal t_{2g}-orbital. If the sequence is bipy < 4-dmbipy < 5-dmbipy, the excess electron occupies a ligand π^*-orbital.

(2) A comparison between the reduction half-wave potential of a complex and that of free ligand. In deriving eqns. (10) and (11), it was assumed that the difference in solvation energy between the reductant and the oxidant species is held invariant on methyl-substitution of ligand. Success in finding experimental evidence for the validity of these equations may suggest that the methyl-substitution was indeed a small perturbation with respect to the solvation energy. However, when a comparison of half-wave potential

is made between a pair of complexes with different central metals of different ionic charge, the contribution of the solvation energy to the half-wave potential cannot be an invariant quantity. When the treatment of Case et al.[6] and Peover[7] based on the Born equation is followed, the solvation energy of an ionic species bearing charge z, α^z, is expressed as

$$-\alpha^z = z^2S + zF\chi \qquad (12)$$

with

$$S = Ne^2(1 - 1/D_s)/2r \qquad (13)$$

where r is the radius of the molecule when it is assumed to be a sphere, χ the surface potential of the solution, D_s the static dielectric constant, N the Avogadro number and F the Faraday. When it is assumed that the standard potential is practically identical with the reversible half-wave potential, the gas-phase electron affinity A_C of a complex is

$$A_C = E^{red}_{1/2,C} + \alpha_C^{z-1} - \alpha_C^z + c \qquad (14)$$

and the same quantity of a free ligand substance, i.e. bipy, 4-dmbipy and 5-dmbipy, is

$$A_L = E^{red}_{1/2,L} + \alpha_L^{-1} - \alpha_L^0 + c \qquad (15)$$

where the subscripts L and C designate a complex and a free ligand substance respectively and c is a constant appropriate to the reference electrode employed.

In view of the large molecular dimension of the ligand,

the radii of the bipyridine complexes may be constant, regardless of their central metals. In the following discussion, the term S is assumed to be a constant of all complexes and designated by a sysmbol S_C. The S terms for the free ligands may be also nearly identical. They are designated by a common symbol S_L. Naturally S_C is smaller than S_L. On the basis of these assumptions the difference in energy levels of complexes can be discussed on the basis of their half-wave potentials referred to those of free ligands.

(3) The difference between the half-wave potentials of the oxidation and reduction waves of a complex. The ionization potential of a complex bearing a charge z is related with the oxidation half-wave potential by an equation analogous to eqn. (14) as

$$I_C = E^{ox}_{1/2,C} - \alpha_C^{z+1} + \alpha_C^z + c \qquad (16)$$

The half-wave potential difference defined by $E^{ox}_{1/2,C} - E^{red}_{1/2,C}$ can thus be written as

$$\Delta E_{1/2} = I_C - A_C - 2S \qquad (17)$$

where I_C is the ionization potential of a complex.

Consequently, the quantity $\Delta E_{1/2}$ can be a measure of a sort of intrinsic energy of a complex irrespetive of solvation energies of the species with charges z+1, z and z-1, and the following aspects can be discussed on the basis of the $\Delta E_{1/2}$ values.

(i) If the molecular orbitals occupied by the added electron and the removed one are the same or the degenerate orbitals, the energy of electronic repulsion can be estimated from $\Delta E_{1/2}$.

(ii) If an electron is added to a high-lying vacant orbital or an electron is removed from a low-lying fully occupied orbital, difference in energy between these orbitals can be estimated from $\Delta E_{1/2}$, though it is biassed by the repulsion energy between a couple of electrons in the latter orbital. The $\Delta E_{1/2}$ values are listed in Table 7 together with those for iron, ruthenium, osmium and cobalt complexes. The latter data are obtained from Sections A and B of this chapter.

Figure 28 is a schematic diagram showing the half-wave potentials of these complexes. The half-wave potential order among bipy, 4-dmbipy and 5-dmbipy complexes is also shown. Such a half-wave potential as becomes more negative in the order bipy < 4-dmbipy < 5-dmbipy (Group I), on methyl-substitution, is more negative than -1.22 V and that of the other type, bipy < 5-dmbipy < 4-dmbipy (Group II), is more positive than -1.11 V. Table 7 shows the number of unpaired electrons in these complexes estimated form the literature data on the magnetic moment. As described in Section A, the reduction half-wave potentials of the complexes ML_3^{2+}, ML_3^{+} and

ML_3 (M = Fe, Ru, Os) satisfied eqn. (10) and the half-wave potentials for complexes with the same oxidation state were held constant within 80 mV regardless of the kind of metals. On the basis of this and some other experimental facts the added electron was concluded to occupy a triply degenerate π^*-orbital of which energy might be nearly identical irrespective of M. Table 7 shows that in the circumstances of case (i) the $\Delta E_{1/2}$ values are small compared with those in case (ii). This correlation is used as a general rule in the following discussion.

From eqns. (12), (14) and (15) the electron affinities of $Fe(bipy)_3^{2+}$, $A_C^{Fe^{2+}}$, and free bipyridine, A_L, are

$$A_C^{Fe^{2+}} = E^{red}_{1/2,C} + 3\,S_C + c$$

$$A_L = E^{red}_{1/2,L} - S_L + c$$

Thus

$$A_C^{Fe^{2+}} - A_L = E^{red}_{1/2,C} - E^{red}_{1/2,L} + 3S_C + S_L > 0.85 \text{ eV}$$

The π^*-orbitals of ML_3^{2+}(M = Fe, Ru, Os) are lower than that of free bipyridine by more than 0.85 eV.

The half-wave potentials of the redox systems CrL_3^+/CrL_3 and VL_3/VL_3^- satisfied eqn. (10). According to the empirical rule described above, each excess electron in the reductant complexes, i.e. CrL_3 and VL_3^-, should occupy a ligand π^*-orbital. This is in conflict with the experimental fact that these complexes are diamagnetic

as seen in Table 8 . Strong π-bondings between the t_{2g}-orbitals of a central metal ion and the ligand π-orbitals caused by the decrease in the charge of the central metal ion may account for this apparent π-character of the excess electron. If necessary, they should be classified into a group intermediate between Group I and II.

The methyl substitution effect, the number of reduction waves and the small $\Delta E_{1/2}$ values for CrL_3^- and CrL_3^{2-} suggest that the added electron in the reduction of CrL_3, CrL_3^- and CrL_3^{2-} may occupy a molecular orbital contributed mainly by ligand π^*-orbitals. The $\Delta E_{1/2}$ values are as small as those of iron, ruthenium and osmium complexes. The number of unpaired electrons in Table 8 also points to the degeneracy of these π^*-orbitals.

The differerce in electron affinity between CrL_3 and free bipyridine is given by

$$A_C^{Cr^o} - A_L = E_{1/2,C}^{red} - E_{1/2,L}^{red} - S_C + S_L + c > 0.25 \text{ eV}$$

since $S_C < S_L$. The difference between electron affinities of FeL_3^{2+} and CrL_3 is given by

$$A_C^{Fe^{2++}} - A_C^{Cr^o} = 0.6 \text{ eV} + 4S_C > 0.6 \text{ eV}$$

In the same way , comparison between the half-wave potentials of $V(bipy)_3^-/V(bipy)_3^{2-}$ and $Cr(bipy)_3/Cr(bipy)^-$ yields the following relation:

$$A_C^{Cr^o} - A_C^{V^-} = 0.38 \text{ eV} + 2S_C > 0.38 \text{ eV}$$

These estimates show that the lowest π^*-orbitals of these

complexes are more stabilized in the order $V(bipy)_3^-$ < $Cr(bipy)_3$ < $Fe(bipy)_3^{2+}$. The order is in accordance with the increasing order of positive charges on the central metals. This may suggest that the electrostatic interaction between a π^*-electron and the residual charge on the central metal ion is account for the observed π^*-level shift.

In connection with Table 7 it may be reasonable to predict that the $\Delta E_{1/2}$ values for d^4 and d^5 complexes are nearly equal to each other and smaller than those for d^6 complexes, because the $\Delta E_{1/2}$ values for only d^6 complexes are contributed by the energy difference between the t_{2g}- and π^*-orbitals through the A values in eqn. (17). Table 7 shows that the prediction is valid for all complexes studied except $V(bipy)_3^+$. The $\Delta E_{1/2}$ value of 0.10 V for the latter complex is anomalously small. An explanation for this may tentatively be given as follows: It is known that $Ti(bipy)_3$ (d^4, S = 0)[8], an isoelectronic compound with $V(bipy)_3^+$ and $Cr(bipy)_3^{2+}$, is diamagnetic. The diamagnetism of this complex has been considered to be caused by the strong splitting of the t_{2g}-orbitals within the partly-filled d-shell, $t_{2g} \rightarrow e_g' + a$, with the e_g' orbital being the lowest. This large splitting has been interpreted by Orgel[11] to be caused by the strong π-type interaction of the e_g' orbital with antibonding ligand orbitals. As for the magnetism

of vanadium complexes, on the other hand, the measurements of the magnetic susceptibility of $V(bipy)_3^+$ has not yet been successful and a methanolic solution of $V(bipy)_3I$ exhibited no e.s.r. signals[12]. $V(bipy)_3^{2+}$ and $V(bipy)_3$ are known to be paramagnetic and to have total spins of 3/2 and 1/2 respectively[12]. If the $V(bipy)_3^+$ ion in solution is assumed to be diamagnetic, the electronic configurations of $V(bipy)_3^{2+}$, $V(bipy)_3^+$ and $V(bipy)_3$ can be t_{2g}^3, $e_g'^4$ and $e_g'^4a$ respectively. Then the small $\Delta E_{1/2}$ value for $V(bipy)_3^+$ may be explained.

DuBois et al.[1] have concluded that the unpaired electron in $Mo(bipy)_3^-$ occupies a metal e_g-orbital, on the basis of the e.s.r. spectrum exhibiting a hyperfine structure due to the Mo nucleus. An alternative explanation can be made as follows: the $\Delta E_{1/2}$ data shows that the molecular orbital occupied by the unpaired electron in $Mo(bipy)_3^-$ is a π^*-orbital, in the sense defined in this paper, namely it is a linear combination of ligand π^*-orbitals with metal t_{2g}-orbitals. The mixing of the latter orbitals may account for the observed hyperfine splittings.

It is probable that in the reduction of $Ti(bipy)_3$ and $Ti(bipy)_3^-$ each added electron occupies a molecular orbital contributed mainly from t_{2g}-orbitals. The reason is that the half-wave potential for $Ti(bipy)_3$/

$Ti(bipy)_3^-$ was more positive than that of $Cr(bipy)_3$/$Cr(bipy)_3^-$, and $Ti(bipy)_3^-/Ti(bipy)_3^{2-}$ than $V(bipy)_3^-$/$V(bipy)_3^{2-}$. The magnetic moment data also support this.

e. REFERENCES

1 D. W. DuBois, R. T. Iwamoto and J. Kleinberg, Inorg. Nucl. Chem. Lett., 6, 53 (1970).

2 A. Misono, Y. Uchida, M. Hidai, T. Yamagishi and H. Kageyama, Bull. Chem. Soc. Japan, 46, 2769 (1973).

3 V. F. Hein and S. Herzog, Z. Anorg. Allgem. Chem., 267, 337 (1952).

4 S. Herzog, K. Renner and W. Schön, Z. Naturforsch. B, 12, 809 (1957).

5 S. Herzog and R. Taube, Z. Anorg. Allgem. Chem., 306, 159 (1960).

6 B. Case, N. S. Hush, R. Parsons and M. E. Peover, J. Electroanal. Chem., 10, 360 (1965).

7 M. E. Peover, Electrochim. Acta, 13, 1083 (1968).

8 S. Herzog and R. Taube, Z. Anorg. Allgem. Chem., 306, 159 (1960).

9 L. E. Orgel, J. Chem. Soc., 1961, 3683.

10 S. Herzog, Z. Anorg. Allgem. Chem., 294, 155 (1958).

11 S. Herzog and R. Taube, Z. Chem., 2, 208 (1962).

12 S. Herzog, J. Inorg. & Nucl. Chem., 8, 557 (1958).

13 R. Perthel, Z. Physik. Chem, 211, 74, (1959).

14 W. R. Mcwhinnie and J. D. Miller in H. J. Emeleus and A. G. Sharpe (Eds.), Advances in Inorganic Chemistry and Radiochemistry, Vol. 12, Academic Press, New York.

15 Y. Kaizu, T. Yazaki, Y. Torii and H. Kobayashi, Bull. Chem. Soc. Japan, 43, 2068 (1970).

TABLE 5

THE HALF-WAVE POTENTIALS FOR TRIS-BIPYRIDINE COMPLEXES OF CHROMIUM AND VANADIUM, $E_{\frac{1}{2},C}$, AND THOSE CORRECTED FOR REDUCTION POTENTIALS OF FREE LIGAND MOLECULES, $E_{\frac{1}{2},C} - E_{\frac{1}{2},L}$, IN DMF CONTAINING 0.2 M TBAP

Redox system	$E_{\frac{1}{2},C}$/V vs. SCE			$(E_{\frac{1}{2},C} - E_{\frac{1}{2},L})$/V		
	bipy	4dmbipy	5dmbipy	bipy	4dmbipy	5dmbipy
CrL_3^{3+}/CrL_3^{2+}	-0.23	-0.37	-0.31	1.87	1.78	1.92
CrL_3^{2+}/CrL_3^{+}	-0.72	-0.82	-0.78	1.38	1.33	1.45
CrL_3^{+}/CrL_3	-1.22	-1.34	-1.37	0.88	0.81	0.86
CrL_3/CrL_3^{-}	-1.85	-1.93	-2.02	0.25	0.22	0.21
CrL_3^{-}/CrL_3^{2-}	-2.22	-2.27	-2.37	-0.10	-0.12	-0.14
CrL_3^{2-}/CrL_3^{3-}	-2.45	-2.49	-2.73	-0.35	-0.34	-0.37
VL_3^{2+}/VL_3^{+}	-1.01	-1.14	-1.11	1.09	1.01	1.12
VL_3^{+}/VL_3	-1.11	-1.23	-1.21	0.99	0.92	1.02
VL_3/VL_3^{-}	-1.55	-1.64	-1.71	0.55	0.51	0.52
VL_3^{-}/VL_3^{2-}	-2.23	-2.31	-2.39	-0.13	-0.16	-0.16
VL_3^{2-}/VL_3^{3-}	-2.73	——	——	-0.63	——	——

TABLE 6

THE HALF-WAVE POTENTIALS FOR TRIS-BIPYRIDINE COMPLEXES OF TITANIUM IN DMF AND MOLYBDENUM IN DMF AND THF CONTAINING 0.2 M TBAP

Redox system	Solvent	$E_{\frac{1}{2},C}$/V vs. SCE
$Ti(bipy)_3/Ti(bipy)_3^-$	DMF	-1.51
$Ti(bipy)_3^-/Ti(bipy)_3^{2-}$	DMF	-1.97
$Mo(bipy)_3^+/Mo(bipy)_3$	DMF	-1.13
$Mo(bipy)_3/Mo(bipy)_3^-$	DMF	-1.72
$Mo(bipy)_3^-/Mo(bipy)_3^{2-}$	DMF	-2.14
$Mo(bipy)_3^+/Mo(bipy)_3$	THF	-1.11
$Mo(bipy)_3/Mo(bipy)_3^-$	THF	-1.80
$Mo(bipy)_3^-/Mo(bipy)_3^{2-}$	THF	-2.15
$Mo(bipy)_3^{2-}/Mo(bipy)_3^{3-}$	THF	-2.9

TABLE 7

THE NUMBER OF UNPAIRED ELECTRONS OF TRIS-BIPYRIDINE COMPLEXES OF TRANSITION METALS ESTIMATED FROM THE LITERATURE DATA ON MAGNETIC MOMENTS[b]

Oxidation state	d-electron number						
	3	4	5	6	7	8	9
+3	Cr(3)		Fe(1)	Co(0)			
+2	V(3)	Cr(2)	Mn(5)	Fe(0)	Co(3)		
+1		V(?)	Cr(1)		Fe(p)[a]	Co(2)	
0		Ti(0)	V(1)	Cr(0)	Mn(3?)	Fe(p)[a]	Co(1)
-1			Ti(1)	V(0)	Cr(1)	Mn(2?)	Fe(p)[a]
-2				Ti(0)	V(1)	Cr(2)	
-3						V(2)	Cr(3)

a Magnetic-moment data is lacking but an e.s.r. spectrum is observed.

b Ref. 11 - 14.

TABLE 8

THE $\Delta E_{\frac{1}{2}}$ VALUES FOR TRIS-BIPYRIDINE COMPLEXES OF TRANSITION METALS

Central metal	$\Delta E_{\frac{1}{2}}$/V				
	d-electron number				
	4	5	6	7	8
Ti		0.46			
V	0.10	0.44	0.68	0.50	
Cr	0.49	0.50	0.63	0.35	0.25
Mo			0.59	0.42	0.7-0.8
Mn			0.17	0.22	0.22
Fe			2.32	0.18	0.26
Ru			2.58	0.18	0.25
Os			2.02	0.18	0.32

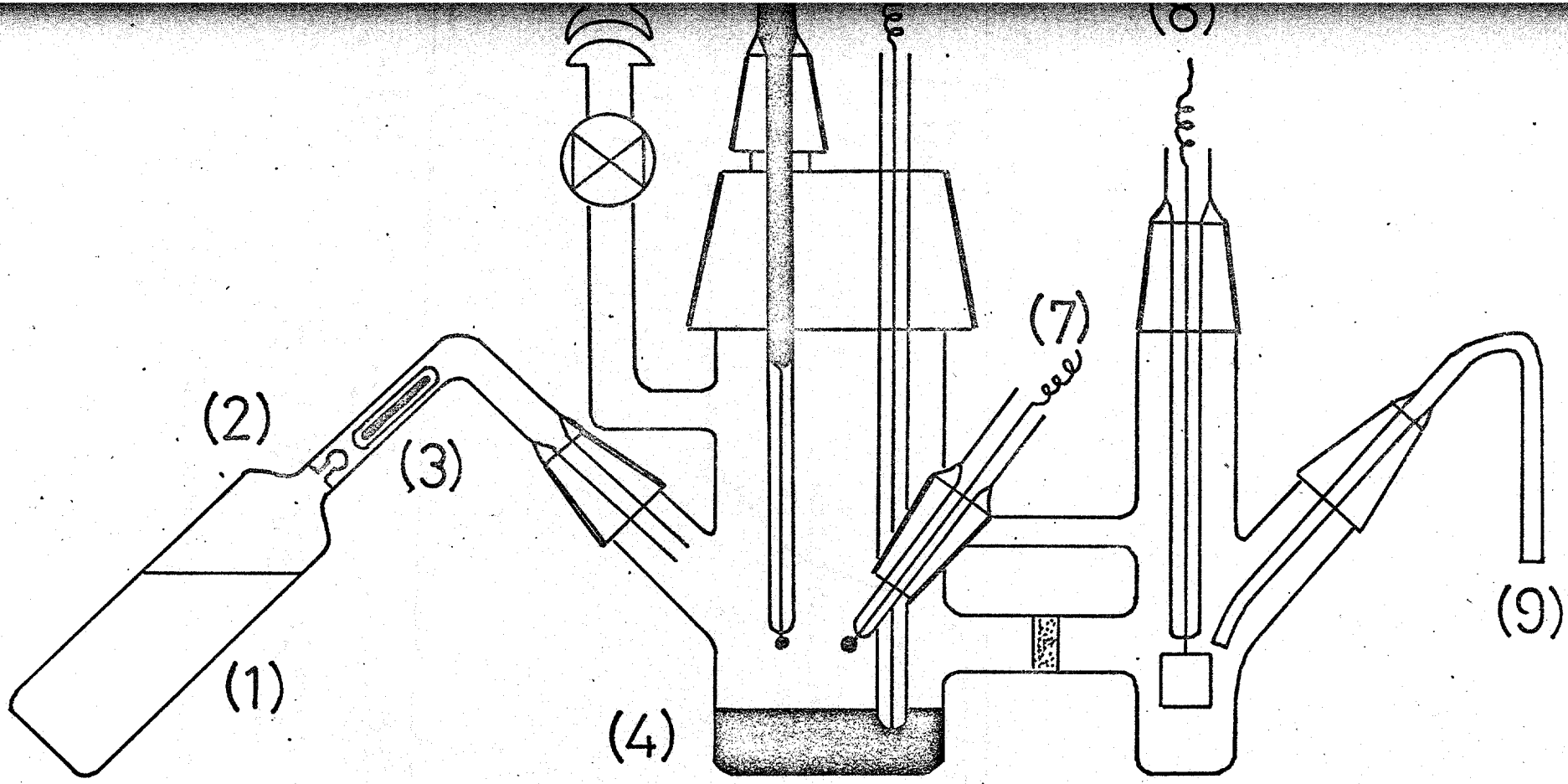

Fig. 16. Electrolysis cell: (1) electrolytic soln., (2) breakable seal, (3) hammer, (4) mercury pool, (5) joint to vacuum line and inlet for nitrogen gas, (6) dropping mercury electrode, (7) platinum electrode A, (8) platinum electrode B, (9) agar bridge, connected to SCE.

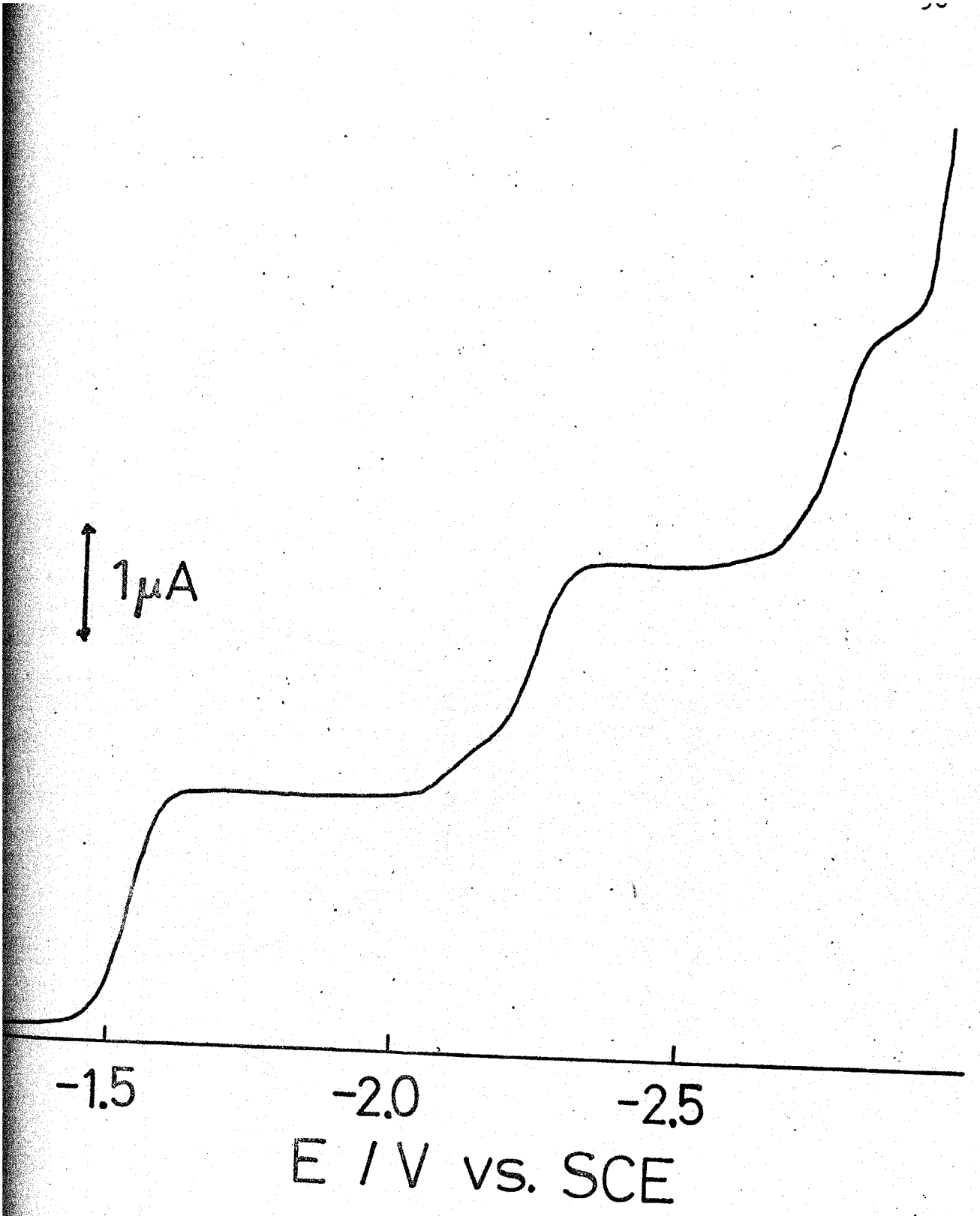

Fig. 17. Cathodic polarogram for 1 mM $V(bipy)_3$ in DMF soln. of 0.2 M TBAP.

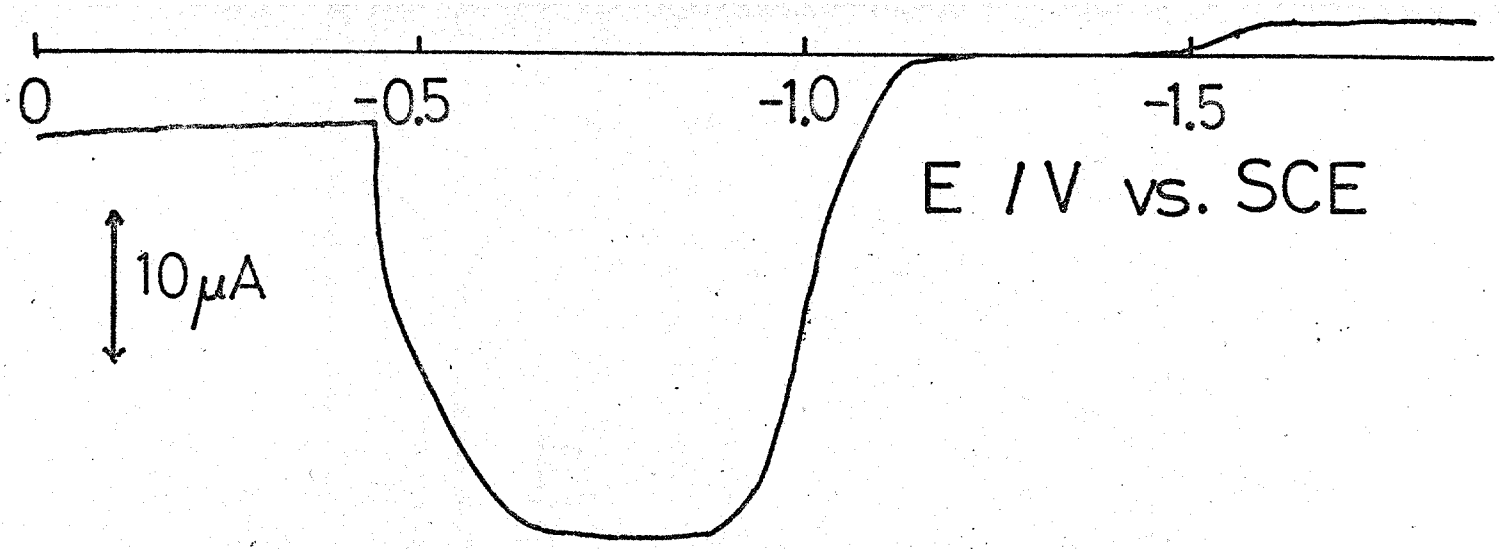

Fig. 18. Cathodic-anodic polarogram for 1 mM $V(bipy)_3$ in DMF soln. of 0.2 M TBAP.

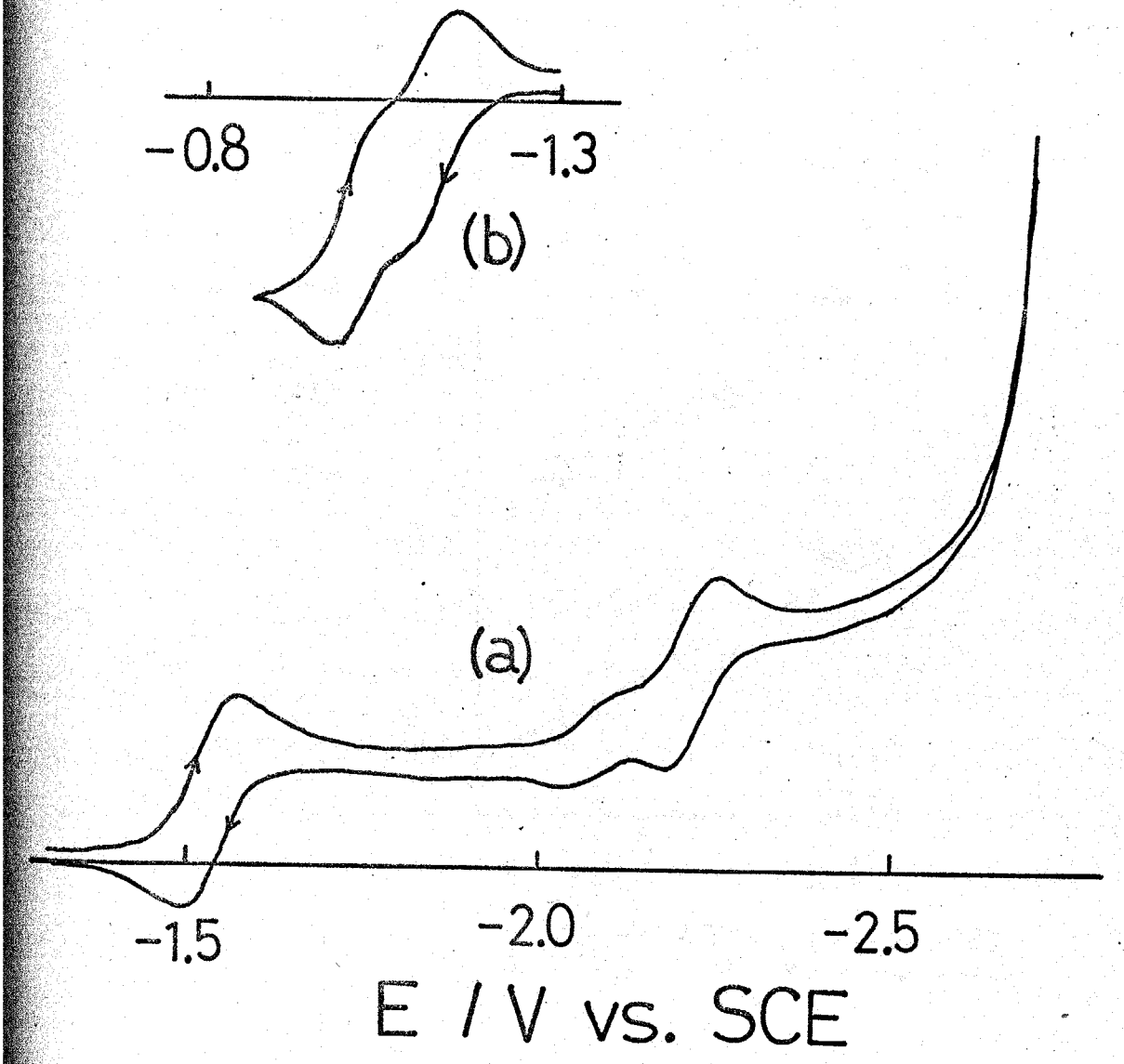

Fig. 19. Cyclic voltammograms with initial (a) cathodic scan and (b) anodic scan for 1 mM $V(bipy)_3$ in DMF soln. of 0.2 M TBAP. Scan rate 0.1 V s^{-1}.

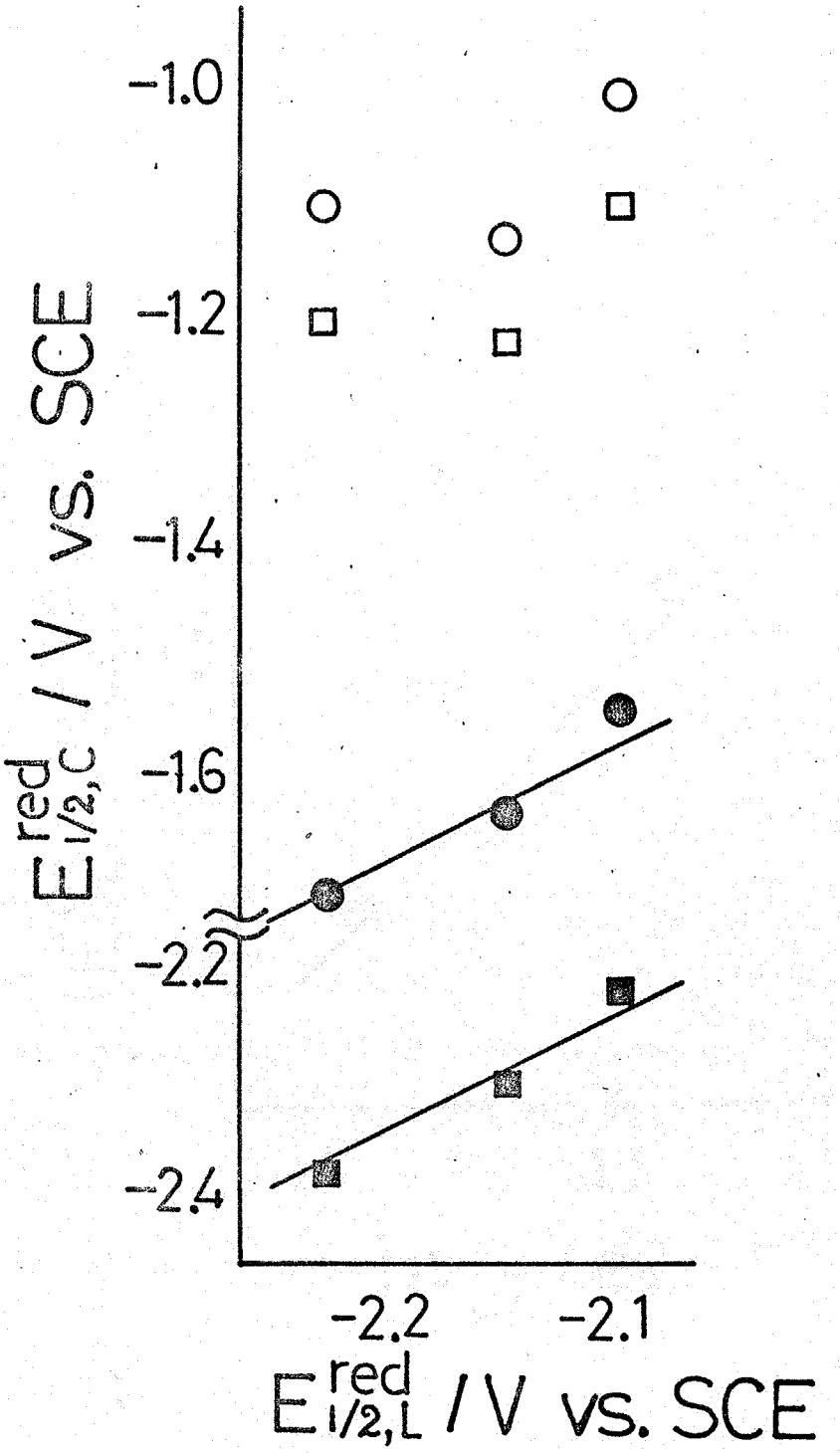

Fig. 20. Plot of reduction half-wave potentials for (○) VL_3^{2+}/VL_3^{+}, (□) VL_3^{+}/VL_3, (●) VL_3/VL_3^{-}, (■) VL_3^{-}/VL_3^{2-}, $E^{red}_{½,C}$, vs. those for L/L^{-}, E^{red}_{L}. L = bipy, 4-dmbipy, 5-dmbipy.

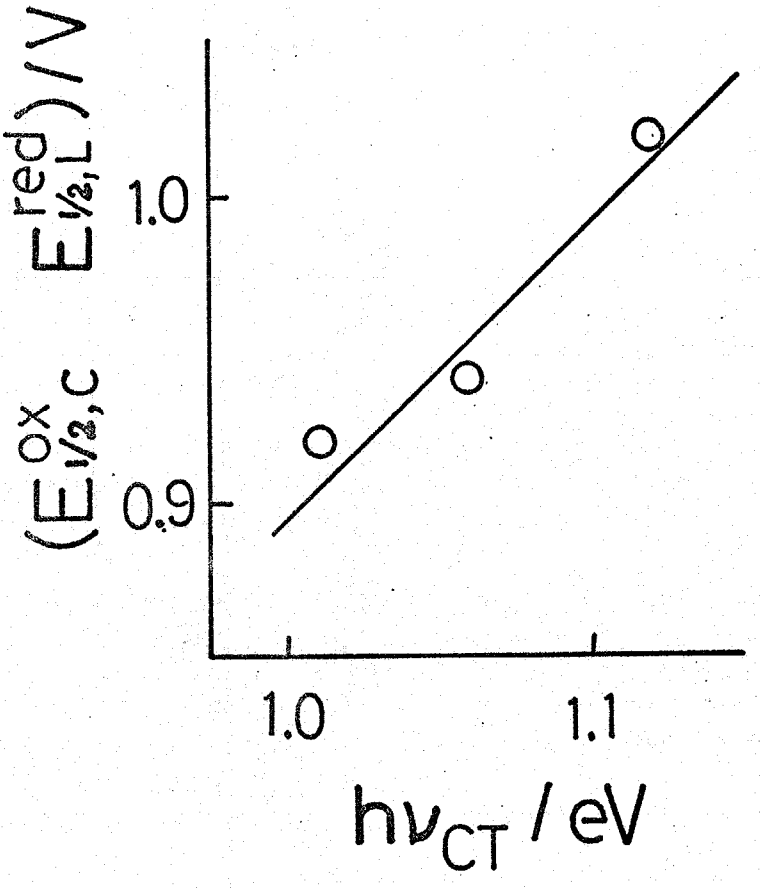

potential

Fig. 21. Plot of half-wave difference, $E^{ox}_{½,C} - E^{red}_{½,L}$, vs. charge transfer energy for VL_3 in DMF soln. of 0.2 M TBAP. L = bipy, 4-dmbipy; 5-dmbipy.

Data of charge transfer energies are obtained from Ref. 15.

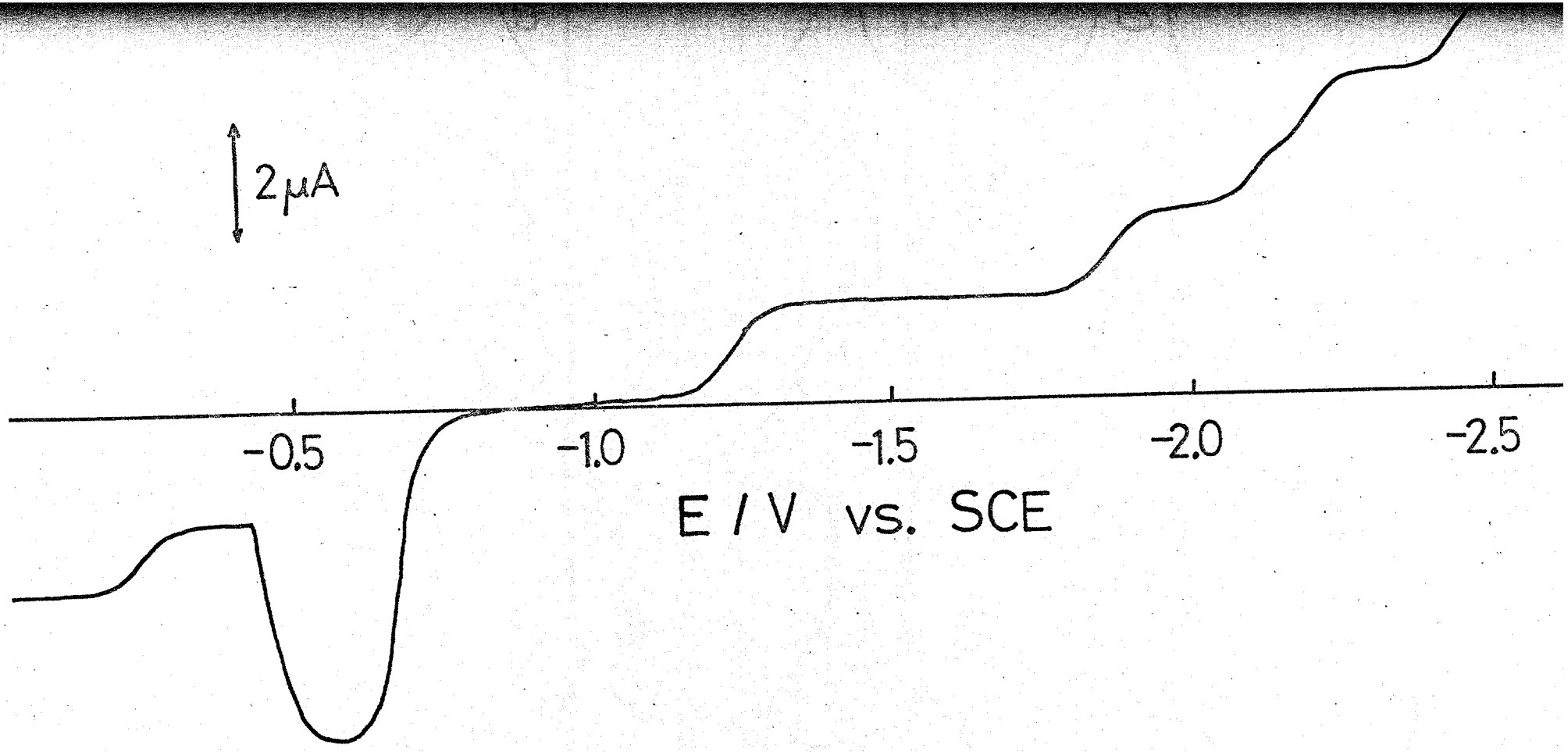

Fig. 22. Cathodic-anodic polarogram for 1 mM $Cr(bipy)_3ClO_4$ in DMF soln. of 0.2 M TBAP.

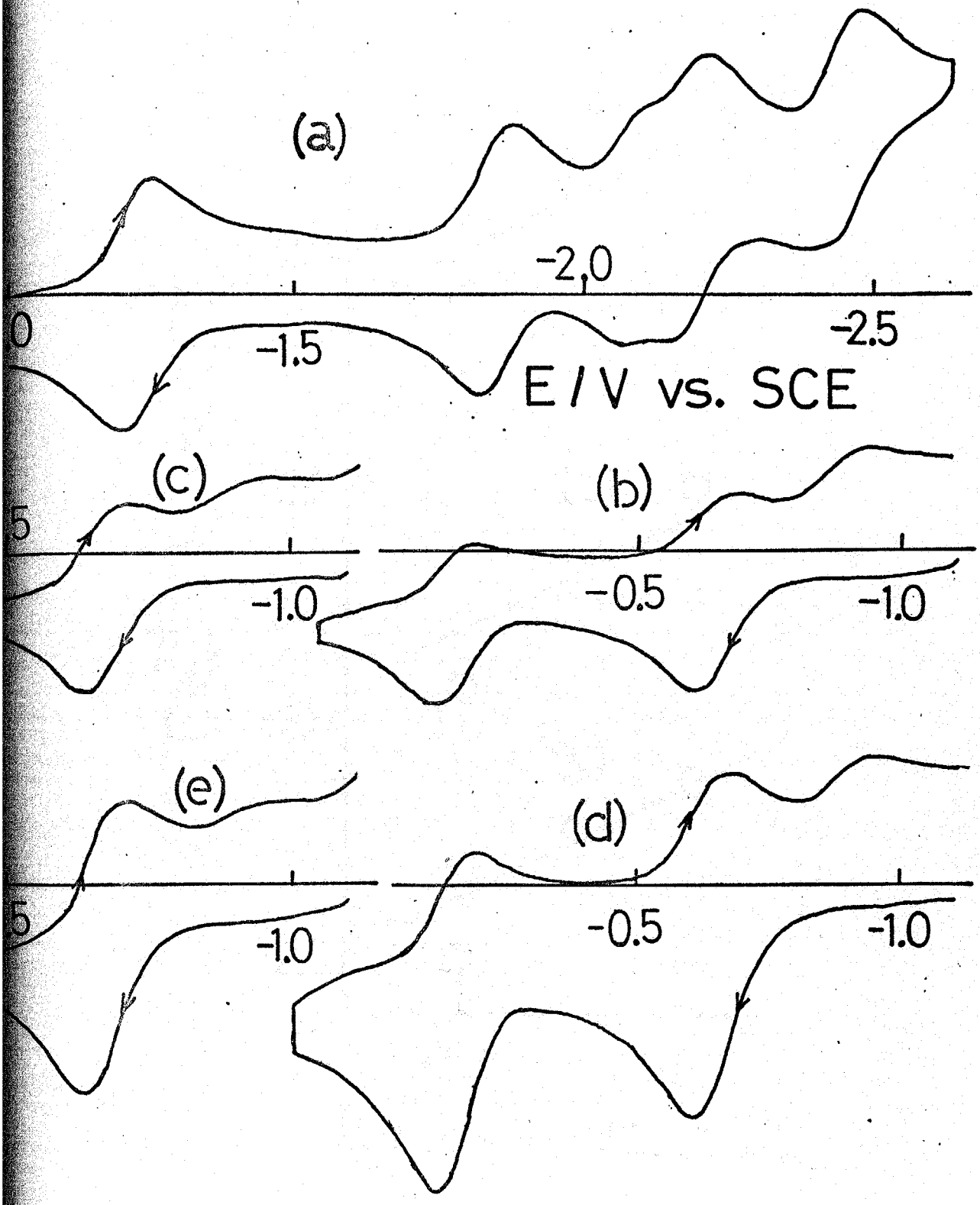

Fig. 23. Cyclic voltammograms with initial (a) cathodic scan and (b), (c), (d), (e) anodic scan for 1 mM $Cr(bipy)_3$-ClO_4 in DMF soln. of 0.2 M TBAP. Scan rate (a), (b), (c)

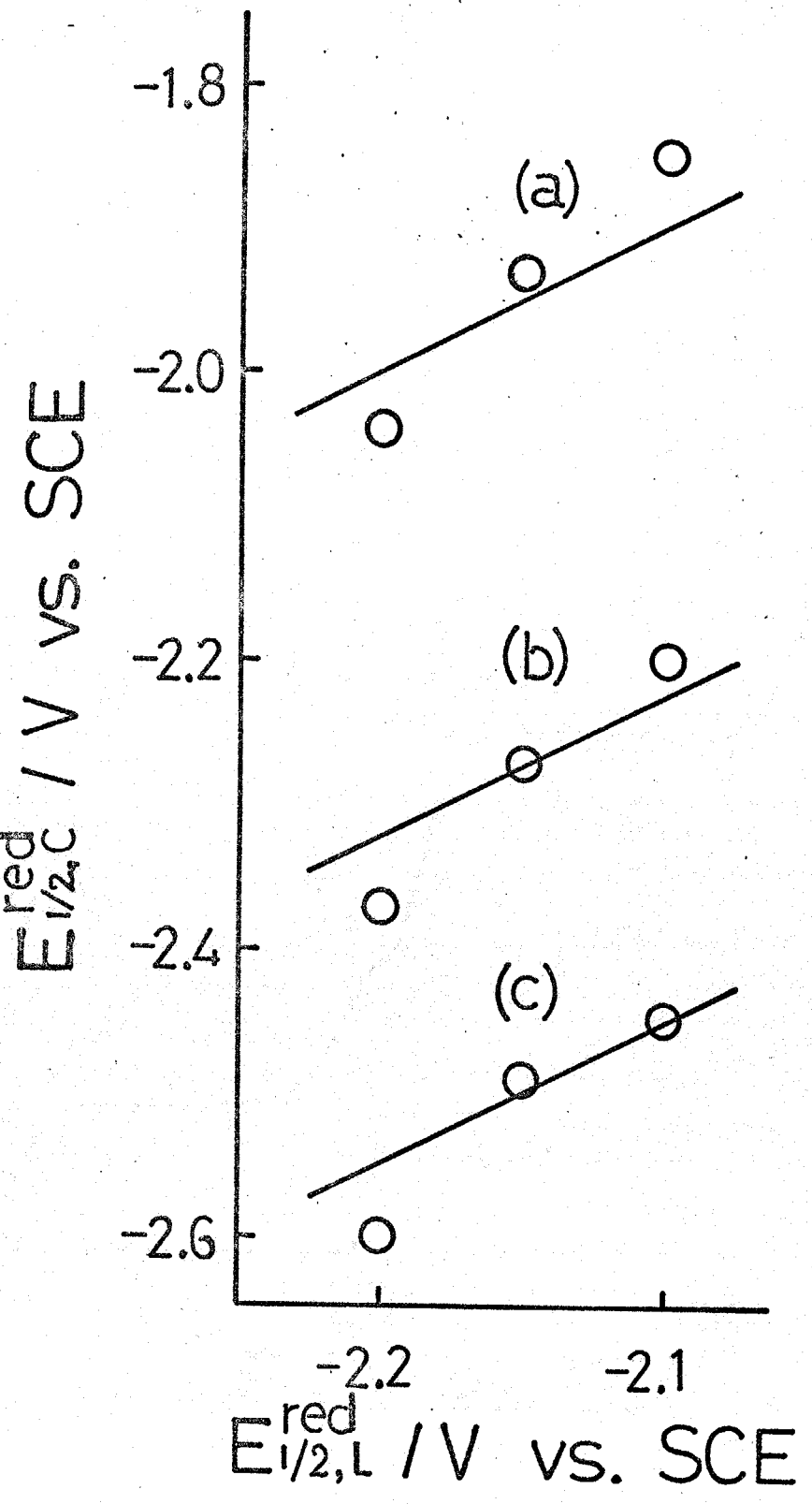

Fig. 24. Plot of reduction half-wave potentials for (a) CrL_3/CrL_3^-, (b) CrL_3^-/CrL_3^{2-} and (c) CrL_3^{2-}/CrL_3^{3-} systems, $E^{red}_{½,C}$, vs. those for L/L^- systems, $E^{red}_{½,L}$. L = bipy, 4-dmbipy, 5-dmbipy.

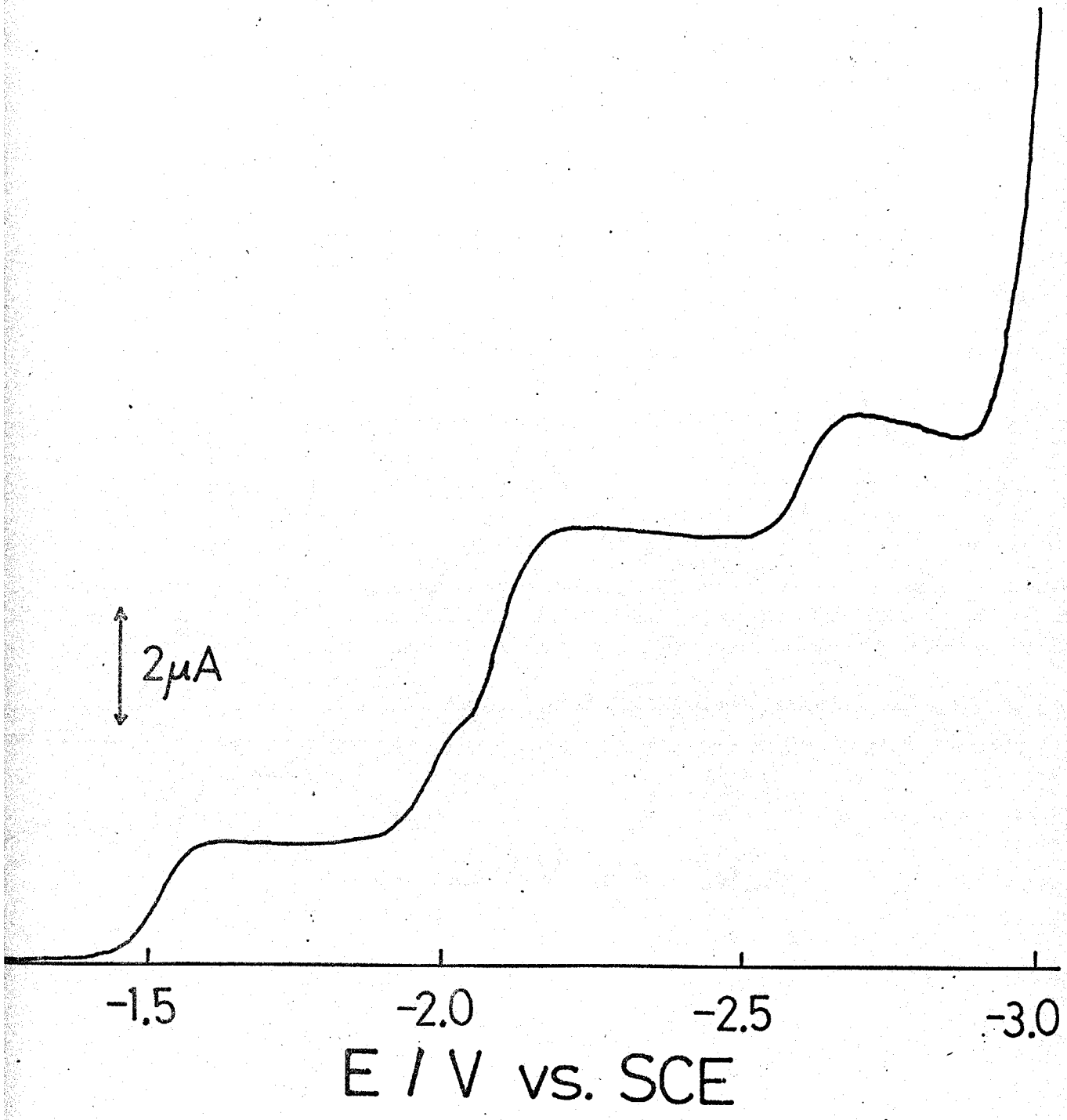

Fig. 26. Cathodic polarogram for 1 mM $Ti(bipy)_3$ in DMF soln. of 0.2 M TBAP.

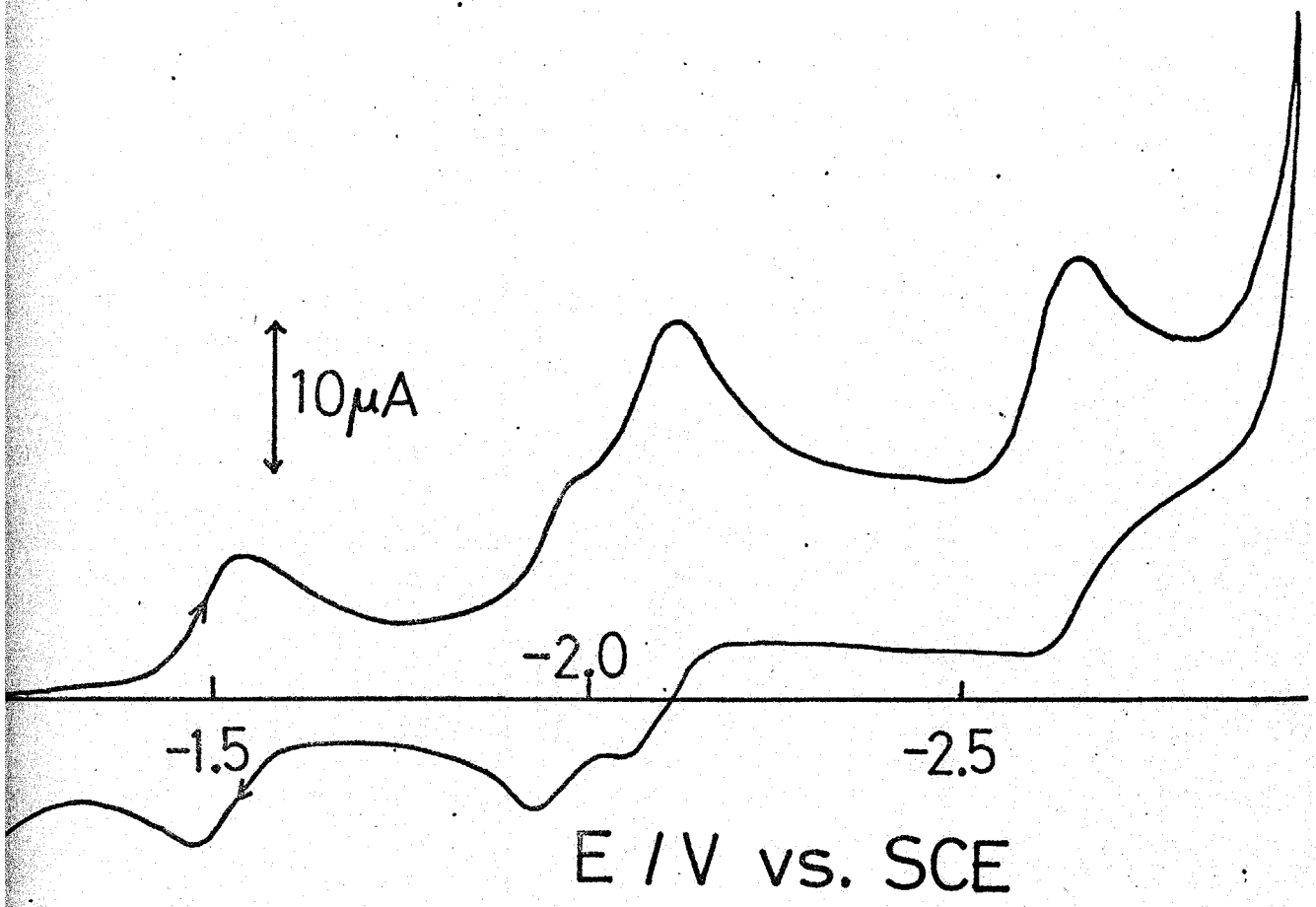

Fig. 26. Cyclic voltammogram with initial cathodic scan for 1 mM $Ti(bipy)_3$ in DMF soln. of 0.2 M TBAP.

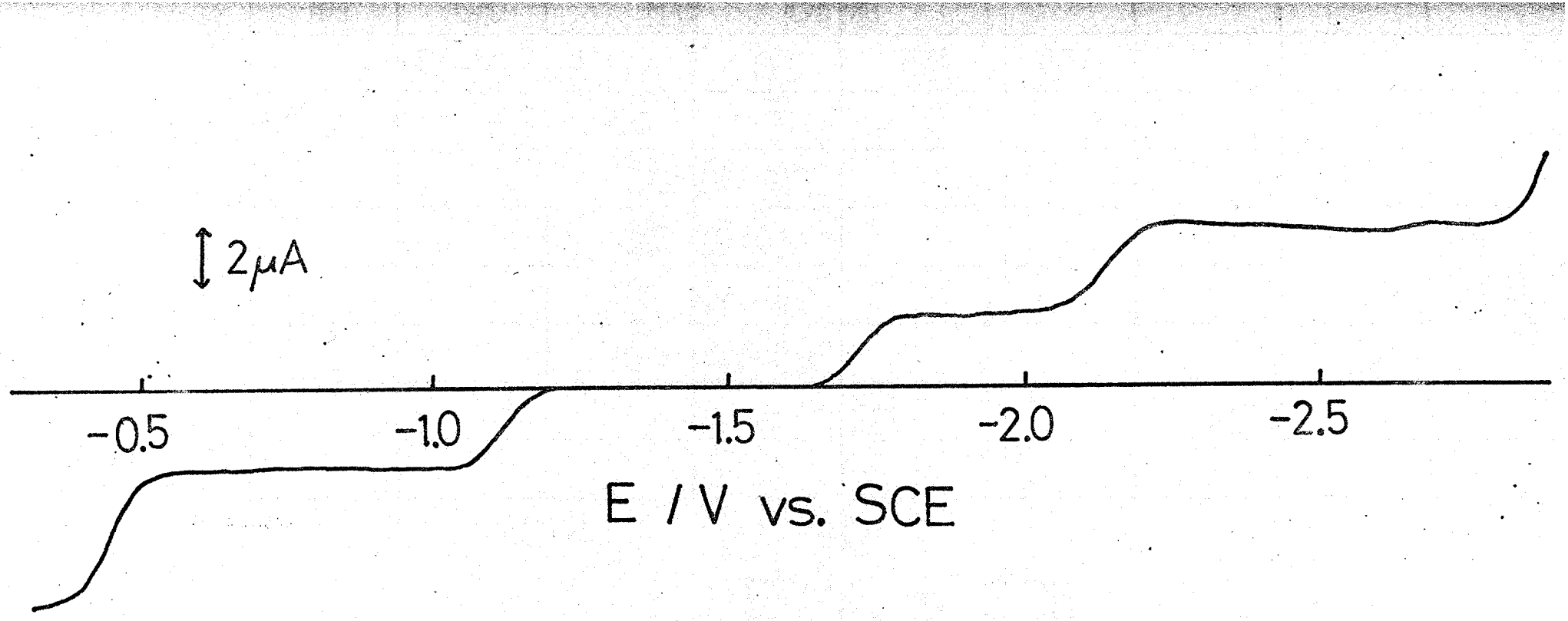

Fig. 27. Cathodic-anodic polarogram for 1 mM $Mo(bipy)_3$ in DMF soln. of 0.2 M TBAP.

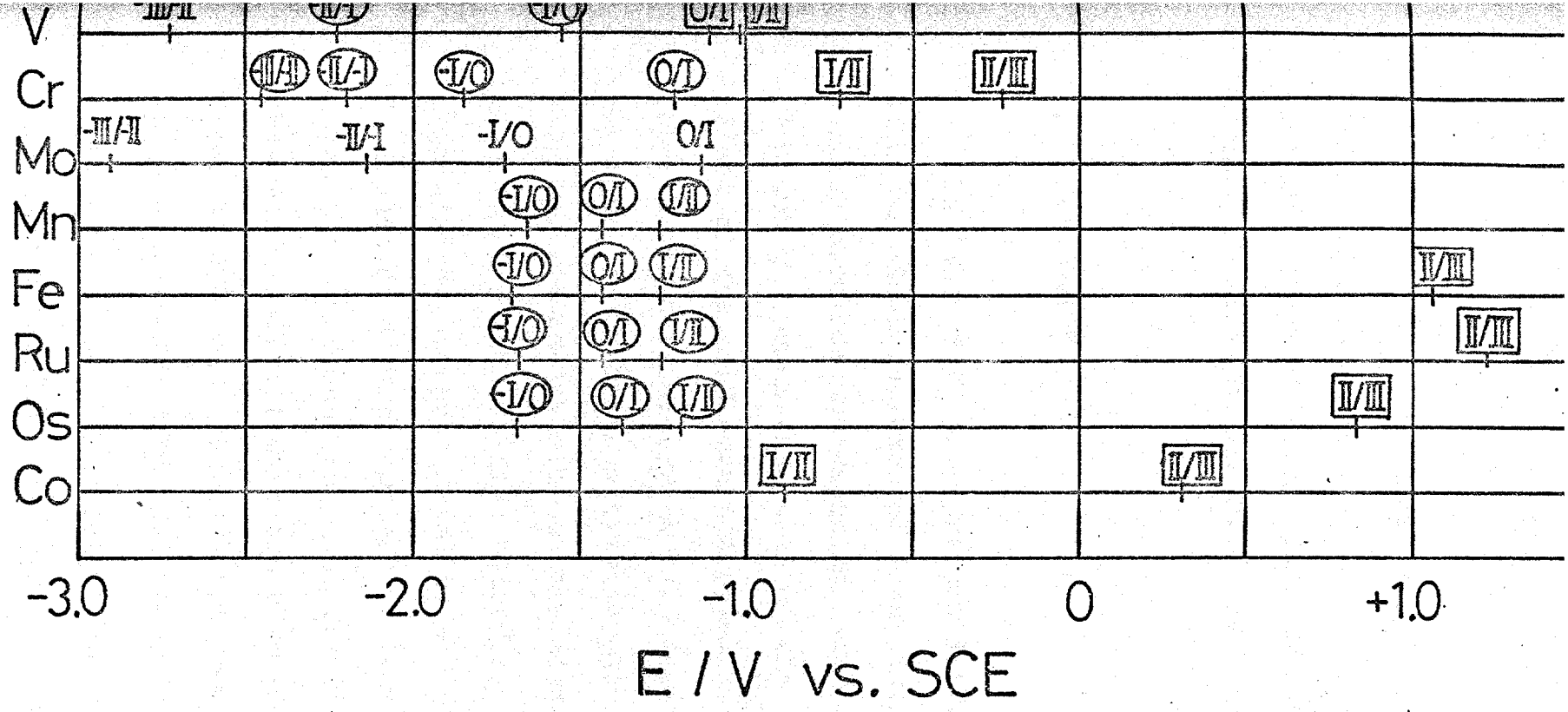

Fig. 28. Schematic illustration of the half-wave potentials of trisbipyridine complexes of transition metals in DMF and their shifts on methyl substitution. (I/II) means that the half-wave potentials for ML_3^{+}/ML_3^{2+} become more negative in the order bipy < 4-dmbipy < 5-dmbipy and [I/II], in the order bipy < 5-dmbipy < 4-dmbipy.

CHAPTER III

ELECTROCHEMICAL ELECTRON-TRANSFER RATES OF TRIS(2,2'-BIPYRIDINE) COMPLEXES OF IRON, RUTHENIUM, OSMIUM, CHROMIUM, TITANIUM, VANADIUM AND MOLYBDENUM

a. INTRODUCTION

In Chapter II and Appendix I twenty seven systems of bipyridine complexes of iron, ruthenium, osmium, cobalt, chromium and vanadium have been classified into two groups on the basis of the methyl-substitution effect on the half-wave potential. The half-wave potetial of a redox system of one group becomes more negative, on methyl-substitution, in the order bipy < 5-dmbipy < 4-dmbipy. The excess electron in the reductant species of a redox system belonging to this group was concluded to occupy a metal t_{2g}-orbital on the basis of the discussion on the correlation between half-wave potentials and frequencies of the charge-transfer bands. This was consistent with the data on their magnetic moments. Only exception was the CoL_3^{3+}/CoL_3^{2+} system whose electronic configuration was believed to be $t_{2g}^6/t_{2g}^5e_g^2$. Here L is bipy, 4-dmbipy, or 5-dmbipy. The half-wave potential of a redox system of the other

group becomes more negative in the order bipy < 4-dmbipy < 5-dmbipy. A discussion on the correlation between the half-wave potential of a complex and that of the free ligand led to the prediction that the excess electron occupies a ligand π^*-orbital of the reductant complex. The $CrL_3^+(t_{2g}^5)/CrL_3(t_{2g}^6)$ and $VL_3(t_{2g}^5)/VL_3^-(t_{2g}^6)$ systems were exceptions. It has been discussed in Chapter II.

The aim of this chapter is to find the correlation between the electron-transfer rates and the electronic configurations of these complexes and some other related ones.

b. EXPERIMENTAL

All chemicals and voltammetric measurements were described in Chapter II. Every solution contained a 2 mM complex and 0.2 M TBAP in DMF. A platinum spherical electrode or a dropping mercury electrode (DME) was served as a working electrode. Before each run of experiments, the platinum electrode was treated as follows: it was washed in distilled water, wiped with a filter paper and then polished with a finest abrasive paper. The surface area of the platinum electrode was determined by a geometric method as 6.1×10^{-2} cm^2. That of the mercury pool electrode

was about 10 cm^2. Solutions were prepared with the procedure described in Chapter II-C. The Pyrex-glass electrolysis cell shown in Fig. 16 was used for kinetic measurements by the galvanostatic double-pulse (g.d.p.) mehtod with a preceding polarographic electrolysis[1]. Measurements were performed on an apparatus deviced in this laboratory[1,2]. The cell responce to a g.d.p. was observed with an Iwatsu SS5157 cathode-ray oscilloscope. A standard rate constant was assumed to be identical with the rate constant at a reversible half-wave potential. Analysis procedure is found in the literature cited[1]. Voltammetric and g.d.p. measurements were carried out at room temperature maintained at 25 ± 2 °C.

c. RESULTS

The polarograms and cyclic voltammograms for FeL_3^{2+}, $FeL_2(CN)_2$, RuL_3^{2+}, OsL_3^{2+}, CrL_3^{+}, CrL_3, VL_3, TiL_3, and MoL_3 in DMF solutions have been given in Chapter II and Appendix I. L designates 2,2'-bipyridine in this chapter. The stability and assignment of the complexes in various oxidation states were confirmed in the following way.

Figure 29 typically shows the polarograms for OsL_3^{2+}, OsL_3^{+} and OsL_3 taken in the course of a controlled-potential electrolysis at -2.0 V of a solution initially containing OsL_3^{2+}. Their wave-heights and half-wave potentials are almost invariant. This indicates that the complexes are sufficiently stable for kinetic measurements to be performed on them and that the half-wave potentials in the polarogram for OsL_3^{2+} can be assigned to the redox systems OsL_3^{2+}/OsL_3^{+}, OsL_3^{+}/OsL_3 and OsL_3/OsL_3^{-}. Further electrolysis yielded a polarogram for OsL_3^{-}. The OsL_3/OsL_3^{-} system was also concluded to be stable on the same basis. The same kind of experiments were performed on FeL_3^{2+}/FeL_3^{+}, FeL_3^{+}/FeL_3, FeL_3/FeL_3^{-}, RuL_3^{2+}/RuL_3^{+}, RuL_3^{+}/RuL_3 and RuL_3/RuL_3^{-} with the result that they are stable and the assignment of the oxidation states described in Chapter II is correct. It was found in Chapter II-C that CrL_3^{2+} and TiL_3 were insufficiently stable in DMF solutions. Thus the standard rate constant for the CrL_3^{2+}/CrL_3^{+} redox system obtained by the g.d.p. method with in situ generation of CrL_3^{2+} should be a lower limit. The complex TiL_3 in DMF was found to decompose slowly. Its concentration was determined polarographically assuming that the diffusion coefficient of TiL_3 is equal to that of VL_3. The diffusion coefficients for most complexes were determined polarographically

with the aid of the controlled-potential electrolysis as shown in Fig. 29.

The slope of every linear plot of overpotential vs. square root of the first-pulse width obtained by g.d.p. measurements was fairly in good agreement with the slope calculated [2], by use of the known diffusion coefficients of the reductant and the oxidant species. When the diffusion coefficient of either species was not available, the slope was calculated by assuming that both diffusion coefficients were identical. The observed standard rate constants (k^o) are listed in Tables 9 and 10 together with the half-wave potentials ($E_{1/2}$). The excess electron of the reductant species of a redox system in Table 9 occupies a metal t_{2g}-orbital and that of a redox system in Table 10 a ligand π^*-orbital. The Tables involve also the standard rate constants corrected for the potential of the diffuse double-layer (k^o_{cor}) with the procedure of Frumkin. The double-layer correction was not performed on the data obtained with the platinum electrode, because the data on ϕ_2-potential were not avalable. The direction of shift of each standard rate constant when it is corrected with the point of zero-charge being assmed to fall within the range 0.4 to -0.4 V vs. SCE[3] is shown in the Tables.

d. DISCUSSION

The observed rate constants in Table 9, as a whole, are larger than those in Table 10: the former ones range from 1.3 to 0.8 cm s^{-1}, while the latter ones from 0.3 to 0.1 cm s^{-1}. The rate constant for the VL_3^{2+}/VL_3^{+} system is exceptionally small. This will be discussed later. It is worth noting that the rate constants in either Table were affected much by neither the intrinsic nor the extrinsic conditions: redox potentials ranging from +1.03 to -1.54 V (Table 9) and from -1.18 to -1.86 V (Table 10), oxidation states of the oxidant species ranging from +3 to 0 (Table 9) and +2 to 0 (Table 10), kinds of solvent (DMF and water) or kinds of electrode (DME and platinum). This fact suggests that the electron transfer complexes at electrodes are governed predominantly by their electronic configurations.

The dependende of the electron-transfer rate on the electronic configurations of the reactants has been discussed by a few authors[5-9]. The following experimental facts are known concerning the electron-exchange of metal complexes in solution: the electron-exchange rate is high when the electronic configuration of a reactant complex differs from that of the other

reactant by one in the number of electrons in the low-lying t_{2g}-orbitals. The rate is much lower in the cases where an e_g-electron is transferred or where the central metals in the reduction and the oxidant are in different crystal fields. This has been explained as follows: the t_{2g}-orbitals are delocalized over the molecule under the formation of metal-to-ligand π-bondings. This may cause little change in molecular geometry between the oxidant and the reductant and, in its turn, small activation energy. The energy for changing the molecular geometry is formulated in the Marcus-Hush theory as the inner-sphere reorganization energy[5-9]. Consequently the rate is high when a t_{2g}-electron is transferred, but otherwise lower, because more extensive changes in bond lengths and molecular geometry are required.

The correlation between the electronic configuration and the electron-transfer rate at electrode has been discussed from the analogy to the homogeneous reactions[6-8]. Such an explanation may be reasonable because there is some evidence for the mechanistic parallelism between homogeneous and electrochemical electron-transfer reactions[10]. However, the discussion has been made on the basis of a few data and no systematic studies have been reported before this investigation. Moreover, the inorganic redox reactions cited above are limited to those in

which either a t_{2g}- or an e_g-electron is transferred and comparison is established among inert complexes and labile ones. Almost all the complexes in Tables 9 and 10 are inert under the experimental conditions. Thus it may be more rational to ascribe the difference in the rate constant between these Tables to the difference in electronic configuration. The previous discussion was based on a notable difference in rate constants caused by a notable change in molecular geometry and it led to an explanation that the electronic configuraiton affects indirectly the rate constant via the atomic configuration. The results of the present investigation can be explained in the same way: noting that the metal t_{2g}- and the ligand π^*-orbitals are both of π-character, a smaller change in the electronic configuration caused a smaller change in molecular geometry and in turn a smaller change in electron-transfer rate. However, the fact that the rate constant for the bipy/bipy$^-$ system was nearly equal to the rate constants in Table 10 suggests that a certain factor other than the atom-reorganization energy is operative as a rate determining factor. The reasons are as follows: according to the Chapter II the π-electron in the complexes in Table 10 is partly localized on a ligand bipyridine molecule and consequently the chemical environment of the excess π^*-electron of the free bipyridine anion and that of the coordinated one may be

nearly identical. Combined with the fact that the electron-transfer rates for the redox systems with the electronic configurations $t_{2g}^6/t_{2g}^6\pi^*$, $t_{2g}^6\pi^*/t_{2g}^6\pi^{*2}$ and $t_{2g}^6\pi^{*2}/t_{2g}^6\pi^{*3}$ are nearly equal, this points to a small contribution of the inner-sphere reorganization energy to the total activation free energy, as is known for the systems of the type R/R^-, where R is an aromatic hydrocarbon. The contribution from the outer-sphere reorganization energy is also considered to be small, because a large difference in the molecular dimension between the complex and the free ligand caused only a little difference in the rate constant. This suggests the direct contribution of the electronic states of the reductant and the oxidant to the rate constant.

The redox systems in Table 9 and those of the form R/R^- are nearly identical in both the homogeneous and electrochemical rate constants: the homogeneous rate constant is about 10^9 M^{-1} s^{-1} for a reaction where coulomb repulsion energy is negligible and the latter about 1 cm s^{-1} when no double-layer correction is applied. The homogeneous exchange rate constants for the redox systems in table 10 except the bipy/bipy$^-$ system have not yet been reported. By analogy they should be of the same order with the rate constant for the bipy/bipy$^-$ system[11], 5×10^6 M^{-1} s^{-1}. The difference in the

homogeneous rate constant between the systems R/R^- and $bipy/bipy^-$ can be attributed to the difference in the degree of delocalization of the π-orbitals and in its turn to the difference in the inner-sphere reorganization energy.

The above discussion is based on the observed rate constants uncorrected for the potential of the diffuse double-layer. As seen from Tables 9 and 10 when a double-layer correction is applied on them, some become larger and others become smaller than the uncorrected ones. Thus the resultant values in each Table scatter over two or three orders of magnitude and the classification of the redox systems into two groups makes no sense. The corrected rate constants become smaller in the order ML_3^{3+}/ML_3^{2+} $(t_{2g}^{n}/t_{2g}^{n+1}) > ML_3/ML_3^{-}$ $(t_{2g}^{n}/t_{2g}^{n+1}$, $t_{2g}^{6}\pi^{*}/t_{2g}^{6}\pi^{*2})$ ML_3^{2+}/ML_3^{+} $(t_{2g}^{n}/t_{2g}^{n+1}$, $t_{2g}^{6}/t_{2g}^{6}\pi^{*}$, $t_{2g}^{6}\pi^{*2}/t_{2g}\pi^{*3}) > ML_3^{+}/ML_3$ $(t_{2g}^{n}/t_{2g}^{n+1}$, $t_{2g}^{6}/t_{2g}^{6}\pi^{*})$, where M is any one of the central metals Fe, Ru, Os, Cr, Mo, V and Ti and n is an integer within 3 - 6. This should be taken to imply that the electrostatic interaction between the electrode and the oxidant or the reductant is a predominant factor determining the rate constant and is not a small perturbation. The corrected rate constant for a redox system should be an intrinsic property of the system; in other words, it should reflect the molecular properties which may affect the electron-transfer rate. In view of this, the corrected rate constants cannot be better rate constants than uncorrected

ones. One of the reasons is the absence of the superiority of the t_{2g}-electron transfer over the π^*-electron transfer in the above sequence of the rate constants. The absence of the parallelism between corrected rate constants and their respective homogeneous rate constants is another reason. The homogeneous rate constant for the CrL_3^+/CrL_3 system[12] is 1.5×10^9 M^{-1} s^{-1}, indicating that this reaction belongs to a category of the fastest reaction to which several redox systems of the type R/R^- also belong [14]. The uncorrected electrochemical rate constant of a reaction of this category is of the order 1 cm s^{-1}. When a double-layer correction is applied, the rate constant for a R/R^- system is shifted to a direction different from that to which the CrL_3^+/CrL_3 system is shifted. The corrected rate constants are of the order of 10 cm s^{-1} and 0.3 cm s^{-1} for the R/R^- system[14,15] and the CrL_3^+/CrL_3 system respectively. In conclution a set of uncorrected rate constants may provide a more reasonable basis for discussion than that of corrected ones.

The standard rate constant for the VL_3^{2+}/VL_3^+ system, 0.35 cm s^{-1}, is exceptionally small anong others in Table 9. This may be caused by the crystal-field splitting of the d-orbitals of the VL_3^+ complex in a way different from that of other complexes in this Table. In Chapter II, the anomalous proxity of the half-wave potentials for

the VL_3^{2+}/VL_3^{+} and VL_3^{+}/VL_3 systems was explained tentatively, assuming the electronic configurations t_{2g}^{3}, $e_g'^{4}$ and $e_g'^{4}a$ for VL_3^{2+}, VL_3^{+} and VL_3 respectively. A change in electronic configuration from t_{2g}^{3} to $e_g'^{4}$ may require more extensive change in the molecular geometry than from t_{2g}^{3} to t_{2g}^{4}, which may account for the small rate constant.

e. REFERENCES

1 H. Mizota, H. Matsuda, Y. Kanzaki and S. Aoyagui, J. Electroanal. Chem., 45, 385 (1973).

2 T. Rohko, M. Kogoma and S. Aoyagui, J. Electroanal. Chem., 38, 45 (1972).

3 R. S. Perkins and T. N. Andersen in J. O'M. Bockris and B. E. Conway (Eds.), Modern Aspects of Electrochemistry, No. 5, Butterworths, London, 1969, p. 253, Table 1.

4 F. Basolo and R. G. Pearson, Mechanisms of Inorganic Reactions, John Wiley, New York, 1967.

5 N. S. Hush, Electrochim. Acta, 13, 1005 (1968).

6 R. A. Marcus, Background Material and Lecture Note for First and Second International Summer Schools on Quantumn Mechanical Aspects of Electrochemistry, Ohrid, Yugoslavia, 1971-1972, p. 72.

7 A. A. Vlček, Collection Czech. Chem. Commun., 20, 894 (1955).

8 A. A. Vlček in F. A. Cotton (Eds.), Progress in Inorganic Chemistry, Vol. 5, Interscience, New York, 1963, p. 289.

9 R. A. Marcus, J. Chem. Phys., 43, 679 (1965).

10 R. A. Marcus, J. Phys. Chem., 67, 853 (1963).

11 W. L. Reynolds, J. Amer. Chem. Soc., 67, 2866 (1963).

12 T. Saji and S. Aoyagui, Bull. Chem. Soc. Japan, 46, 2101 (1973), (Chapter IV-A).

13 K. Suga, S. Ishikawa and S. Aoyagui, Bull. Chem. Soc. Japan, 46, 808 (1973).

14 H. Mizota, K. Suga, Y. Kanzaki and S. Aoyagui, J. Electroanal. Chem., 44, 471 (1973).

15 M. E. Peover in N. S. Hush (Ed.), Reactions of Molecules at Electrodes, Wiley-Interscience, London, 1971, p. 259.

TABLE 9

DATA ON RATES OF ELECTRODE REACTIONS INVOLVING ELECTRON TRANSFER OF A t_{2g}-ELECTRON L = 2,2'-BIPYRIDINE

Redox systems	Electrode	$E_{\frac{1}{2}}$/V SCE	k°/cm s^{-1}	ϕ_2/mV	k°_{cor}/cm s^{-1}
$TiL_3(t_{2g}^4)/TiL_3^-(t_{2g}^5)$	DME	-1.506	(~0.5)	-91	~3
$VL_3^{2+}(t_{2g}^3)/VL_3^+(t_{2g}^4)$	DME	-1.012	0.35	-76	0.05
$VL_3^+(t_{2g}^4)/VL_3(t_{2g}^5)$	DME	-1.113	1.2±0.2	-80	0.3
$VL_3(t_{2g}^5)/VL_3^-(t_{2g}^6)$	DME	-1.540	0.66±0.05[a]	-91	~4
$CrL_3^{2+}(t_{2g}^4)/CrL_3^+(t_{2g}^5)$	DME	-0.72	(>0.4)	-59	>0.01
$CrL_3^{2+}(t_{2g}^4)/CrL_3^+(t_{2g}^5)$	Pt	-0.68	(>0.5)		<0.5
$CrL_3^+(t_{2g}^5)/CrL_3(t_{2g}^6)$	DME	-1.20	1.3±0.2	-82	0.3
$CrL_3^+(t_{2g}^5)/CrL_3(t_{2g}^6)$	Pt	-1.22	0.88±0.13		<0.9
$MoL_3^+(t_{2g}^5)/MoL_3(t_{2g}^6)$	DME	-1.127	1.3±0.2	-80	0.3
$FeL_3^{3+}(t_{2g}^5)/FeL_3^{2+}(t_{2g}^6)$	Pt	+1.03	0.80±0.08		>0.8
$FeL_3^{3+}(t_{2g}^5)/FeL_3^{2+}(t_{2g}^6)$	Pt	+0.81	0.80[b]		>0.8
$OsL_3^{3+}(t_{2g}^5)/OsL_3^{2+}(t_{2g}^6)$	Pt	+0.83	0.87		>0.8

(a) α = 0.48 ± 0.08. (b) Aq. soln. contn. 0.2 M KF.

TABLE 10

DATA ON RATES OF ELECTRODE REACTIONS INVOLVING ELECTRON TRANSFER OF A π^*-ELECTRON L = 2,2'-BIPYRIDINE

Redox systems	Electrode	$E_{\frac{1}{2}}$/V SCE	k°/cm s^{-1}	ϕ_2/mV	k°_{cor}/cm s^{-1}
$CrL_3(t_{2g}^6)/CrL_3^-(t_{2g}^6\pi^*)$	DME	-1.86	0.23±0.02	-97	~2
$MoL_3(t_{2g}^6)/MoL_3^-(t_{2g}^6\pi^*?)$	DME	-1.719	0.22±0.02	-95	~1
$FeL_3^{2+}(t_{2g}^6)/FeL_3^+(t_{2g}^6\pi^*)$	DME	-1.26	0.14		0.001
$FeL_3^{2+}(t_{2g}^6)/FeL_3^+(t_{2g}^6\pi^*)$	Pt	-1.26	0.16		
$RuL_3^{2+}(t_{2g}^6)/RuL_3^+(t_{2g}^6\pi^*)$	DME	-1.243	0.10	-83	0.001
$RuL_3^{2+}(t_{2g}^6)/RuL_3^+(t_{2g}^6\pi^*)$	Pt	-1.24	0.24		<0.2
$RuL_3^+(t_{2g}^6\pi^*)/RuL_3(t_{2g}^6\pi^{*2})$	DME	-1.432	0.25	-89	0.05
$RuL_3^+(t_{2g}^6\pi^*)/RuL_3(t_{2g}^6\pi^{*2})$	Pt	-1.43	0.24		<0.2
$RuL_3(t_{2g}^6\pi^{*2})/RuL_3^-(t_{2g}^6\pi^{*3})$	DME	-1.690	0.22	-94	~1
$RuL_3(t_{2g}^6\pi^{*2})/RuL_3^-(t_{2g}^6\pi^{*3})$	Pt	-1.69	0.26		>0.3

TABLE 10(continued)

$OsL_3^{2+}(t_{2g}^6)/OsL_3^{+}(t_{2g}^6\pi^*)$	DME	-1.173	0.15	-83	0.001
$OsL_3^{2+}(t_{2g}^6)/OsL_3^{+}(t_{2g}^6\pi^*)$	Pt	-1.18	0.26		<0.2
$OsL_3^{+}(t_{2g}^6\pi^*)/OsL_3(t_{2g}^6\pi^{*2})$	DME	-1.253	0.25	-86	0.05
$OsL_3(t_{2g}^6\pi^{*2})/OsL_3^{-}(t_{2g}^6\pi^{*3})$	DME	-1.672	0.18	-94	~1
bipyridine/bipyridine$^-$	DME	-2.10	0.13[a]	-104	~1
bipyridine/bipyridine$^-$	Pt	-2.09	0.21[a]		>0.2

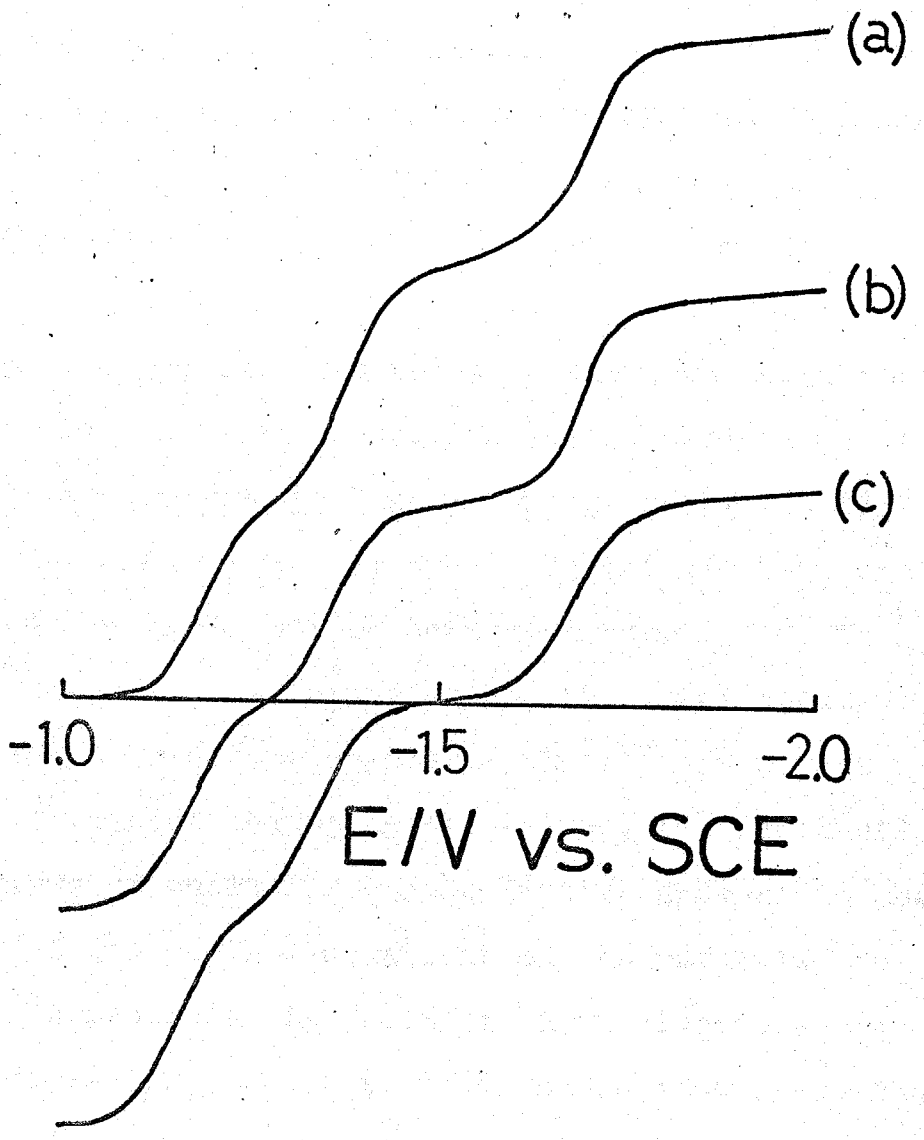

Fig. 29. Cathodic-anodic polarograms for (a) 2 mM $OsL_3(ClO_4)_2$, (b) and (c) reduction products of $OsL_3(ClO_4)_2$ obtained by the controlled-potential electrolysis at -2.0 V vs. SCE in DMF containing 0.2M TBAP.

CHAPTER IV

THE CORRELATION BETWEEN THE ELECTROCHEMICAL AND HOMOGENEOUS RATES OF ELECTRON-TRANSFER REACTIONS

A. Electron Spin Resonance Measurements of the Homogeneous Electron-exchange Rate between $Cr(bipy)_3^+$ and $Cr(bipy)_3$.

a. INTRODUCTION

From the mechanistic point of view, the electron-transfer reactions of transition metal complexes may be divided into two groups: one is the group of reactions proceeding via an outer-sphere activated complex, and the other, an inner-sphere activated complex[1,2]. In the reactions of the former group, the inner coordination shells of the reactant complex ions are left intact in the transition state; in the latter, two reactants share the ligands of their first coordination spheres in the transition state. In general, it may be difficult to show which mechanism is realized in an electron-transfer reaction. However, it is known that reactions of some kind proceed with the outer-sphere mechanism: they are the fast electron-transfer reactions between substitution-inert complexes. Particularly, the electron-exchange rate constant is very large for a pair of complexes differing by one in the number of electrons in the lower t_{2g}-orbitals which are not used in ligand

bondings[1]. For example, the electron-exchange reaction between $Fe(phen)_3^{3+}(t_{2g}^5)$ and $Fe(phen)_3^{2+}(t_{2g}^6)$ is too fast to be measured by the NMR method; the largest second-order rate constant obervable by this method is of the order of 10^7 M^{-1} s^{-1}. The lower limit of the rate constant of this reaction has been reported by Larsen and Wahl to be 3×10^7 $M^{-1}s^{-1}$ at 25 °C in aqueous solutions[3].

Among the methods for measuring the rates of isotopic exchange-reactions, the e.s.r method is probably the only one which is applicable to such fast reactions as described above. This method has been applied extensively to electron-transfer reactions between aromatic hydrocarbons and their anion radicals. On the other hand, there has been only one report on the application of this procedure to the transition-metal complexes[4]. This may be because of the following difficulties: most of the e.s.r spectra of these complexes thus far reported are very broad at ordinary temperatures, and they scarcely ever exhibit a hyperfine structure. Moreover, the rate constants measurable by this method must be larger than 10^6 $M^{-1}s^{-1}$.

The present investigation deals with the e.s.r measurement of the rate of electron-exchange between $Cr(bipy)_3^+$ and $Cr(bipy)_3$ in DMF. The latter complex

is diamagnetic[5], while the former complex yields the e.s.r spectra with the most resolved nitrogen hyperfine splittings of all the tris-bipyridine complexes of transition metals ever reported[6,7]. Furthermore, the electronic configurations of $Cr(bipy)_3^+$ and $Cr(bipy)_3$ are t_{2g}^5 and t_{2g}^6 respectively, as in $Fe(phen)_3^{3+}$ and $Fe(bipy)_3^{2+}$; it may thus be expected that the reaction rate for this pair of complexes is sufficiently fast for it to be measured by the e.s.r method. The determination of the hyperfine linewidth is made by comparing the observed e.s.r spectrum with the computer-simulated one. The observed rate constants are discussed in comparison with those predicted by the theory of R. A. Marcus on the electron-transfer reactions with the adiabatic outer-spher mechanism[8].

The present discussion is based on the following premises: (1) both complexes, $Cr(bipy)_3^+$ and $Cr(bipy)_3$ are substitution inert, and (2) the electron transfer reaction between them proceeds via an outer-sphere activated complex. There is no data which assures us of the validity of these premises. However, it may be reasonable to considered that this reaction has a fair chance of being an outer-sphere reaction because of its very large rate constant, which will be seen in the later part of this article.

b. EXPERIMENTAL

Reagents.

All the reagents and solvents were commercially obtained. The DMF was stored in an evacuated ampoule containing solid $Cr(bipy)_3(ClO_4)_2$ and magnesium power in order to remove the trace of oxygen.

Complexes

Both complexes, tris(2,2'-bipyridine) chromium(I) perchlorate and tris(2,2'-bipyridine)chromium(0), are very sensitive to oxygen. They were prepared and handled in a vacuum or in a nitrogen atmosphere. The preparation and analysis of these complexes were described in Chapter I.

Solutions

Solutions of $Cr(bipy)_3ClO_4$ with various concentrations were required in order to evaluate the contribution to the linewidth of the $Cr(bipy)_3^+$ spectrum from the Heisenberg spin-exchange process. They were prepared separately in e.s.r sample tubes *in vacuo* by diluting each aliquot from the stock solution of $Cr(bipy)_3ClO_4$ to a desired concentration with the solvent distilled from the stock solvent. Their concentrations were determined e.s.r spectroscopically.

The sample solutions used in the measurement of the electron exchange rates contained both $Cr(bipy)_3ClO_4$ and $Cr(bipy)_3$; they were prepared by dissolving a known amount of solid $Cr(bipy)_3$ into a $Cr(bipy)_3ClO_4$ solution of a known concentration in such an ampoule as shown in Fig. 30.

In handling the sample solutions, all the operations were performed on a vacuum line by the use of glassware fitted with a breakable seal.

E.s.r measurements

The e.s.r spectra of $Cr(bipy)_3^+$ were measured in solutions with and without $Cr(bipy)_3$ added, under experimental conditions otherwise identical. A JEOL-3SB spectrometer was operated at a frequency near 9.7 kMHz, with a 100 kHz field modulation and with a modulation amplitude of 0.5 gauss. The measurements were carried out at room temperature maintained at 25 ± 1 °C. Calculations of the linewidth were performed on a FACOM 270-20/30 computer using a FORTRAN program.

c. RESULTS AND DISCUSSION

Let the rate of the electron transfer reaction between a diamagnetic and a paramagnetic molecule be

described by the following equation:

$$\text{rate} = k[P][D] = [P]/\tau_p$$

where k is the second-order rate constant and τ_p, the mean life of the paramagnetic species; [D] and [P] are the concentrations of $Cr(bipy)_3$ and $Cr(bipy)_3^+$ respectively, in this case. The hyperfine linewidth as a function of τ_p can be linearlized with regard to τ_p and $1/\tau_p$ respectively, under the following fast-limit and slow-limit conditions[12]:

fast-limit: $|\omega_i - \omega_j|\tau_p \ll 1$ for all i's

slow-limit: $|\omega_i - \omega_j|\tau_p \gg 1$ for all i's

where ω's are the resonance frequencies of the designated hyperfine lines. As will be seen below, it is necessary that [D] be larger than 1 M to fulfill the fast-limit condition. This is not possible in the present incestigation, however, because of the poor solubility of the D species; thus, in the present experiment the rate constant is determined by the line-broading procedure, with the slow-limit approximation. The rate constant is, then, given by eqn. (18), when the broadened hyperfine lines are assumed to maintain the Lorentzian lineshape[13]:

$$k = (1.5 \times 10^7)\,\Delta(\Delta H_{pp})/[D] \qquad (18)$$

where $\Delta(\Delta H_{pp})$ is the increase in the peak-to-peak linewidth of the first derivative spectra caused by

electron exchange.

Although evidence has been reported for the disproportionation of $Cr(bipy)_3^+$ ions[14], their absorption spectrum obtained in DMF exhibited no sign of absorption due to either $Cr(bipy)_3^{2+}$ or $Cr(bipy)_3$; it was identical with the spectrum reported by König and Herzog in methanol[11]. Hence, the disproportionation was not taken into consideration.

The e.s.r spectrum of $Cr(bipy)_3^+$, shown in Fig. 31, exhibits eleven poorly resolved lines with a spacing of about 3.05 gauss. They may be attributed to the hyperfine interaction due to six equivalent nitrogen nuclei of three bipyridines. Such an interaction would give rise to thirteen lines. Because of the broadening in linewidth and poor signal-to-noise ratio, not all the thirteen lines were observed. The following procedure was used in order to determine the hyperfine linewidth of such a poorly resolved spectrum as this. A linewidth parameter is defined here as l_2/l_1, where l_1 and l_2 are taken in the way shown in Fig. 31. The parameter was calculated for each given width of the hypothetical unoverlapping hyperfine lines and is shown plotted vs. the latter quantity in Fig. 32. From the observed values for the linewidth parameter, the true or unoverlapped hyperfine linewidths are obtained by the use of this figure.

Figure 33 illustrates a plot of the linewidth vs. the concentration of $Cr(bipy)_3ClO_4$. The experimental points lie on a straight line; this may serve to support this procedure for the linewidth determination. From the slope of this line, the second-order rate constant of the Heisenberg spin-exchange process[15] was estimated to be 1.8×10^9 $M^{-1}s^{-1}$. An inevitable increase in the concentration of $Cr(bipy)_3ClO_4$ is caused by the addition of $Cr(bipy)_3$[16]; this can be corrected by the procedure of Suga and Aoyagui[17]. The increase, however, was less than 0.02 mM; its effect on the linewidth is negligible.

Figure 34 shows with circles the observed increase in the linewidth plotted vs. the concentration of added $Cr(bipy)_3$. The second-order rate constant of the electron-exchange reaction was determined from the slope of the straight line drawn through the point of origin and the circles as $k_{obs} = (1.5 \pm 0.4) \times 10^9$ $M^{-1}s^{-1}$. No such a large rate constant exceeding 10^9 $M^{-1}s^{-1}$ has, to our knowledge, ever been reported for the electron-exchange reactions of transition metal complexes. The observed rate constant must be corrected for diffusion because of its large value, approaching the value for the diffusion-controlled rate constant. The correction was performed using the following relation:

$$k_{act}^{-1} = k_{obs}^{-1} - k_{dif}^{-1}$$

where k_{act} is the corrected or activation-controlled rate constant, and k_{obs} and k_{dif} are the observed and the diffusion-controlled rate constant respectively. The last one was estimated in the following way. When one of the reactants is neutral and when, accordingly, the electrostatic interaction between the reactants is negligibly small or zero, the diffusion-controlled second-order rate constant in $M^{-1}s^{-1}$ may be given by [18]:

$$k_{dif} = 4\pi\sigma DN/1000 \qquad (19)$$

where σ is the collision diameter; D, the sum of the diffusion coefficients of the two reactants, and N, Avogadro's number. The value for σ was assumed to be equal to the sum of the molecular radii of the reactants; the latter quantities were estimated from the molecular geometry of $Cr(bipy)_3$, drawn in Fig. 35 on the basis of the X-ray diffraction data[19] and the van der Waals radius of the hydrogen atom (1.2 Å). It may reasonably be assumed that a common value can be attributed to the radii of $Cr(bipy)_3^+$ and $Cr(bipy)_3$. In the subsequent calculations, this common molecular radius is designated by a and taken in the two ways shown in Fig. 35: 7.1 and 6.1 Å. The diffusion coefficients of $Cr(bipy)_3$ and $Cr(bipy)_3^+$ are both 3.2×10^{-6} cm^2s^{-1} at 25 °C in DMF[20]. The diffusion-

controlled rate constants calculated from eqn. (19) with the $\underline{a}$ values of 7.1 and 6.1 A were 7×10^9 and 6×10^9 $M^{-1}s^{-1}$ respectively. Both k_{dif} values, however, actually yielded the same k_{act} value, 2.0×10^9 $M^{-1}s^{-1}$. The limiting condition for slow-exchange is obviouly fulfilled with the observed k value of 1.5×10^9 $M^{-1}s^{-1}$ and the minimum value for $|\omega_i - \omega_j|$, 3.05 gauss, as well as the maximum value for [D], 0.7 mM. On the other hand, the limiting condition for fast-exchange requires that [D] be significantly larger than 0.4 M when the maximum value for $|\omega_i - \omega_j|$, ca. 30 gauss, is applied.

According to the theory of Marcus[8], the rate constant of the electron-exchange reaction between a neutral and a charged species is, the inner-sphere reorganization being neglected:

$$k_{act} = Z \exp(-\Delta G^*/RT)$$
$$= Z \exp[-(e^2/8\underline{a})(1/D_{op} - 1/D_s)]$$

where Z, the collision number between two uncharged species in solution, is assumed to be 10^{11} $M^{-1}s^{-1}$; ΔG^* is the reorganization free energy of solvent molecules in forming the activated complex; e is the electronic charge, and D_{op} and D_s are the optical and the static dielectric constants respectively. The activation-controlled rate constant was calculated from this equation for each radius mentioned above. They are list

listed in Table 11, together with the corrected rate constant. The agreement between k_{act} and k_{calc} was satisfactory. In order for k_{calc} to be in exact agreement with k_{act}, $\underline{a}$ should be taken as 8.2 Å, a reasonable value in view of the molecular dimensions of $Cr(bipy)_3$. This suggests that the inner-sphere reorganization energy contributes to the activation free energy to only a small extent in this reaction. However, the value of k_{calc} is quite sensitive to that of $\underline{a}$, and unfortunately $\underline{a}$ is not a sufficiently definite quantity for the Marcus theory to be applied to the existing molecules. Thus, the theory must be tested experimentally with regard to a variety of aspects of its theoretical expression for the rate constant before we can consider that the theory is successful in the non-empirical prediction of the electron-exchange rate constant. Such an extensive examination of this theory has recently been attempted for the electron-transfer reactions between aromatic hydrocarbons and their anion radicals[21]. The theoretical calculation of the rate constant can be done more reasonably for the reactions participated by the octahedral complex ions than for those participated by the planar aromatic hydrocarbons, because of the premise of a spherical molecular shape in this theory.

d. REFERENCES

1 F. Basolo and R. G. Pearson, Mechanisms of Inorganic Reactions, 2nd ed., John Wiley & Sons Inc., New York, N. Y. (1967), Chap. 6.

2 W. L. Reynolds and R. W. Lamry, "Mechanisms of Electron Transfer," The Ronald Press Co., New York, N. Y. (1966).

3 D. W. Larsen and A. C. Wahl, J. Chem. Phy., 43, 3765 (1965).

4 R. A. Stewart, L. W. Reeves and S. Fujiwara, Bull, Chem. Soc. Japan, 41, 2832 (1968).

5 S. Herzog and K. Renner, Chem. Ber., 92, 872 (1959).

6 B. Elschner and S. Herzog, Arch. Sci. (Geneva), 11, 160 (1958).

7 E. König, Z. Naturforsch., A, 19, 1139 (1964).

8 R. A. Marcus, J. Chem. Phys., 24, 966, 979 (1956).

9 V. F. Hein and S. Herzog, Z. Anorg. Allgem. Chem., 267, 337 (1952).

10 S. Herzog, K. Renner, and W. Schön, Z. Naturforsch., B, 12, 809 (1957).

11 E. König and S. Herzog, J. Inorg. Nucl. Chem., 32, 585 (1970).

12 J. A. Pople, W. G. Schneider, and H. J. Bernstein, High-resolution Nuclear Magnetic Resonance, McGraw-

Hill, New York, N. Y. (1959), Chap. 10.

13 R. L. Ward and S. I. Weissman, J. Amer. Chem. Soc., 79, 2086 (1957).

14 U. P. Geiger and E. Class, Experientia, 17, 444 (1961).

15 M. P. Eastman, R. G. Kooser, M. R. Das, and J. H. Freed, J. Chem. Phys., 51, 2690 (1969). M. P. Eastman, G. V. Bruno, and J. H. Freed, ibid., 52, 2511 (1970).

16 When a known amount of $Cr(bipy)_3$ is added to the solution of $Cr(bipy)_3^{1+}$, a part of $Cr(bipy)_3$ may inevitably be oxidized by oxygen to yield $Cr(bipy)_3^{1+}$.

17 S. Suga and S. aoyagui, Bull. Chem. Soc. Japan, 45, 1375 (1972).

18 M. V. Smoluchowski, Z. Phys. Chem., 92, 129 (1917).

19 G. Albrecht, Z. Chem., 3, 182 (1963).

20 T. Saji and S. Aoyagui, Bull. Chem. Soc. Japan, 47, 389 (1974).

21 K. Suga and S. Aoyagui, ibid, 46, 755, 808 (1973).

Table 11. Comparison of the corrected observed rate constant with the calculated one in the electron exchange reaction between $Cr(bipy)_3^+$ and $Cr(bipy)_3$

k_{act} ($M^{-1}sec^{-1}$)	Radius (Å)	k_{calc} ($M^{-1}sec^{-1}$)	ΔG^* (kcal/mol)
	6.1	3.7×10^8	3.3
	7.1	1.2×10^9	2.6
2.0×10^9	8.2	2.0×10^9	2.2

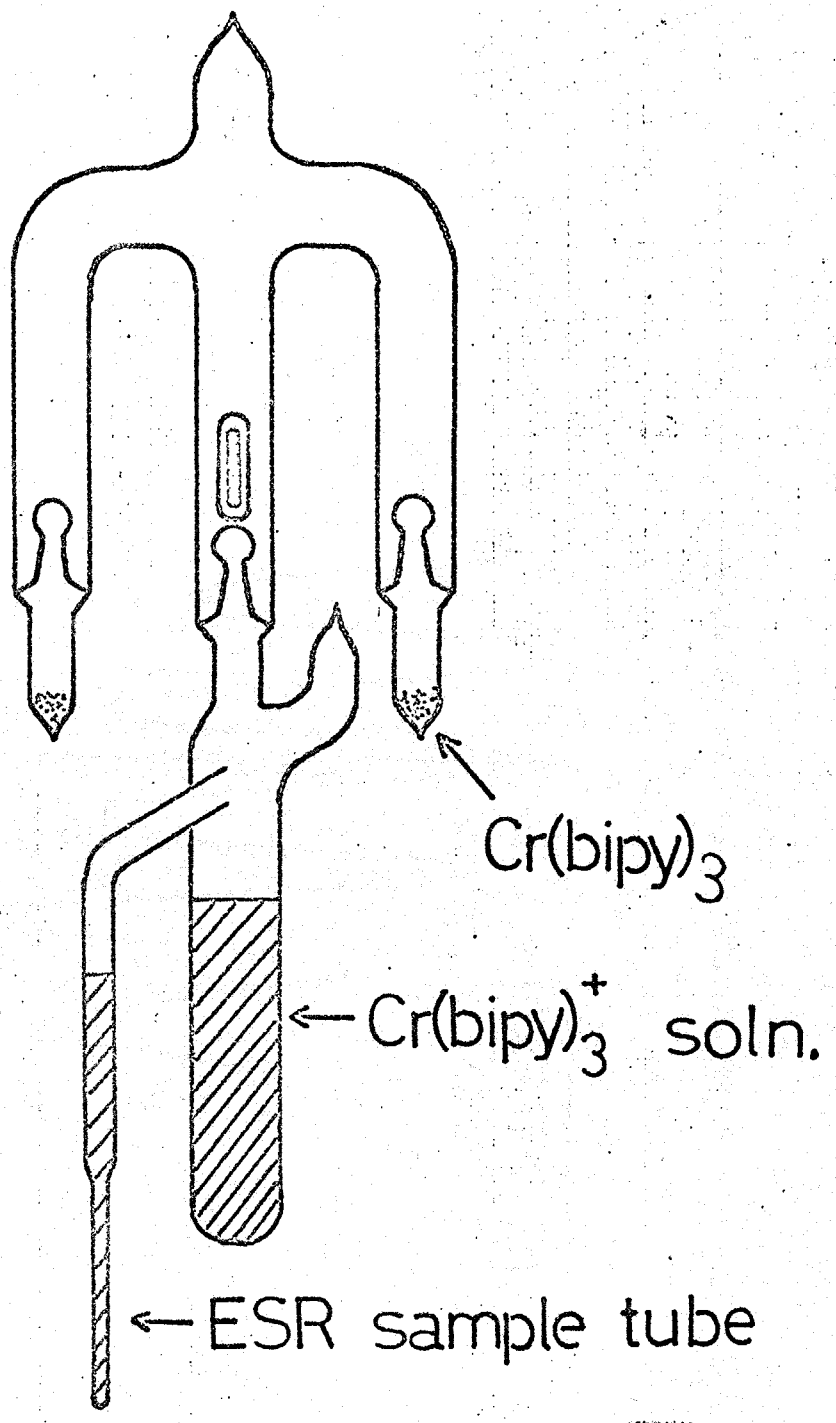

Fig. 30. Apparatus for preparation of e.s.r. sample solution.

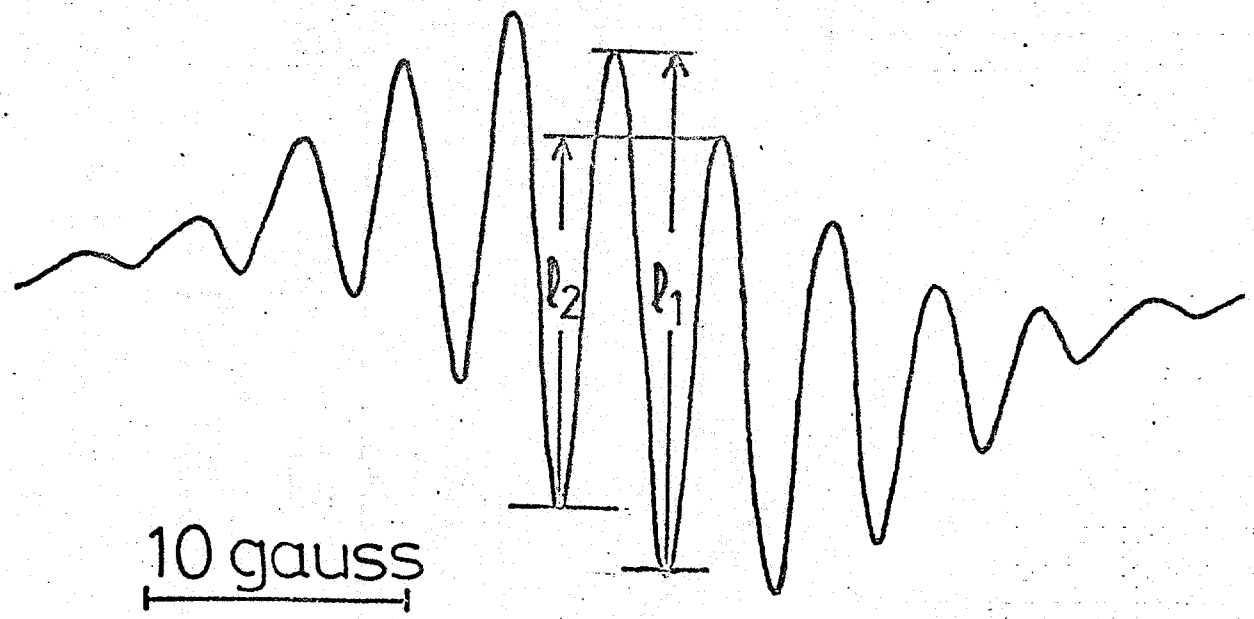

Fig. 31. e.s.r. spectrum of 0.7 mM $Cr(bipy)_3^+$ in DMF.

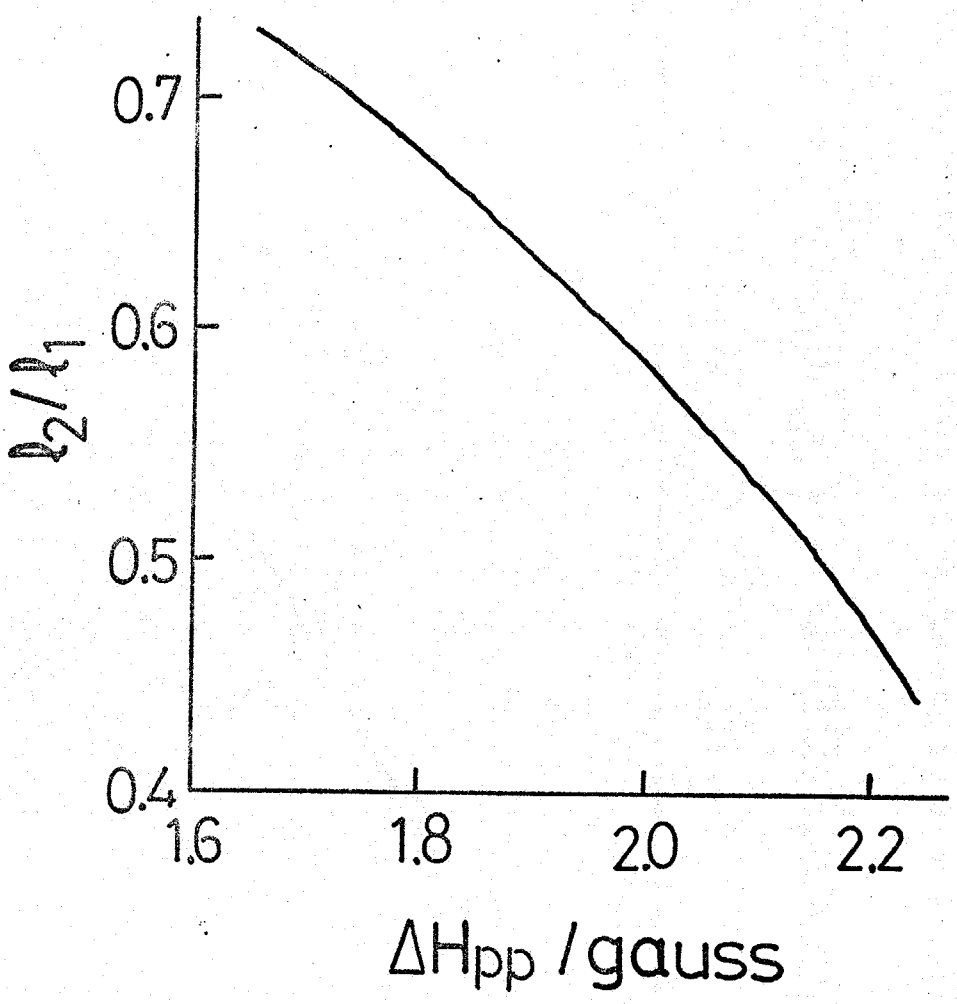

Fig. 32. Linewidth parameter vs. unoverlapped hyperfine linewidth.

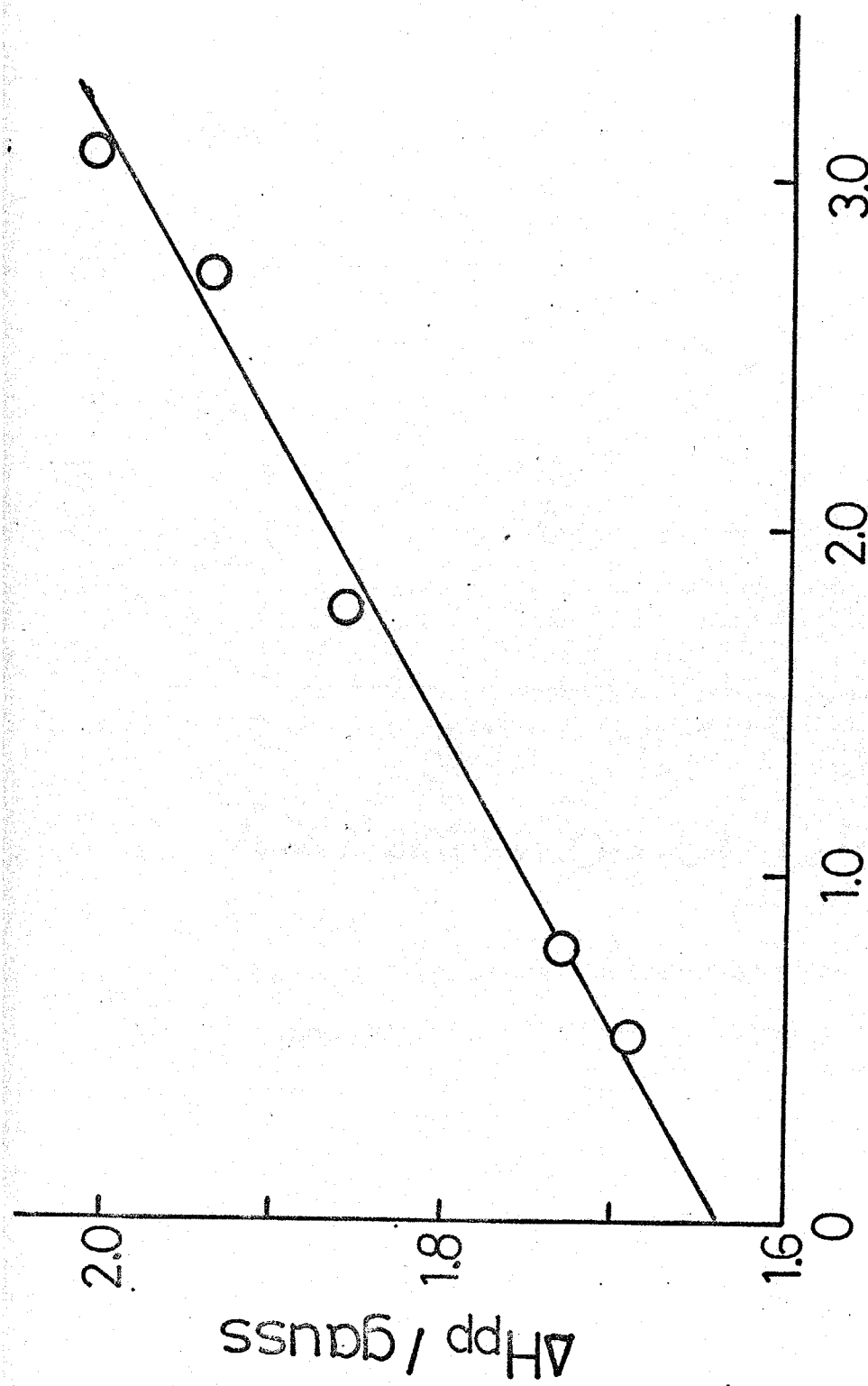

Fig. 33. Observed linewidth of e.s.r. spectrum vs. concentration of $Cr(bipy)_3ClO_4$.

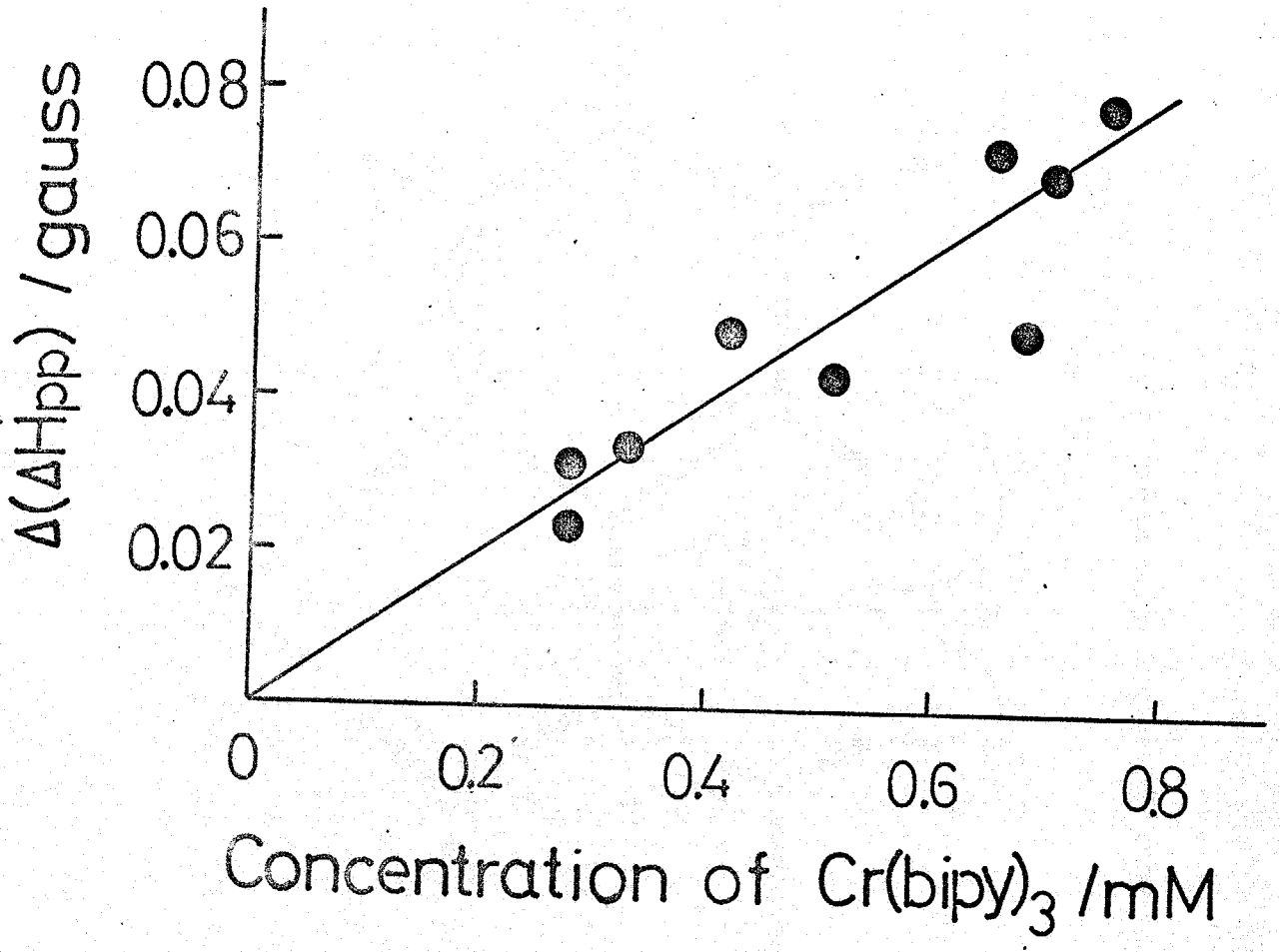

Fig. 34. Increase in linewidth of e.s.r. spectrum vs. concentration of added $Cr(bipy)_3$.

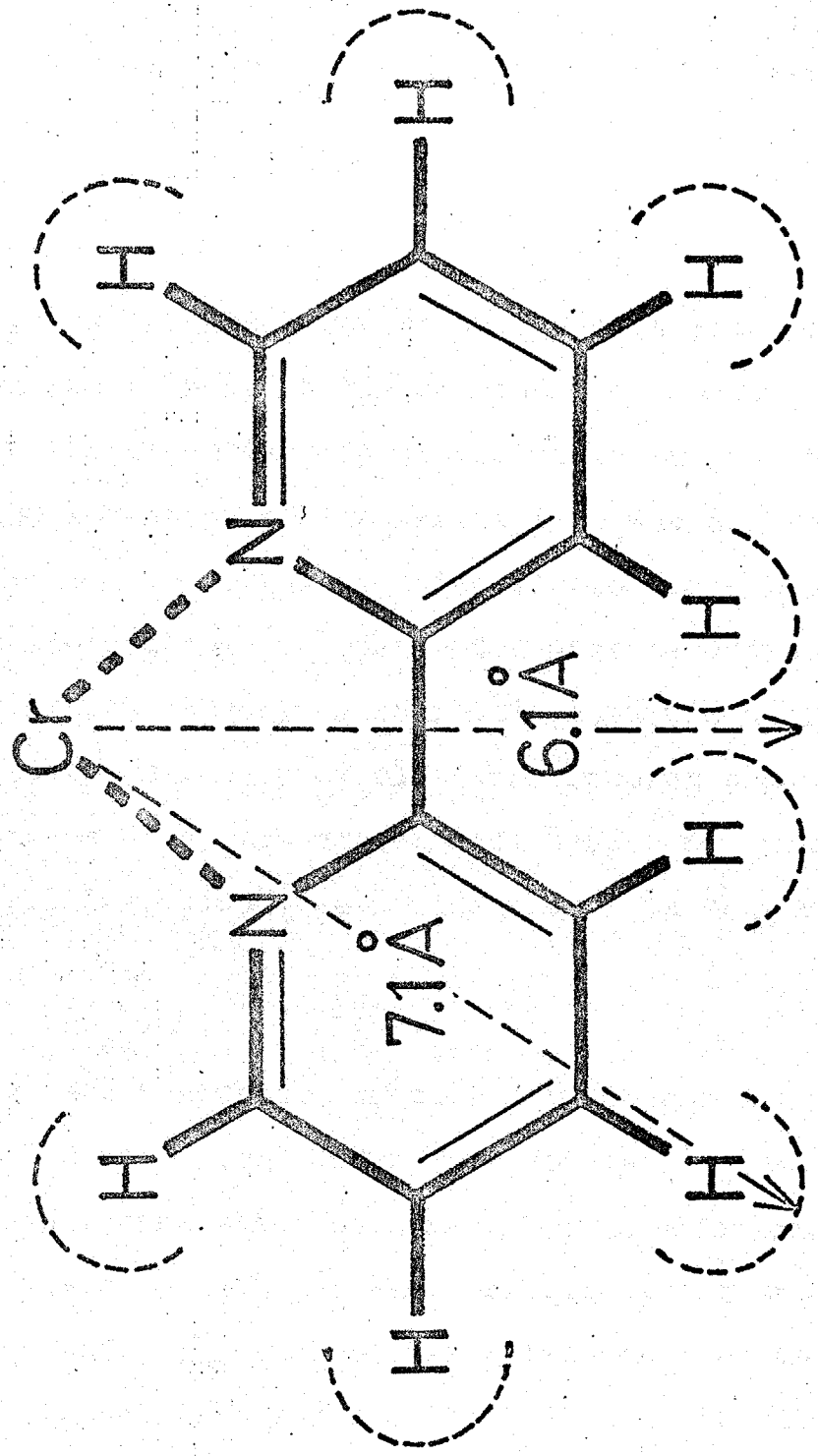

Fig. 35. Molecular geometry of Cr(bipy)3.

B. Electrochemical Electron-transfer Rates of Fe(III)/Fe Fe(II) Complexes with 2,2'-Bipyridine and/or Cyanide Ion

a. INTRODUCTION

The unified treatment of homogeneous electron exchange reaction and heterogeneous i.e. electrochemical electron transfer reaction presented by Marcus[1] has attracted attention of electrochemists who are interested in the non-empirical elucidation of electrode kinetics based on molecularity. One on the most essential feature of this theory is the basic assumption of mechanistic similarity of electron transfer process in homogeneous and electrochemical reactions. However, the concluding expression of the theory in this respect i.e.

$$(k_{ex}/Z_{ex})^{1/2} = k^{o}/Z_{el} \qquad (20)$$

held for fast reactions, neither organic nor inorganic. Here k_{ex} is the second order rate constant of a homogeneous electron exchange reaction occurring in solution, k^{o} the standard rate constant of the corresponding electrochemical redox reaction, Z_{ex} the collision frequency of an uncharged particle in solution and Z_{el} the collision frequency of an uncharged particle with the unit area of the electrode. Usually the Z_{el} and Z_{ex} are set equal to 10^{4} cm s^{-1} and 10^{11} M^{-1} s^{-1} respectively. Inconsistency between theory

and experiment is serious in the following two cases. One is the systems of an aromatic hydrocarbon and its anion radical. It is known that some of them have k_{ex} values of the order 10^9 M^{-1} s^{-1} when anions are not in strong ion-pairing with counter cations[2]. The observed k^o values for these systems are of the order 1 cm s^{-1}, whereas the theoretically predicted ones are of the order 10^3 cm s^{-1}. The latter is far beyond the upper limit measurable with the aid of any existing technique. The other is a system of transition metal complex. The k_{ex} and k^o values for the $Cr(bipy)_3^+/Cr(bipy)_3$ system are 1.5×10^9 M^{-1} s^{-1} and 1.3 cm s^{-1} respectively. An attempt has been made to revise the theory so that the relation between observed values for k_{ex} and those for k^o may be explained[3]. However, in view of the simple model proposed by Marcus for the activated complex in electrochemical electron transfer reactions, it is not so surprising that the relation (1) cannot be valid for a wide variety of reactions. It may be urgently required to find an empirical relation between k_{ex} and k^o for fast reactions. The aim of this chapter is to add a few experimental points to a correlation diagram of k_{ex} vs. k^o by measuring the standard rate constants for a series of iron(III)/iron(II) redox systems with a variety of ligands by the galvanostatic double pulse (g.d.p.) method.

b. EXPERIMENTAL

Reagent

The analytical grade potassium fluoride were used without further purification.

Complexes

Potassium hexacyanoferriate and hexacyanoferrate were commercially obtained. Tris(2,2'-bipyridine)iron(II) perchlorate[4], dicyano-bis(2,2'-bipyridine)iron(II) trihydrate[5] and potassium tetracyano-mono(2,2'-bipyridine) iron(II) trihydrate[5] was prepared according to the procedure in the literature cited. The hydrated dicyano-complex was dried in vacuo at 150 °C for eight hours to remove water of crystallization, because this complex was to be used as a solute in DMF solution. Complexes were identified by the elementary analysis.

Calcd. for $Fe(bipy)_3(ClO_4)_2$: C, 49.8; H, 3.32; N, 1 N, 11.6. Found: C, 49.2; H, 3.41; N, 11.5.

Calcd. for $Fe(bipy)_2(CN)_2.3H_2O$: C, 55.7; H, 4.64; N, 17.7. Found: C, 55.5; H, 4.82; N, 17.1.

Calcd. for $Fe(bipy)_2(CN)_2$: C, 62.8; H, 3.81; N, 20.0. Found: C, 59.7; H, 4.22; N, 18.8.

Calcd. for $K_2Fe(bipy)(CN)_4.3H_2O$: C, 37.5; H, 3.12; N, 18.8. Found: C, 36.9; H, 2.92; N, 18.2.

Solutions

Two kinds of DMF solutions and five kinds of aqueous solutions were prepared: DMF solutions of (1) 2mM $Fe(bipy)_3(ClO_4)_2$ and (2) 2 mM $Fe(bipy)_2(CN)_2$; aqueous solutions of (3) 2 mM $Fe(bipy)_3(ClO_4)_2$, (4) 0.5 mM $Fe(bipy)_2(CN)_2$, (5) 1 mM $K_2Fe(bipy)(CN)_4$, (6) 2 mM $K_4Fe(CN)_6$ and (7) 1 mM $K_4Fe(CN)_6$ + 1 mM $K_3Fe(CN)_6$. supporting electrolytes in DMF solutions and aqueous solutions were TBAP and potassium fluoride respectively. Their concentrations were 0.2 M.

c. RESULTS AND DISCUSSION

Cyclic voltammograms with initial anodic scan were taken in solutions (1) to (6) using the platinum electrode. According to the reversibility criteria based on the peak-potential separation and the peak-current ratio, the oxidation steps for the iron(II) complexes were all reversible one-electron steps. The polarographic half-wave potentials obtained from these voltammograms are listed in Table 12. The diffusion coefficients of the complexes, $Fe(bipy)_3^{2+}$, $Fe(bipy)_2(CN)_2$, $Fe(bipy)(CN)_4^{2-}$ and $Fe(CN)_6^{4-}$, were determined from the cyclic voltammograms as well as the cathodic polarograms obtained by the use of the DME. They are listed in

Table 13. Previous data are available only for $Fe(CN)_6^{4-}$. A recent data obtained by voltammetry with a rotating disk electrode is 8.0×10^{-6} cm^2 s^{-1} which is in fair agreement with the present data[6]. The trend of diffusion coefficients as a function of the number of ligand bipyridine molecules is reasonable, considering the molecular dimensions of the complexes. The slope of every linear plot of overpotential vs. square root of the first-pulse width obtained by g.d.p. mesurements was fairly consistent with the slope calculated[7] by use of a diffusion coefficient in Table 13. The standard rate constants obtained are listed in Table 12. It is noted that the difference in kinds of solvent and supporting electrolyte did not affect much the apparent standard rate constant.

The validity of the g.d.p. method with in situ generation of a redox substance was proved by the fact that the rate constant for the $Fe(CN)_6^{3-}/Fe(CN)_6^{4-}$ system obtained by this procedure was in good agreement with the rate constant obtained by use of a solution containing both the oxidant and the reductant species. Previous data on the standard rate constant for this syatem are available though they have been obtained under conditions different from those in this experiment. They are scattered[6,8-11] between 0.02 and 0.24 cm s^{-1}. The present data are close the data 0.13 cm s^{-1} obtained in a 0.5 M potassium sulphate solution by means of the coulostatic pulse method[11].

The rate constants for the homogeneous electron exchange reactions corresponding to the three of the electrochemical reactions treated in this section are known. The second order rate constant for the $Fe(CN)_6^{3-}/Fe(CN)_6^{4-}$ system has been reported by two authors[12,13]. The rate constants for the systems $Fe(bipy)(CN)_4^{-}/Fe(bipy)(CN)_4^{2-}$ and $Fe(bipy)_3^{3+}/Fe(bipy)_3^{2+}$ have been evaluated indirectly by the use of cross electron transfer reactions between $Fe(CN)_6^{4-}$ and a reactant of these couples[14], though they have never been obtained directly. These homogeneous rate constants are also involved in Table 12. From the data in this table it is seen that the standard rate constant increases as the number of the coordinated 2,2'-bipyridine increases. The same relation holds for the $Fe(bipy)_3^{3+}/Fe(bipy)_3^{2+}$ and $Fe(bipy)_2(CN)_2^{-}/Fe(bipy)_2(CN)_2$ systems in DMF solution. On the other hand, the rate constants for the homogeneous electron exchange reactions for the $Fe(bipy)_3^{3+}/Fe(bipy)_3^{2+}$, $Fe(bipy)(CN)_4^{-}/Fe(bipy)(CN)_4^{2-}$ and $Fe(CN)_6^{3-}/Fe(CN)_6^{4-}$ systems decrease in this order. The identity of the qualitative trend in both kinds of rate constants may support the paralellism between the mechanism of an electrochemical redox reaction and that of the corresponding homogeneous electron-exchange reaction.

Discussion has so far been based on the apparent uncorrected standard rate constant for the potential in the diffuse double-layer. Because the present kinetic data were obtained with a platinum electrode and the transfer coefficients have not yet been measured, the double-layer correction was not performed. The sixth column in Table 12 shows the direction of shift of the k^o values when they are corrected with the potential of zero charge being assumed to be more negative than 0.18 V vs. SCE[8]. It is probable that the parallelism also holds between the k_{ex} values and the corrected k^o values, k^o_{cor}.

Table 12 shows that the homogeneous and the electrochemical rate constants seem to depend on the extension of the ligand π-orbital in the same way. This fact may be explained as follows: if the ligands are unsaturated compounds, metal-to-ligand π-bondings occur. When the reactants have large conducting unsaturated ligands, they are characterized by a highly delocalized π-electron distribution, and hence the geometries of the oxidant and the reductant species will be nearly equal. Consequently, in the case where an electron in a low-lying orbital is transferred, the larger the π-orbital of the ligand is, the faster is the electron transfer of the complex.

d. REFERENCES

1 (a) R. A. Marcus, J. Chem. Phys., 43, 479 (1965), (b) J. Phys. Chem., 67, 853 (1963).

2 K. Suga, S. Ishikawa and S. Aoyagui, Bull. Chem. Soc. Japan, 46, 808 (1973).

3 N. S. Hush, Electrochim. Acta, 13, 1005 (1968).

4 F. H. Burstall and R. S. Nyholm, J. Chem. Soc., 1952, 3570.

5 A. A. Shilt, J. Amer. Chem. Soc., 82, 3000 (1960). H. Mizota, H. Matsuda, Y. Kanzaki and S. Aoyagui, J. Electroanal. Chem., 45, 385 (1973). H. Matsuda, S. Oka and P. Delahay, J. Amer. Chem. Soc., 81, 385 (1957).

6 D. H. Angell and T. Dickinson, J. Electroanal. Chem., 35, 55 (1972).

7 T. Rohko, M. Kogoma and S. Aoyagui, J. Electroanal. Chem., 38, 45 (1972).

8 D. Jahn, and W. Vielstich, ibid, 109, 849 (1962).

9 H. P. Agarwal, J. Electrochem. Soc., 110, 237 (1963).

10 J. E. B. Randles and K. W. Somerton, Trans. Faraday Soc., 48, 937 (1952).

11 P. H. Daum and C. G. Enke, Anal. Chem., 41, 653 (1969).

12 M. Shporer, G. Ron, A. Loemenstein and G. Novon, Inorg. Chem., 4, 361 (1965).

13 C. F. Deck and A. C. Wahl, J. Amer. Chem. Soc., 76, 4054 (1954).

14 R. Strasiw and R. G. Wilkins, Inorg. Chem., 8, 156 (1969).

TABLE 12

HOMOGENEOUS AND ELECTROCHEMICAL RATE CONSTANTS FOR THE SYSTEMS OF Fe(III)/Fe(II) COMPLEXES WITH LIGANDS OF 2,2'-BIPYRIDINE AND/OR CYANIDE ION

System	Soln	Solv	$E_{\frac{1}{2}}$ / V	k_{ex} / M^{-1} s^{-1}	k° / cm s^{-1}	k°_{cor} / cm s^{-1}
$Fe(bipy)_3^{3+}/Fe(bipy)_3^{2+}$	(3)	aq	0.81	$>10^8$	0.80	>0.8
$Fe(bipy)_3^{3+}/Fe(bipy)_3^{2+}$	(1)	DMF	1.03		1.1	
$Fe(bipy)_2(CN)_2^{+}/Fe(bipy)_2(CN)_2$	(4)	aq	0.53		0.63	>0.6
$Fe(bipy)_2(CN)_2^{+}/Fe(bipy)_2(CN)_2$	(2)	DMF	0.47		0.41	
$Fe(bipy)(CN)_4^{-}/Fe(bipy)(CN)_4^{2-}$	(5)	aq	0.31	$4x10^7$	0.43	< 0.4
$Fe(CN)_6^{3-}/Fe(CN)_6^{4-}$	(6)	aq	0.18	$9x10^4$	0.18	< 0.2
$Fe(CN)_6^{3-}/Fe(CN)_6^{4-}$	(7)	aq	0.18		0.15	

TABLE 13

DIFFUSION COEFFICIENTS OF Fe(II) COMPLEXES WITH LIGANDS 2,2'-BIPYRIDINE AND/OR CYANIDE ION AT 25 °C.

Complex	$D/10^{-6}$ cm^2 s^{-1}	
	a	b
$Fe(bipy)_3^{2+}$	3.6	3.6
$Fe(bipy)_2(CN)_2$	3.8	4.3
$Fe(bipy)(CN)_4^{2-}$	---	7.7
$Fe(CN)_6^{4-}$	---	8.3

a: obtained by polarography with DME in DMF soln.

b: obtained by cyclic voltammetry with platinum electrode in aq. soln.

C. Conclusion

Figure 36 shows the relation between $\log k_{ex}$ and $\log k^{o}$. The data for the redox systems Tl^{3+}/Tl^{+}, Eu^{3+}/Eu^{2+}, V^{3+}/V^{2+}, Fe^{3+}/Fe^{2+} and MnO_4^{-}/MnO_4^{2-} were obtained from the paper of Marcus[1] and the data for perylene/perylene^{-} system from the recent papers from this laboratory[2,3]. Several experimental points for systems composed of an aromatic hydrocarbon and its anion radical should lie near the experimental point for the perylene/perylene^{-} system. The data obtained in this work are designated by solid circles. Figure 36 shows that there is slight doubt about as to existence of a close parallelism between the mechanism of a homogeneous electron-exchange reaction and the corresponding electrochemical electron-transfer reaction. However, it also shows that the rate constants of the two processes cannot be related to each other by a simple equation.

According to the theory of Marcus[1,4,5], the homogeneous and electrochemical electron-transfer rate constants are expressed by eqns. (21) and (25) respectively.

Homogeneous:

$$k_{ex} = \kappa Z_{ex} \exp(-\Delta F^{*}_{ex}/RT) \qquad (21)$$

with

$$\Delta F^{*}_{ex} = \frac{w^{r} + w^{p}}{2} + \frac{1}{4}(\lambda)_{ex} = \frac{w^{r} + w^{p}}{2} + \frac{1}{4}\{(\lambda_{o})_{ex} + (\lambda_{i})_{ex}\} \qquad (22)$$

$$(\lambda_o)_{ex} = n^2e^2\left(\frac{1}{2a_1} + \frac{1}{2a_2} - \frac{1}{r}\right)\left(\frac{1}{D_{op}} - \frac{1}{D_s}\right) \qquad (23)$$

$$(\lambda_i)_{ex} = \sum_j \frac{k_j^r k_j^p}{k_j^r + k_j^p} (\Delta q_j)^2 \qquad (24)$$

Electrochemical:

$$k^o = \kappa Z_{el} \exp(-\Delta F_{el}^*/RT)$$

with

$$\Delta F_{el}^* = \frac{w^r + w^p}{2} + \frac{1}{4}(\lambda)_{el} = \frac{w^r + w^p}{2} + \frac{1}{4}\left\{(\lambda_o)_{el} + (\lambda_i)_{el}\right\} \qquad (26)$$

$$(\lambda_o)_{el} = \frac{n^2e^2}{2}\left(\frac{1}{a} - \frac{1}{r}\right)\left(\frac{1}{D_{op}} - \frac{1}{D_s}\right) \qquad (27)$$

$$(\lambda_i)_{el} = \frac{1}{2}(\lambda_i)_{ex} \qquad (28)$$

The following symbols are employed in these equations:

w^r, w^p = Works required to bring the reactant and product from infinity to the positions they would occupy in the activated complex. For the electrode system, w denotes the work required to transport the reactant and product to the so-called pre-electrode site.

n = Number of electrons transferred from one reactant to the other or, in the electrochemical case, from a reactant to the electrode.

e = unit of electronic charge.

a_1, a_2 = Ionic radii.

r = Interionic distance in the activated complex (Marcus has taken $r = a_1 + a_2$) or, for the electrochemical case, twice the distance from the electrode to the center of the ion.

D_{op} = Square of the refractive index.

D_s = Static dielectric constant.

Δq_j = Difference in equilibrium values of bond coordidates.

k_j^r, k_j^p = Force constants of the j-th vibrational coordinates in a reactant and a product.

κ = The transmission coefficient ($\kappa = 1$).

When it is assumed that r is twice the radius of the reactant (in the electrochemical case).

$$(\lambda_o)_{el} = \frac{n^2e^2}{4a}\left(\frac{1}{D_{op}} - \frac{1}{D_s}\right) \qquad (29)$$

When $a_1 = a = a$ and $r = 2a$ (in the homogeneous case)

$$(\lambda_o)_{ex} = \frac{n^2e^2}{2a}\left(\frac{1}{D_{op}} - \frac{1}{D_s}\right) \qquad (30)$$

A discussion in Chapter III on the correlation between the electrochemical rates and electronic configurations of bipyridine complexes has led us to a conclusion that a set of uncorrected rate constants provids a more reasonable basis for discussion than that of corrected ones. This conclusion means that the work term, w, is negligible in electrochemical reactions of this kind.

Equation (20) can be obtained from eqns. (21), (25), (29) and (30) with work terms neglected. The straight line (A) in Fig. 36 is drawn in accordance with eqn. (20). The experimental points corresponding to homogeneous rate constants larger than 10^3 M^{-1} s^{-1} deviate from this line.

An alternative explanation for the relation between the homogeneous and the electrochemical rate constants has been presented by Peover[6] on the basis of the theory of Hush[8] with the reasoning of Hale[7]. If the pre-electrode site is located at a position a few Å or more apart from the outer Helmholtz plane towards the solution bulk, the contribution from the image potential can be neglected in calculating the acitivation free energy. This condition is consistent with the conclusion of Chapter III that the pre-electrode site is located far apart from the outer Helmholtz plane. When $r = \infty$ holds, the following equations can be led from eqns. (23), (24), (27) and (28)

$$(\lambda_o)_{el} = (\lambda_o)_{ex} \tag{31}$$

$$(\lambda_o)_{el} = (\lambda_o)_{ex} + \frac{1}{2}(\lambda_i)_{ex} \tag{32}$$

A parameter is defined by the following equation:

$$\gamma = (\lambda_o)_{ex}/(\lambda_i)_{ex} \tag{33}$$

This is a measure of the contribution from the inner-sphere reorganization energy to the total reorganization energy. The homogeneous rate constant can then be related with the electrochemical one by the following equation:

$$\log k_{ex} = \frac{2(\gamma + 1)}{2\gamma + 1} \log k^o + \frac{14\gamma + 3}{2\gamma + 1} \tag{34}$$

with the Z_{el} and Z_{ex} values set equal to 10^4 cm s^{-1} and 10^{11} M^{-1} s^{-1} respectively.

The equations for various values of the parameter γ are as follows:

$$\log k_{ex} = \log k^{o} + 7 \qquad \text{for } \gamma = \infty \qquad (35)$$

$$\log k_{ex} = 2\log k^{o} + 3 \qquad \text{for } \gamma = 0 \qquad (36)$$

$$\log k_{ex} = 1.5\log k^{o} + 5 \qquad \text{for } \gamma = 1/2 \qquad (37)$$

$$\log k_{ex} = 1.3\log k^{o} + 5.7 \qquad \text{for } \gamma = 1 \qquad (38)$$

The eqn. (35) agrees with the following equation derived by Peover[6]:

$$k_{ex}/Z_{ex} = k^{o}/Z_{el}$$

The eqn. (36) agrees with eqn. (20) given by Marcus.

Each straight line in Fig. 36 is drawn in accordance with eqn. (35), (36), (37) or (38). Eqn. (35) fits the experimental points for fast reactions but does not for slow nor intermediate reactions. The $Cr(bipy)_3^{+}/Cr(bipy)_3$ reaction is one of such fast reactions. As shown in Section A of this chapter, the observed homogeneous rate constant for this system was in good agreement with the one calculated with the aid of the theoretical equation of Marcus with λ_i being neglected. From these facts, it may be inferred that the contribution of λ_i is also negligible in the electrochemical reactions with large rate constants approaching or exceeding 1 cm s^{-1}.

As described above, only experimental points corresponding to very slow reactions obey eqn. (36).

This fact suggests that the slowness of a reaction should be attributed predominantly to a large λ_i value. The reasons are as follows: (1) a large λ_o value cannot account for a very small k_{ex} value, because the difference in molecular radius between $Cr(bipy)_3$ (7.1 Å) and $V(H_2O)_6^{2+}$ (3.5 Å) can cause only a difference in order by one. (2) The ionic repulsion (w terms) cannot account for this, too. This is evident from the fact that a reaction between a pair of highly chargedspecies, $Fe(CN)_6^{3-}$/ $Fe(CN)_6^{4-}$, can have a fairly large k_{ex} value ($10^3 \sim 10^5$ M^{-1} s^{-1}).

Eqns. (36) and (37) fit the experimental points for moderately fast reactions, i.e. $Fe(CN)_6^{3-}/Fe(CN)_6^{4-}$ and MnO_4^-/MnO_4^{2-}. This suggests that λ_i is comparable with λ_o in these systems.

Figure 36 shows that a Z_{el} value about two order of magnitude smaller than 10^4 cm s^{-1} is more favourable; it is quite likely that some saturation occurs in the value of k^o. The latter aspect indispensably relates to the problem of the upper limit of the standard rate constant of the electrode process. In view of the presumed Z_{ex} value of the 10^{11} M^{-1} s^{-1}, saturation in k_{ex} values at about 10^{10} M^{-1} s^{-1} is reasonable. However, it cannot be the case for the saturation in the k^o value.

REFERENCES

1 R. A. Marcus, J. Phys. Chem., 67, 853 (1963).

2 K. Suga, S. Ishikawa and S. Aoyagui, Bull. Chem. Soc. Japan, 46, 808 (1973).

3 H. Mizota, K. Suga, Y. Kanzaki and S. Aoyagui, J. Electroanal. Chem., 44, 471 (1973).

4 R. A. Marcus, J. Chem. Phys., 43, 679 (1965).

5 R. A. Marcus, Can. J. Chem., 37, 155 (1959).

6 M. E. Peover in N. S. Hush (Ed.), Reactions of Molecules at Electrode, Wiley-Interscience, London, 1971, p. 259.

7 J. M. Hale, ibid. p229.

8 N. S. Hush, Electrochim. Acta, 13, 1005 (1968).

9 H. Bartelt, ibid. 16, 629 (1971).

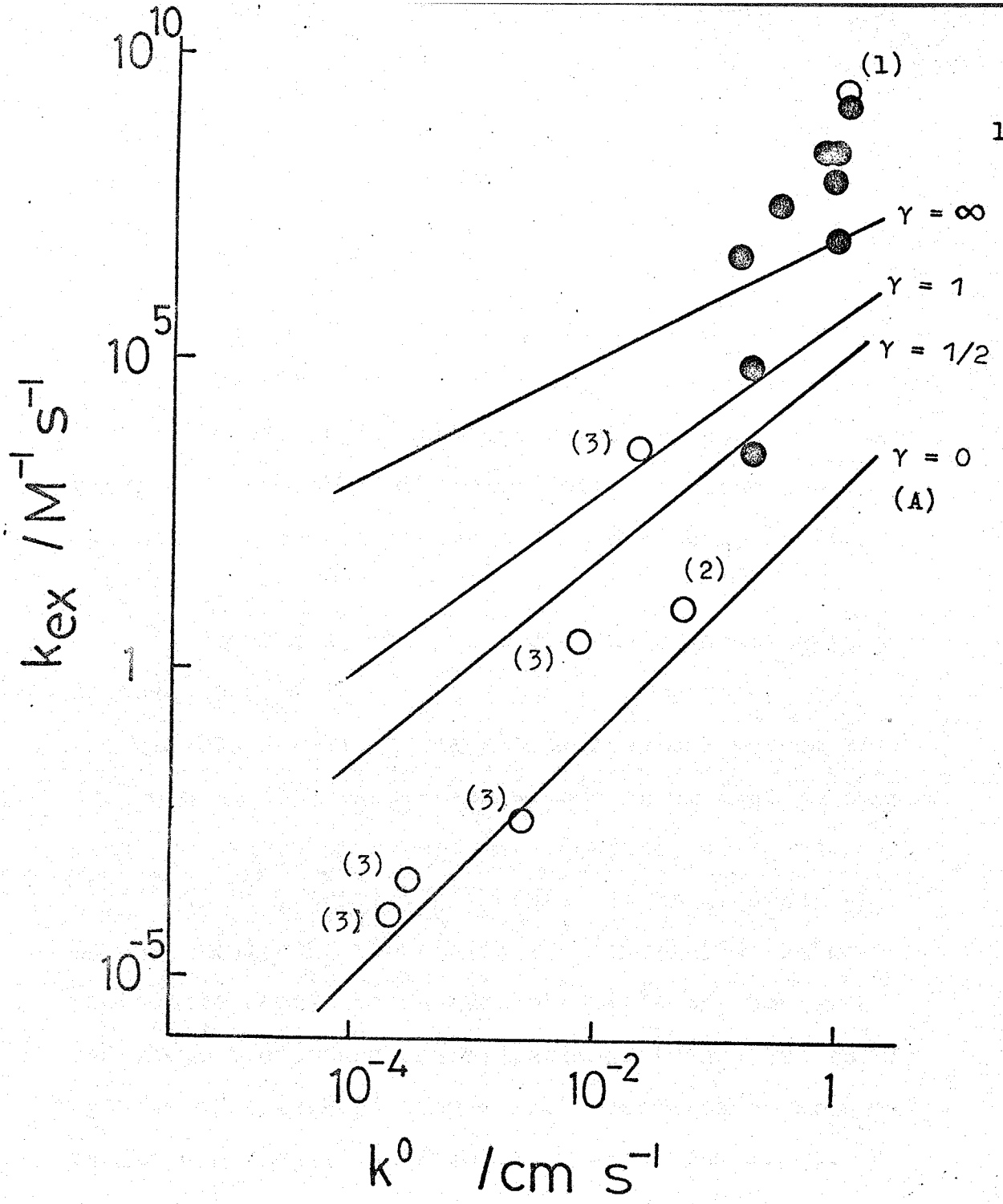

Fig. 36. Correlation between homogeneous electron-exchange rate constants and electrochemical rate constants. (1) Perylene/Perylene$^-$, Refs. 2 and 3. (2) Data from Ref. 9. (3) Data from Ref. 1. Solid circles represent the values measured in this work. Straight lines are drawn in accordance with eqn.(34) for various values of the parameter γ.

CHAPTER V

SUMMARY

The aim of this thesis is to find the correlation between the electrochemical electron-transfer rates and the electronic configurations of the reactants on the basis of the mechanistic similarity of electron-transfer process in homogeneous and electrochemical reactions.

In Chapter I, the purpose of this investigation is described.

In Chapter II, a new electrochemical method is proposed to determine which molecular orbital an excess electron of reductant species occupies, a ligand π^*-orbital or a metal t_{2g}-orbital. It is based on an empirical rule concerning the correlation between the polarographic half-wave potentials of complexes and their electronic configurations. Twenty two redox systems of tris(2,2'-bipyridine) complexes of transition metals are classified into two groups. The excess electron in the reductant species of redox systems, ML_3^{2+}/ML_3^{+}(M = Fe, Ru, Os), ML_3^{+}/ML_3(M = Fe, Ru, Os), ML_3/ML_3^{-}(M = Fe, Ru, Os, Cr), ML_3^{-}/ML_3^{2-}(M = Cr, V), CrL_3^{2-}/CrL_3^{3-} (L = 2,2'-bipyridine) is concluded to occupy a ligand π^*-orbital. The excess electron in the

reductant species of redox systems ML_3^{3+}/ML_3^{2+}(M = Fe, Ru, Os, Cr, Co), ML_3^{2+}/ML_3^{+}(M = Co, Cr, V) and VL_3^{+}/VL_3 is concluded to occupy a metal t_{2g}-orbital.

In Chapter III, the standard rate constants, k^o, for tris(2,2'-bipyridine) complexes of transition metals are measured by the galvanostatic double-pulse method. The standard rate constant for a redox system falls within 0.1~0.3 cm s^{-1}, when a ligand π^*-orbital is occupied by the excess electron of the reductant species, and within 0.5~1.3 cm s^{-1}, when a metal t_{2g}-orbital is occupied. A set of rate constants uncorrected for the potential of the diffuse double-layer provides a more reasonable basis for discussion than that of corrected ones. The difference in rate constant between these two groups is explained by the difference in inner-sphere reorganization energy, λi.

In Chapter IV, the correlation between the rate constants for the homogeneous electron-exchange reactions and those for the electrochemical electron-transfer reactions is discussed on the basis of the theoretical equation of Marcus. It is inferred that the contribution of λi is negligible in the electrochemical reactions with large rate constants approaching or exceeding 1 cm s^{-1} and large in those with very small rate constants. The λi is comparable with λo in the moderately fast reactions.

APPENDIX I

Polarography of Dicyano-bis(2,2'-bipyridine) Iron(II) Complexes

Figure 37 shows a cathodic polarogram for $Fe(bipy)_2(CN)_2$ in DMF containing 0.1 M TBAP. It exhibited four waves with half-wave potentials -1.59, -1.90, -2.1 and -2.5 V. The wave at -2.1 V was lower in height than others. It may be the first reduction wave for free bipyridne. The first three waves at -1.59, -1.90 and -2.1 were concluded to be reversible one-electron waves on the basis of the cyclic voltammogram for $Fe(bipy)_2(CN)_2$ in Fig. 38 taken with an initial cathodic scan. The waves at -1.59 and -1.90 V may be assigned to the redox systems $Fe(bipy)_2(CN)_2/Fe(bipy)_2(CN)_2^-$ and $Fe(bipy)_2(CN)_2^-/Fe(bipy)_2(CN)_2^{2-}$ respectively. The cyclic voltammogram with an anodic scan exhibited a reversible one-electron step corresponding to the redox system $Fe(bipy)_2(CN)_2^+/Fe(bipy)_2(CN)_2$.

Similar polarograms and cyclic voltammograms were also observed for the methyl-substituted complexes. The half-wave potentials of the two redox systems, Fe(CN) $FeL_2(CN)_2/FeL_2(CN)_2^-$ and $FeL_2(CN)_2^-/FeL_2(CN)_2^{2-}$ (L = bipy, 4-dmbipy, 5-dmbipy), became more negative in the order of ligand, bipy < 4-dmbipy < 5-dmbipy (Table 14) and those of $FeL_2(CN)_2^+/FeL_2(CN)_2$ in the order bipy < 5-dmbipy < 4-dmbipy.

The absorption band for $Fe(bipy)_2(CN)_2$ in the vicinity of 19,000 cm^{-1} has been assigned to a charge-transfer transition[1]. The charge-transfer bands for the dimethyl derivatives were measured and assigned by analogy to this. The charge-transfer bands for $FeL_2(CN)_2$ were blue-shifted according to the order of ligand, 4-dmbipy < bipy < 5-dmbipy (Table 14).

The $E^{red}_{1/2,C}$ vs. $E^{red}_{1/2,L}$ plots for the $FeL_2(CN)_2$/$FeL_2(CN)_2^-$ and $FeL_2(CN)_2^-$/$FeL_2(CN)_2^{2-}$ systems satisfied eqn. (5) as shown in Fig. 39. On the other hand, the $(E^{ox}_{1/2,C} - E^{red}_{1/2,L})$ vs. $h\nu_{CT}$ plot for the $FeL_2(CN)_2^+$/$FeL_2(CN)_2$ system satisfied eqn. (9) as shown in Fig. 40.

Thus it is concluded that in the first two reduction steps for $FeL_2(CN)_2$ each added electron occupies a ligand π^*-orbital and in the oxidation step an electron is removed from a metal t_{2g}-orbital.

REFERENCES

1 A. A. Shilt, J. Amer. Chem. Soc., 82, 3,000 (1960).

Table 14. Polarographic data and charge-transfer energies $h\nu_{CT}$ for $FeL_2(CN)_2$ and half-wave potentials corrected for reduction half-wave potentials for L/L^- systems. L = bipy, 4-dmbipy, 5-dmbipy.

Complex	$E_{1/2}$/V vs. SCE				$h\nu_{CT}$/eV (aq)
	DMF(0.1 M TBAP)			aq(0.5 M KCl)	
	2-/-	-/0	0/+	0/+	
$Fe(bipy)_2(CN)_2$	-1.96	-1.59	+0.48(2.58)[a]	+0.52(2.62)[a]	2.42
$Fe(4\text{-dmbipy})_2(CN)_2$	-1.98	-1.69	+0.39(2.54)	+0.43(2.58)	2.38
$Fe(5\text{-dmbipy})_2(CN)_2$	-2.05	-1.73	+0.42(2.65)	+0.46(2.69)	2.46

a: $(E^{ox}_{1/2,C} - E^{red}_{1/2,L})$/V

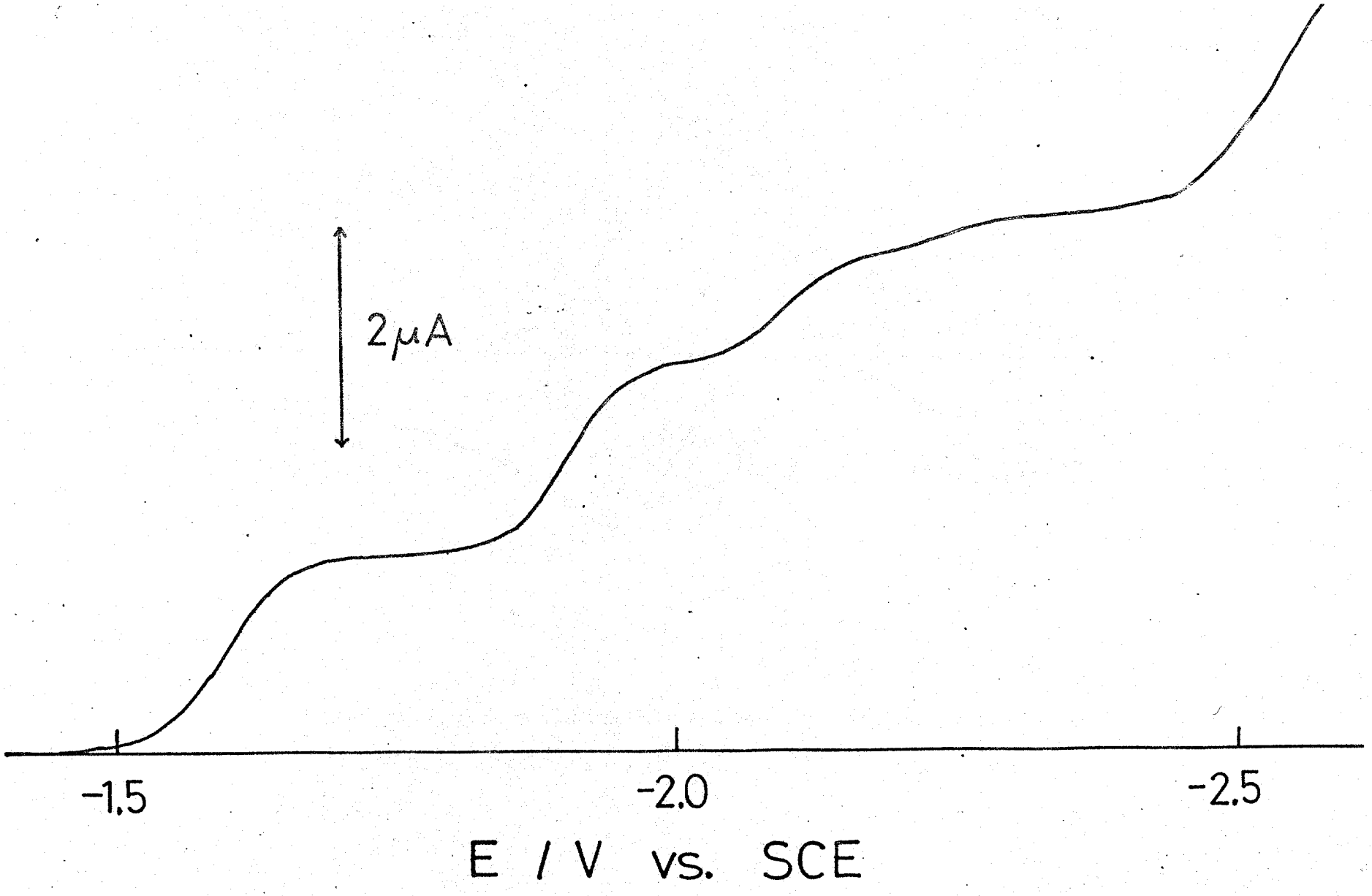

Fig. 37 Cathodic polarogram for 1mM $Fe(bipy)_2(CN)_2$ in DMF soln. of 0.1M TBAP.

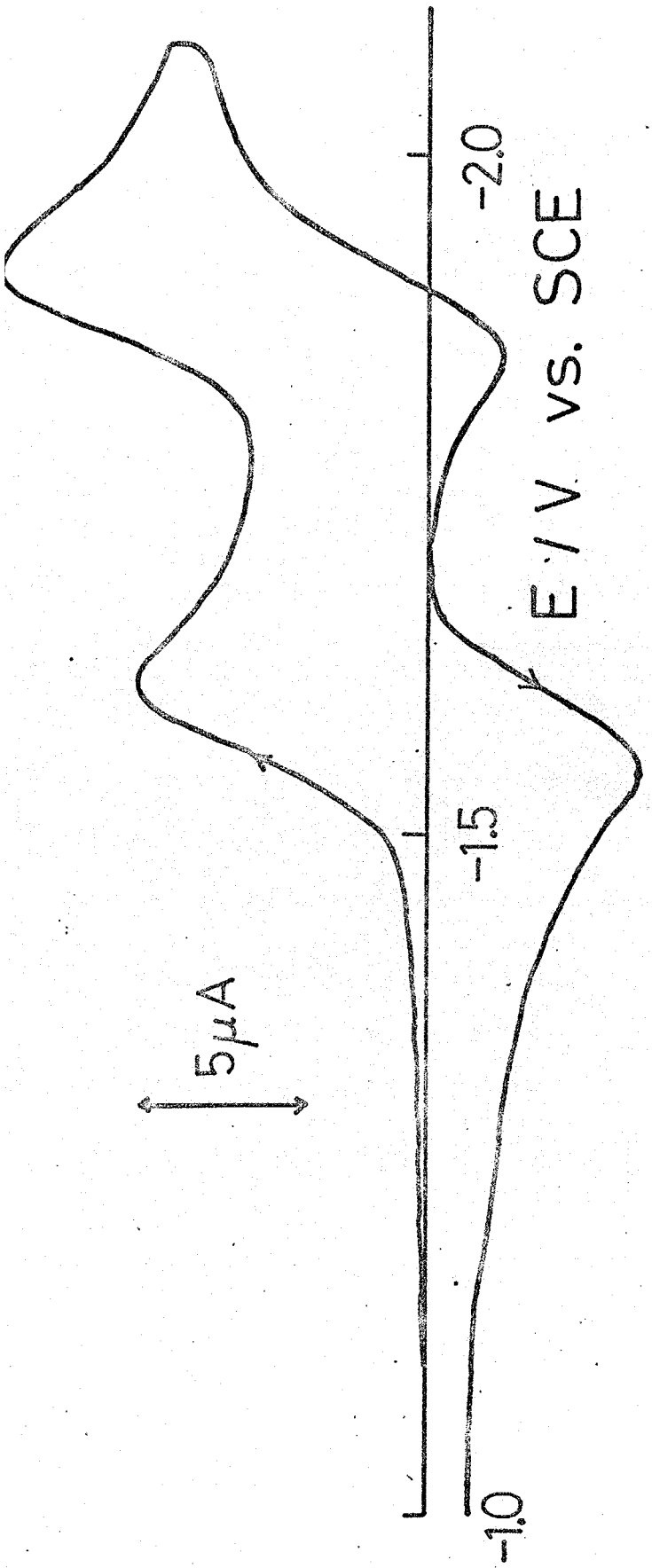

Fig. 38 Cyclic voltammogram with initial cathodic scan for 1mM $Fe(bipy)_2(CN)_2$ in DMF soln. of 0.1M TBAP. Scan rate 0.1V s^{-1}.

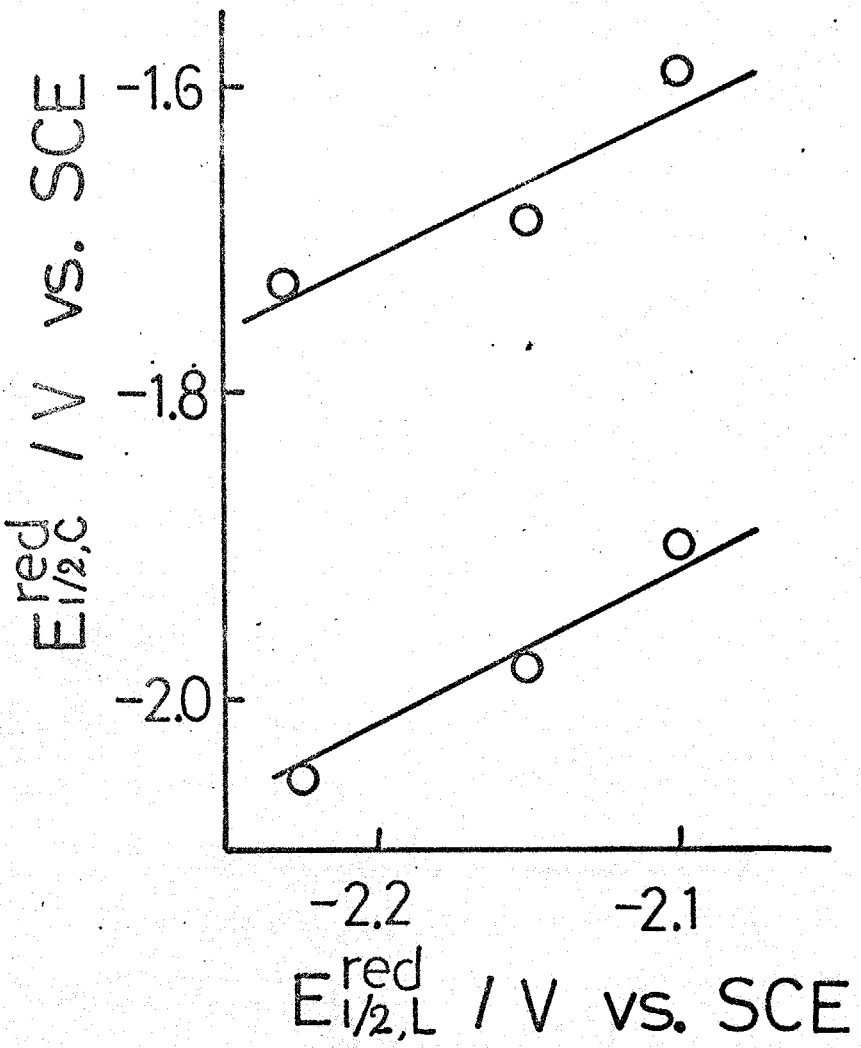

Fig. 39 Plot of half-wave potentials for (a) $FeL_2(CN)_2$/ $FeL_2(CN)_2^-$ and $FeL_2(CN)_2^-/FeL_2(CN)_2^{2-}$, $E^{red}_{1/2,C}$, vs. those for L/L^- systems, $E^{red}_{1/2,L}$, in DMF soln. of 0.1M TBAP. L = bipy, 4-dmbipy, 5-dmbipy.

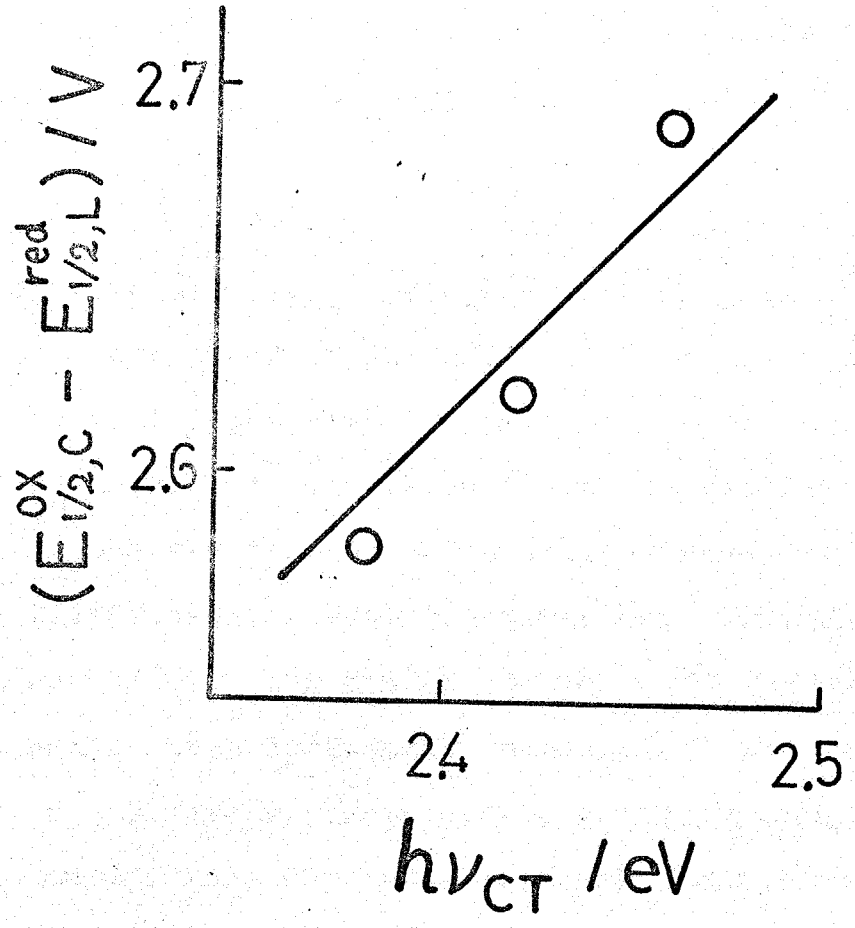

Fig. 40. Plot of half-wave potential difference, $E^{ox}_{1/2,C} - E^{red}_{1/2,L}$, vs. charge trasfer energy $h\nu_{CT}$ for $FeL_2(CN)_2^+/FeL_2(CN)_2$ in aqueous soln. of 0.5 M KCl.

APPENDIX II

The Electrochemical Rate Constants for the Redox Systems $Fe(C_5H_5)_2^+/Fe(C_5H_5)_2$ and $Fe(phen)_3^{3+}/Fe(phen)_3^{2+}$

The homogeneous electron-exchange reactions of the redox systems $Fe(C_5H_5)_2^+/Fe(C_5H_5)_2$ and $Fe(phen)_3^{3+}/Fe(phen)_3^{2+}$ were presumed in Chapter I to proceed via outer-sphere activated complexe because of their large rate constants. They may be suitable for testing the theory of the electrochemical electron-transfer reactions. Their electrochemical rate constants were measured by the g.d.p. method with the aim of adding a few experimental points to a correlation diagram of k_{ex} vs. k^o. Figure 41 shows cyclic voltammograms with initial anodic scan for (a) a methanolic solution containing 2 mM $Fe(C_5H_5)_2$ and 0.5 M LiCl and (b) an aqueous solution containing 2 mM $FeSO_4$, 6 mM phen and 0.5 M LiCl. The oxidation steps for $Fe(C_5H_5)_2$ and $Fe(phen)_3^{2+}$ were concluded to be reversible one-electron steps on the basis of the usual reversibility criteria. The observed standard rate constants are listed in Table 15 together with the literature values for the corresponding homogeneous rate constants [1,2].

Table 15. Homogeneous and electrochemical rate constants for the systems $Fe(C_5H_5)_2^{+}/Fe(C_5H_5)_2$ and $Fe(phen)_3^{3+}/Fe(phen)_3^{2+}$

System	Soln.	Electrode	$E_{1/2}$	k^o(cm s^{-1})	k_{ex}($M^{-1}s^{-}$
$Fe(C_5H_5)_2^{+/o}$	methanol(0.5M LiCl)	Pt	+0.37	0.72	$3x10^8$ a
$Fe(phen)_3^{3+/2+}$	aqueous (0.5M LiCl)	Pt	+0.84	0.69	$3x10^8$ b

a: Ref. 1, b: Ref. 2.

REFERENCES

1 J. R. Pladziewicz and J. H. Espenson, J. Amer. Chem. Soc., 95, 56 (1973).

2 I. Ruff and M. Zimonyi, Electrochimica Acta, 18, 515 (1973).

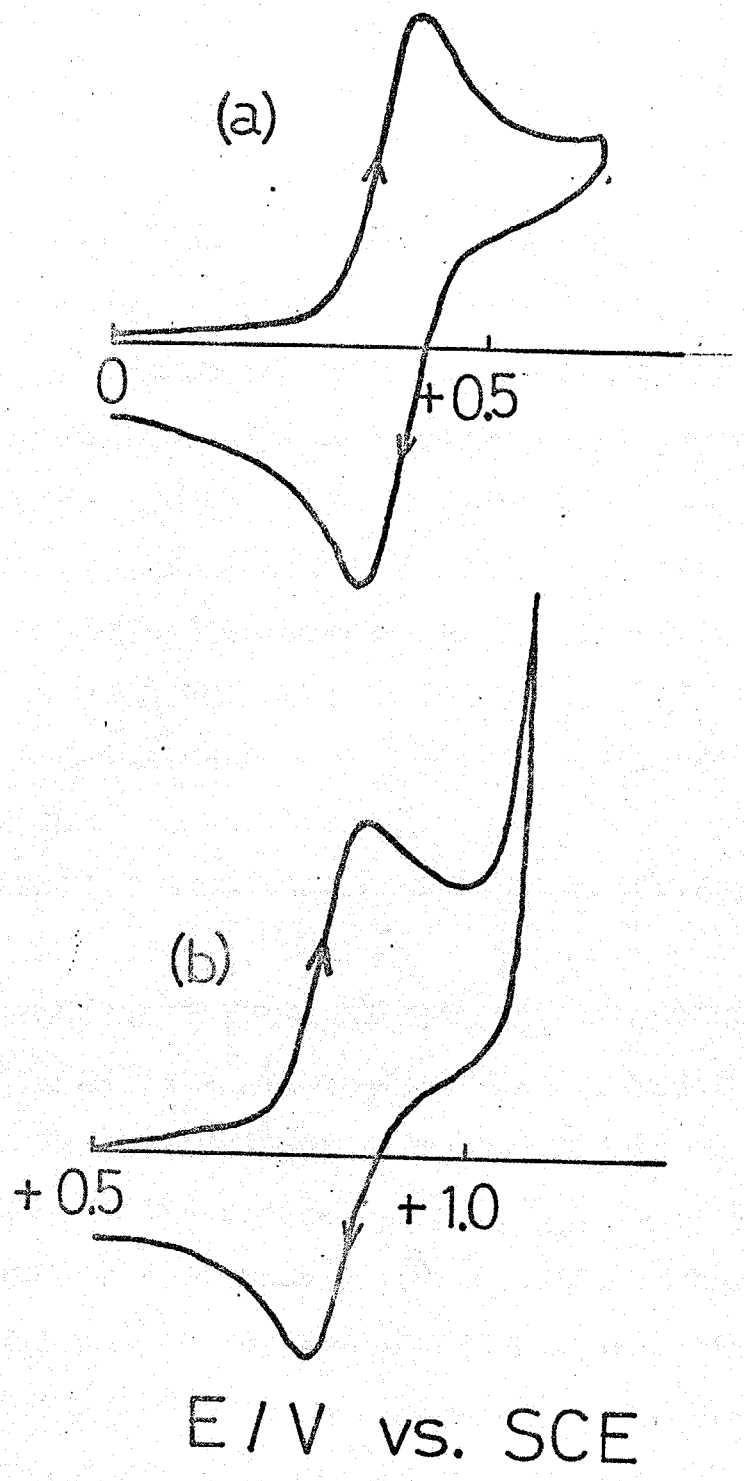

Fig. 41. Cyclic voltammograms with initial anodic scan for (a) a methanolic soln. containing 2 mM $Fe(C_5H_5)_2$ and 0.5M LiCl and (b) an aqueous soln. containing 2 mM $FeSO_4$, 6 mM phen and 0.5 M LiCl. Scan rate 0.1 V s^{-1}.

LIST OF PUBLICATIONS

1) ELECTRON-TRANSFER KINETICS OF TRANSITION-METAL COMPLEXES IN LOWER OXIDATION STATES. PART I. ELECTRON SPIN RESONANCE MEASUREMENTS OF THE ELECTRON-EXCHANGE RATE BETWEEN $Cr(bipy)_3^+$ and $Cr(bipy)_3$, Bull. Chem. Soc. Japan, 46, 2101 (1973), (S. Aoyagui).

2) ELECTRON-TRANSFER KINETICS OF TRANSITION-METAL COMPLEXES IN LOWER OXIDATION STATES. PART II. THE ELECTROCHEMICAL ELECTRON-TRANSFER RATE OF THE $Cr(bipy)_3^+/Cr(bipy)_3$ SYSTEM AS MEASURED BY THE GALVANOSTATIC DOUBLE-PULSE METHOD, Bull. Chem. Soc. Japan, 47, 389 (1974), (S. Aoyagui).

3) POLAROGRAPHY OF TRIS(2,2'-BIPYRIDINE)VANADIUM(O), Chem. Lett., 1974, 203, (S. Aoyagui).

4) POLAROGRAPHIC STUDIES ON BIPYRIDINE COMPLEXES I. CORRELATION BETWEEN REDUCTION POTENTIALS OF IRON(II), RUTHENIUM(II), OSMIUM(II) COMPLEXES AND THOSE OF FREE LIGANDS, J. Electroanal. Chem., 58, 401 (1975), (S. Aoyagui).

5) POLAROGRAPHIC STUDIES ON BIPYRIDINE COMPLEXES II. CORRELATION BETWEEN CHARGE-TRANSFER FREQUENCIES AND OXIDATION POTENTIALS OF TRIS(2,2'-BIPYRIDINE) COMPLEXES OF IRON, RUTHENIUM, OSMIUM, COBALT AND CHROMIUM, J. Electroanal. Chem., in press, (S. Aoyagui).

6) ELECTRON-TRANSFER KINETICS OF TRANSITION-METAL COMPLEXES IN LOWER OXIDATION STATES. PART III. ELECTROCHEMICAL RATE CONSTANTS FOR THE Fe(II)/Fe(I) REDOX SYSTEMS, submitted to Bull. Chem. Soc. Japan, (T. Yamada, S. Aoyagui).

7) ELECTRON-TRANSFER RATE CONSTANTS FOR REDOX SYSTEMS OF Fe(III)/Fe(II) COMPLEXES WITH 2,2'-BIPYRIDINE AND/OR CYANIDE ION AS MEASURED BY THE GALVANOSTATIC DOUBLE PULSE METHOD, J. Electroanal. Chem., in press (T. Yamada, S. Aoyagui).

8) ELECTRON-TRANSFER KINETICS OF TRANSITION-METAL COMPLEXES IN LOWER OXIDATION STATES. PART IV. ELECTROCHEMICAL ELECTRON-TRANSFER RATES OF TRIS(2,2'-BIPYRIDINE) COMPLEXES OF IRON, RUTHENIUM, OSMIUM, CHROMIUM, TITANIUM, VANADIUM AND MOLYBDENUM, J. Electroanal. Chem., in press. (S. Aoyagui).

9) POLAROGRAPHIC STUDIES ON BIPYRIDINE COMPLEXES. PART III. POLAROGRAPHY OF TRIS(2,2'-BIPYRIDINE) COMPLEXES OF CHROMIUM(I,0), VANADIUM(0), TITANIUM(0), AND MOLYBDENUM(0), submitted to J. Electroanal. Chem., (S. Aoyagui).

10) POLAROGRAPHIC STUDIES ON BIPYRIDINE COMPLEXES. PART IV. POLAROGRAPHY OF DICYANO-BIS(2,2'-BIPYRIDINE)IRON(II) COMPLEXES, to be submitted to Bull. Chem. Soc. Japan, (S. Aoyagui).